

Aus der Klinik und Poliklinik für Frauenheilkunde und Geburtshilfe

Klinikum der Ludwig-Maximilians-Universität München

Vorstand: Prof. Dr. Sven Mahner

**The alteration of Histone H3 at lysine 4
Trimethylation (H3K4me3) and its significance in ovarian
cancer**



Dissertation

zum Erwerb des Doktorgrades der Medizin

an der Medizinischen Fakultät der

Ludwig-Maximilians-Universität zu München

vorgelegt von

Nan Han

aus

Heilongjiang

Jahr

2022

Mit Genehmigung der Medizinischen Fakultät
der Universität München

Berichterstatter: Prof.Dr. Udo Jeschke

Mitberichterstatter: Prof. Dr. Björn Lampe
Prof. Dr. Jutta Kirfel

Mitbetreuung durch den
promovierten Mitarbeiter: PD Dr.Fabian Trillsch

Dekan: Prof. Dr. med. Thomas Gudermann

Tag der mündlichen Prüfung: 20.01.2022

Affidavit



Affidavit

Han, Nan

Surname, first name

Street

Zip code, town, country

I hereby declare, that the submitted thesis entitled:

The alteration of Histone H3 at lysine 4 Trimethylation (H3K4me3) and its significance in ovarian cancer

.....

is my own work. I have only used the sources indicated and have not made unauthorised use of services of a third party. Where the work of others has been quoted or reproduced, the source is always given.

I further declare that the submitted thesis or parts thereof have not been presented as part of an examination degree to any other university.

München, 06/02/2022

place, date

Nan Han

Signature doctoral candidate

Table of content

Affidavit	3
Table of content	4
List of abbreviations	5
List of publications and contributions	7
Confirmation of co-authors	8
1.1 Paper I.....	8
1.2 Paper II.....	10
2. Introduction	12
2.1 General Outline of Ovarian Cancer.....	12
2.2 H3K4 Trimethylation and its Transcriptional Functions	13
2.2.1 Histone H3 Lysine 4 Trimethylation.....	13
2.2.2 The Enrichment Patterns of H3K4me3 are Different at TSSs	14
2.2.3 H3K4me3 is Strongly Associated with Transcription.....	15
2.3 Known Functions of H3K4me3 in Cancer.....	16
2.3.1 The Role of H3K4 Trimethylation in Tumorigenesis	17
2.3.2 Broad H3K4me3 is involved in tumour suppression	17
2.3.3 The Association between H3K4me3 and human cancer prognosis	18
2.4 Vitamin D receptor (VDR) and H3K4 trimethylation.....	19
2.5 Estrogen Receptors and H3K4 trimethylation	20
3.Publication I	22
4.Publication II	38
5.Summary	66
5.1 H3K4me3 expression in EOC patients and relation to treatment of $1\alpha,25(\text{OH})_2\text{D}_3$ Ovarian Cancer cells.....	66
5.2 The level of H3K4me3 and cell growth are mediated by GPER in ovarian cancer cells.....	66
6. Zusammenfassung	67
6.1 H3K4me3-Expression bei EOC-Patientinnen und Beziehung zur Behandlung von $1\alpha,25(\text{OH})_2\text{D}_3$ -Eierstockkrebszellen	67
6.2 Das Niveau von H3K4me3 und das Zellwachstum werden durch GPER in Eierstockkrebszellen vermittelt.....	67
7. References	69
Acknowledgements	76

List of abbreviations

1,25(OH) ₂ D ₃	1,25-dihydroxycholecalciferol or calcitriol
Akt	also known as PKB, Protein kinase B
ARID1A	AT-Rich interaction Domain 1A
BAP18	chromatin complexes subunit BAP18
cAMP	cyclic adenosine monophosphate
CCC	clear cell carcinomas
CHD1	Chromodomain-helicase-DNA-binding protein 1
ChIP	chromatinic immunoprecipitation
CTNNB1	catenin beta-1, also known as β -catenin
EC	endometrioid carcinomas
EGFR	epidermal growth factor receptor
EMT	epithelial mesenchymal transition
EOC	epithelial ovarian cancer
ERR α	estrogen-related receptor alpha
ERs	estrogen receptors
ESC	embryonic stem cell
FACT/Paf	facilitates chromatin transcription complex/platelet activating factor
FIGO	International Federation of Gynaecology and Obstetrics
FOXA1	Forkhead box protein A1
GPCR	G protein-coupled receptor
GPER	G protein-coupled estrogen receptor 1
H3K4me	Histone H3 lysine 4 methylation
H3K4me3	Trimethylation of lysine 4 on histone H3
H3K9ac	Histone H3 acetylated at lysine 9
HGSC	high-grade serous carcinomas
HMT	histone methyltransferase
ING1	inhibitor of growth 1
JARID1B	lysine-specific demethylase 5B
KDM1A	lysine (K)-specific demethylase 1A
KDM5B	lysine-specific histone demethylase 5B

KMT2A	histone-lysine N-methyltransferase 2A
KMT2D	histone-lysine N-methyltransferase 2D
MAPK	mitogen-activated protein kinase
MC	mucinous carcinomas
MEN-1	multiple endocrine neoplasia type 1
ncRNA	non-coding RNA
OC	ovarian cancer
PARP	poly ADP ribose polymerase
PHD	plant homeodomain
PIC	pre-initiation complex
PI3K	phosphoinositide 3-kinase
PIK3CA	phosphatidylinositol 3-kinase, catalytic subunit alpha
PPP2R1A	protein Phosphatase 2 Scaffold Subunit Alpha
pT	primary tumour
PTEN	phosphatase and tensin homolog
PTM	posttranslational modification
RBBP5	RB Binding Protein 5, Histone Lysine Methyltransferase Complex Subunit
RNAP II	RNA polymerase II
SNAI1	Snail Family Transcriptional Repressor 1
SC	serous carcinomas
Ser5-P CTD	Ser5-phosphorylation C-terminal domain
TAF	TBP-associated factor
TBP	TATA-binding protein
TFIID	transcription factor II D
TFF1	Trefoil factor 1
TGF- β 1	Transforming growth factor beta 1
TSS	transcriptional start site
U2 snRNP	U2 small nuclear ribonucleoprotein
VDR	vitamin D receptor, also known as calcitriol receptor
Wdr82	WD repeat-containing protein 82
WHO	World Health Organization

List of publications

1. H3K4me3 Is a Potential Mediator for Antiproliferative Effects of Calcitriol ($1\alpha,25(\text{OH})_2\text{D}_3$) in Ovarian Cancer Biology

Int. J. Mol. Sci. 2020, 21(6), 2151. doi:10.3390/ijms21062151. Epub: 20th March 2020.

Nan Han, Udo Jeschke, Christina Kuhn, Anna Hester, Bastian Czogalla, Sven Mahner, Miriam Rottmann, Doris Mayr, Elisa Schmoeckel and Fabian Trillsch

2. The G-Protein-Coupled Estrogen Receptor (GPER) Regulates Trimethylation of Histone H3 at Lysine 4 and Represses Migration and Proliferation of Ovarian Cancer Cells In Vitro

Cells 2021, 10(3), 619. doi: 10.3390/cells10030619. Epub: 11st March 2021.

Nan Han, Sabine Heublein, Udo Jeschke, Christina Kuhn, Anna Hester, Bastian Czogalla, Sven Mahner, Miriam Rottmann, Doris Mayr, Elisa Schmoeckel and Fabian Trillsch

Contributions to the publications

Paper I

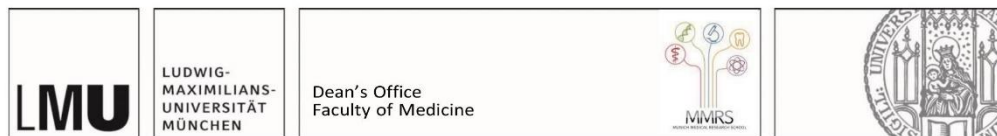
I took the investigations and carried out the experiments. Data visualization was completed by me. I wrote the manuscript with support from PD Dr. Fabian Trillsch.

Paper II

I investigated and performed the experiments. Data visualization was completed by me. I wrote the manuscript with support from PD Dr. Fabian Trillsch.

Confirmation of co-authors

1.1 Paper I



Cumulative Thesis

In accordance with § 4a Paras. 3 and 5 Examination Regulations for Dr. med., Dr. med. dent. and Dr. rer. biol. hum., as well as

with § 7 Para. 4 Doctoral Degree Regulations for Dr. rer. nat. at the Medical Faculty

Please note: for each published article, a separate "Cumulative Thesis" form has to be submitted!

Nan Han

Name of doctoral candidate

The alteration of Histone H3 at lysine 4 Trimethylation (H3K4me3) and its significance in ovarian cancer

Title of dissertation

Title of article	H3K4me3 Is a Potential Mediator for Antiproliferative Effects of Calcitriol (1 α ,25(OH)2D3) in Ovarian Cancer Biology
Title of journal	International Journal of Molecular Sciences
Year	2020
Volume	21
Pages	2151-2166

I hereby confirm that none of the articles submitted for this doctoral degree have been the subject of another (current or completed) cumulative thesis.

Signature of doctoral candidate

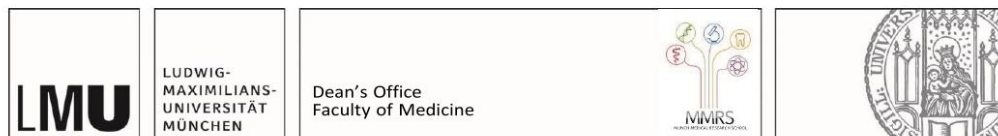
By signing, the following **co-authors** confirm that:

- the extent of their contributions (content-related and volume) in the publications submitted,
- their agreement to the submission of the publications, and
- the article in question is not the subject of another (current or completed) thesis.

Name of co-author	Extent of contribution (content-related and volume)	Signature of co-author
1. Udo Jeschke	Conceptualization; formal analysis; funding acquisition; investigation; methodology; project administration; supervision; validation; writing--review and editing	
2. Christina Kuhn	Investigation	
3. Anna Hester	Investigation; writing—review and editing	
4. Bastian Czogalla	Investigation; writing—review and editing	
5. Sven Mahner	Conceptualization, supervision; validation; writing—review and editing	
6. Miriam Rottmann	Formal analysis	
7. Doris Mayr	Investigation; methodology; supervision; validation; writing—review and editing	
8. Elisa Schmoeckel	Conceptualization; formal analysis; investigation; methodology; writing—review and editing	
9. Fabian Trillsch	Conceptualization, funding acquisition; methodology; project Administration; validation; writing—original draft	

Please list further authors on a separate page

1.2 Paper II



Cumulative Thesis

In accordance with § 4a Paras. 3 and 5 Examination Regulations for Dr. med., Dr. med. dent. and Dr. rer. biol. hum., as well as with § 7 Para. 4 Doctoral Degree Regulations for Dr. rer. nat. at the Medical Faculty
Please note: for each published article, a separate "Cumulative Thesis" form has to be submitted!

Nan Han

Name of doctoral candidate

The alteration of Histone H3 at lysine 4 Trimethylation (H3K4me3) and its significance in ovarian cancer

Title of dissertation

Title of article	The G-Protein-Coupled Estrogen Receptor (GPER) Regulates Trimethylation of Histone H3 at Lysine 4 and Represses Migration and Proliferation of Ovarian Cancer Cells In Vitro
Title of journal	Cells
Year	2021
Volume	10
Pages	619-641

I hereby confirm that none of the articles submitted for this doctoral degree have been the subject of another (current or completed) cumulative thesis.

Signature of doctoral candidate

By signing, the following **co-authors** confirm that:

- the extent of their contributions (content-related and volume) in the publications submitted,
- their agreement to the submission of the publications, and
- the article in question is not the subject of another (current or completed) thesis.

Name of co-author	Extent of contribution (content-related and volume)	Signature of co-author
1. Sabine Heublein	Formal analysis	
2. Udo Jeschke	Conceptualization; formal analysis; funding acquisition; investigation; methodology; project administration; supervision; validation; writing—review and editing	
3. Christina Kuhn	Investigation	
4. Anna Hester	Investigation; writing—review and editing	
5. Bastian Czogalla	Investigation; writing—review and editing	
6. Sven Mahner	Supervision; validation; writing—review and editing	
7. Miriam Rottmann	Formal analysis	
8. Doris Mayr	Investigation; methodology; supervision; validation; writing—review and editing	
9. Elisa Schmoeckel	Conceptualization; formal analysis; investigation; methodology; writing—review and editing	
10. Fabian Trillsch	Conceptualization; funding acquisition; methodology; validation; project administration; writing—original draft	

Please list further authors on a separate page

2. Introduction

2.1 General Outline of Ovarian Cancer

Ovarian cancer (OC) remains the most lethal gynaecological malignancy [1]. An estimated 90-95% of all cases is epithelial ovarian cancer (EOC) [2]. Although approximately two thirds of EOC patients present as an advanced (FIGO stage III or IV) disease, most of patients are either found to be undiagnosed or only shown nonspecific symptoms of early onset of EOC. Hence, 5-year survival rate for ovarian cancer greatly decreases from 92% for patients diagnosed in the early stage to 29% for those diagnosed in advanced disease[3]. The standard therapies of EOC patients are comprised of surgical management followed by platinum-based chemotherapy[4]. Over the past years, the addition of bevacizumab to the combination chemotherapy of carboplatin and paclitaxel has been reported to improve progression-free survival of advanced OC patients[5]. Recently, it has been reported that progression-free survival can be further increased by PARP (poly ADP ribose polymerase) inhibitors treatment alone or in combination with bevacizumab[6,7]. The majority of women respond well to first-line chemotherapeutic drugs initially, but frequently relapses occur, ultimately resulting in chemo-resistance[8]. Deficiency of the early detection biomarkers and acquired resistance to chemotherapeutic drugs are our major problems in EOC management.

Heterogeneity represents a hallmark of cancer cells within the same tumour[9]. EOC is one kind of highly heterogeneous disease, encompassing various morphological and genomic profiling[10]. The histological classifications of EOC by the World Health Organization (WHO) are grouped into several morphological categories as follow: serous carcinomas (SC), mucinous carcinomas (MC), endometrioid carcinomas (EC), clear cell carcinomas (CCC), transitional cell tumour (Brenner tumour), mixed and undifferentiated carcinomas[11]. According to the dualistic theories of tumorigenesis, EOC is characterized by two distinct groups termed type I and type II [12]. In this context type I with low grade histology is opposed to type II featured by high grade histology [13]. Type I tumours are comprised of five types: Brenner tumour, low-grade serous and endometrioid, mucinous and clear cell carcinomas. Type I tumours exhibit typically indolence and present as a favourable prognosis. They are characterized by a relatively stable genomic profile [12]. Type I tumours typically contain a variety of mutations in K-Ras gene, B-Raf gene, PTEN (Phosphatase and tensin homolog) gene, PIK3CA (Phosphatidylinositol 3-kinase, catalytic subunit alpha) gene, CTNNB1 (Catenin beta-1, also known as β -catenin) gene, ARID1A (AT-Rich interaction Domain 1A), and PPP2R1A (Protein Phosphatase 2 Scaffold Subunit Alpha)[13-15], but seldom *TP53* (Figure 1). High-grade serous and endometrioid, undifferentiated and malignant mixed mesodermal carcinosarcomas are examples of Type II tumours [12]. They display in advanced stage and are highly aggressive. HGSC (High-grade serous carcinoma) is a prototypic form of type II tumour, which is characterised by highly unstable and *TP53* and approximately 25% frequent BRCA1/2 abnormalities [1,16,17] (Figure 1). Recently, genetic distinctions between different subtypes of EOC have been gradually identified. So far, there have been implicated at least 15 oncogenes, 16 tumour suppresser genes and more than seven signalling pathways in ovarian cancer[18]. However, classical genetic abnormalities alone cannot elucidate all diversity of cancer[19]. The recent dissection has further highlighted the importance of genetic and epigenetic alterations in the onset and development of cancer[20,21].

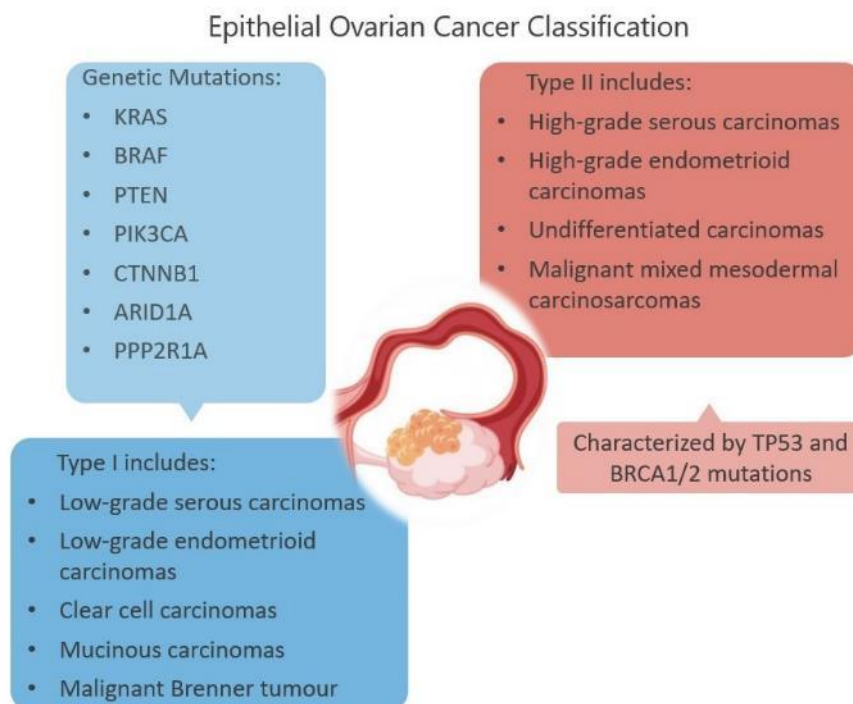


Figure1. The classification of Epithelial Ovarian Cancer (Shown as: Type I and II) and associated molecular genetic mutations.

Epigenetic regulatory mechanism includes methylated DNA, covalence of modified histone, non-coding RNA (ncRNA, such as small RNAs) and their networks with each other [22]. Altered epigenetic landscape is also intimately associated with tumorigenesis of ovarian cancer[23]. Nowadays it is recognized abnormal histone modifications are frequently observed and make a contribution to the initiation and development of ovarian malignancy[24]. The knowledge of how histone modifications associate with ovarian cancer is emerging at present. Tri-methylation of lysine 4 on histone H3 (H3K4me3) is seen as the most widely studies histone modifications in cancer. Nevertheless, the significance for ovarian cancer is still unclear.

2.2 H3K4 Trimethylation and its Transcriptional Functions

2.2.1 Histone H3 Lysine 4 Trimethylation

Histones are small, well-conserved proteins with a ball-shaped C-terminal domain and the flexibility of a short N-terminal tail [25]. The nucleosome, which is the most basic unit of chromatin, is made up of a histone octamer with two duplicates of H2A, H2B, H3 and H4 wrapped around 147 base pairs of DNA [26]. Histone 1 serves as a linking protein that connects the input and output points of DNA on the nucleosome surface [27]. Unstructured and extruding histone N-terminal tails from nucleosomes are gone through extensive covalent, reversible posttranslational modification (PTM) including methylated, acetylated, phosphorylated, ubiquitinated and biotinylated alterations[25,28]. Histone modification is now appreciated as a dynamic and reversible process of PTM[29,30]. The functions of histone modification manifest two categories: global chromatin organization and all sorts of biological events, for instant, transcription, repair and replication of DNA and cellular cycle regulatory in cells[28,31].

Histone H3 lysine 4 methylation (H3K4me) indicates the fourth position of amino-acid residues from N-terminus methylating histone H3[32]. Methylated histones are originally regarded as irreversible[33].

Until the identification of H3K4 demethylase for the first time, KDM1A (lysine K-specific demethylase 1A, also known as LSD1), it is believed to a process with dynamicity and reversibility as well as acetylated modification[34]. Based on the novel terminology, this modification is regulated by two antagonized types of proteinases called methylated histone "Writer" and "Eraser" respectively[35]. The methyl group(s) are added by catalysis of histone methyltransferases ("writers") to the given residue(s) and histone demethylases ("erasers") remove the methylation marks from residues (Figure 2A) [30,36]. The ϵ -amino group (s) of Histone 3 lysine 4 is able to be mono-methylated (H3K4me1), de-methylated (H3K4me2) or tri-methylated (H3K4me3) (Figure 2B)[37]. The subtypes of H3K4 methylation (H3K4me1,H3K4me2 and H3K4me3) display a gradient distribution pattern along actively transcribing genes suggesting distinct roles in transcription[35,38]. H3K4me1 highly accumulates at enhancers [39] and plays a fine-tuning role in enhancer activities and functions[40]. The high level of H3K4me2 is found in the nucleus and associated with the existence and activities of *cis*-regulation elements within the genes[41]. Unlike H3K4me1 and H3K4me2, H3K4me3 has specifically an enrichment around genes' transcriptional start sites (TSSs) in eukaryocyte and is strongly associated with transcriptional activities[42]. Due to reversibility of histone modification, H3K4me3 is seen as a transcriptional on/off switch[43].H3K4me3 has recently gained emerging attention, as it is especially involved in transcriptional mediation [44].

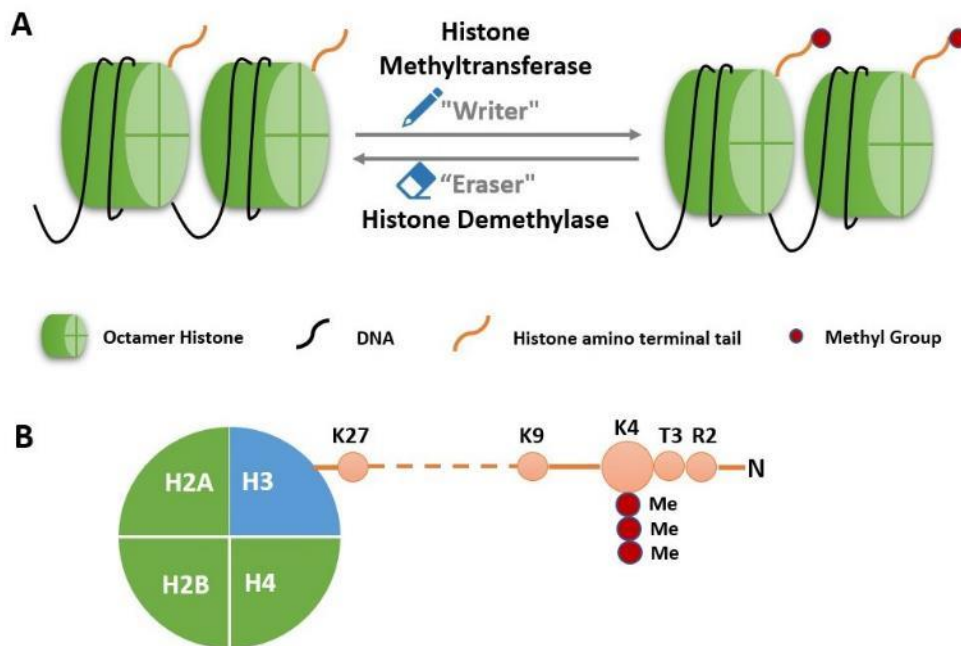


Figure2. (A) Methylated histone is a chemical alteration with dynamicity and reversibility. Histones are catalysed by methyl transferase ("Writer") and demethylase ("Eraser"); (B) H3K4me3: Lysine trimethylation occurs at the fourth residue on histone H3.

2.2.2 The Enrichment Patterns of H3K4me3 are Different at TSSs

By utilizing chromatinic immunoprecipitation (ChIP) and ChIP-on chip techniques, the distribution of H3K4me3 has been mapped in the human genome. Roughly, two-thirds of H3K4me3 are detected at TSS of genes of chromosomes 21 and 22 in human beings [45]. H3K4me3 is discovered about 91% of RNA polymerase II (RNAP II) islands[46]. Many studies have demonstrated that enrichment of trimethylated H3K4 is specifically restricted within TSS region and present sharp and narrow peak with high signal density [46-48]. The sharp and narrow peaks of H3K4me3 are initially known as classical patterns (Figure3 A1). However, some different cases have recently been reported. A few results have early displayed that

relatively small amounts of broad H3K4me3 differs from general sharp, narrow peaks of H3K4me3 at most promoters in mouse cells (Figure 3 A) [49,50]. Meanwhile, the overabundance of broad H3K4me3 has been also observed at some key genes in Wilms tumour cells and embryonic stem cells (ESCs) [51]. Initially, these observations were seen as exceptions and the researchers poorly understand the importance and functions of broad H3K4me3 at enrichment sites. However, two current integrative analyses of large dataset show that the breadth of enrichment site is responsible for the functions of H3K4me3 [52,53]. The H3K4me3 marks show that the width of H3K4me3 is involved with the identities and functions of various cell types, according to a meta-analysis [52]. Moreover, this research has also suggested that genes with the extremely 5% broad H3K4me3 domains improve the consistency of transcription instead of transcriptional rates, implying that the broadness of trimethylated H3K4 exerts a crucial function in cellular identity or function of genetic transcription accuracy [52]. The other known functions of broad H3K4me3 will be referred to later in my dissertation. In brief, the width of H3K4me3 enrichment is not thoroughly investigated so that post-translational properties and its functions should be established in the future.

2.2.3 H3K4me3 is Strongly Associated with Transcription

H3K4me3 is a form of well-known histone modifications that has been found in yeast and humans [54]. In yeast, Set1/COMPASS is the first discovered H3K4 methylating enzyme compound and is capable of catalysing formation of H3K4me3 [55,56]. The presence of H3K4me3 is positively correlated with active transcription [57]. The homologues of human cells comprise KMT2A, KMT2D, KMT2C, KMT2B, KMT2F and SETD1B [54]. For example, the activity of MLL protein takes part in *Hox* gene activation and methylated H3K4 *in vivo* [58]. A previous study has shown that more than 80% of genes taken up by promoter-proximal H3K4me3 is transcribed in an embryonal stem cell line of *Homo sapiens* [59]. Up to date, the molecular mechanisms how H3K4me3 regulates the transcriptional process have been widely studied. It is generally known that transcriptional cycle contains multiple steps from initiation (or pre-initiation) to elongation and termination. Epigenome mapping of humans has manifested that H3K4 trimethylation at the genes' transcriptional start site is tightly linked to the Ser5-phosphorylation C-terminal domain (Ser5-P CTD) of RNAP II [47]. The Wdr82 (WD repeat-containing protein 82) of human SETD1A complex tethers to Ser5-P CTD of RNAP II during transcription initiation for Set1A-mediated H3K4me3 around transcriptional start sites (TSSs) [60]. In addition, the basal transcription factor IID (TFIID) is essential for the initiation of transcription by RNAP II-dependent via assembling nucleated pre-initiation complex (PIC) at core promoters [61]. TFIID complex consists of the TATA-binding protein (TBP) and TAF3 that is considered as a TBP-associated factor (TAF) [62,63]. TFIID binding to DNA is needed, but not sufficient for transcription to start from most of RNAP II promoters. H3K4me3 is shown to directly bind to TFIID through plant homeodomain (PHD) protein of TAF3 [64]. The PHD finger of TAF3 is able to bind to high specificity to H3K4me3 [64]. The interactions between H3K4me3 and TAF3 serve to stabilise PIC assembly and transcription initiation by cooperation between TATA-binding box protein and promoters those are dependent on p53 (Figure 3B) [65].

Besides transcription initiation, the other mechanism is that H3K4me3 is involved in various steps after initiation of transcription like the pre-mRNA splicing. Transcript elongation by RNAP II is acknowledged as a dynamically and extremely mediated stage of the transcriptional loop [66]. The events of mRNA biogenesis include mRNA capping, pre-mRNA splicing, transcript elongation and polyadenylation accompanying mRNA surveillance and nuclear export simultaneously [67,68]. CHD1 (Chromodomain-helicase-DNA-binding protein 1) has been as a crucial factor of cellular processes and functions during transcription elongation via interacting with the components of essential elongation factors [69]. CHD1 is considered as a protein that is capable to bind to H3K4me3 in human cells [70]. H3K4me3 interacts with the spliceosome elements via CHD1, with an optimum for the SF3a subunits of U2 small nuclear ribonucleoprotein (U2 snRNP) [71]. There already exists the evidence to show human splicing factor SF3a playing an extremely

important part in pre-mRNA splicing *in vivo*[72]. Decreasing levels of CHD1 and H3K4me3 by siRNA has shown to weaken correlation of U2 snRNP elements with human chromatin and reduce the rate of pre-mRNA splicing *in vivo* (Figure3 C)[71]. Currently, it is well-known that FACT complex is capable of facilitating transcriptional elongation and impacting the rate of RNAP II[66]. The FACT connects to H3K4me3 through CHD1(Figure3 C)[65]. These findings suggest that CHD1-H3K4me3 contributes the coordinated events of transcriptional elongation and processes of pre-mRNA within the cells[71]. Additionally, the study from Chen *et al.* demonstrates broad H3K4me3 displays a clear peak at the 3' end that has been reported to make a contribution to active transcription elongation at specific genes[53]. By utilizing a well-established pausing index, they suggest that broad H3K4me3 is tightly linked to improvement of transcriptional elongation[53,73]. Taken together, H3K4me3 is strongly involved with active initiation and elongation of transcription via binding and interacting with essential factors.

In addition, H3K4 trimethylation is linked to these molecule memories for present transcriptional activities. It has been observed that hypermethylated status of H3K4 in the mRNA-coding regions still maintain for considerable amount of time after deactivation of transcription and disassociation of H3K4 methyltransferase [74]. However, H3K4me3 loss makes no difference to transcription occurrence in *Drosophila* [75]. Although further detailed data of mechanism by how H3K4me3 impacts active transcription remains enigmatic, it is plausible that H3K4me3 is a mark which has the strong correlations with transcription. The molecular process further impact cell cycle, cell growth and cell apoptosis. Trimethylated H3K4 offers a great deal of flexibility to mediate chromatin dynamics and signalling pathways, thus influencing gene expression. The dynamic plasticity of H3K4me3 is made available as a target for treatment of EOC.

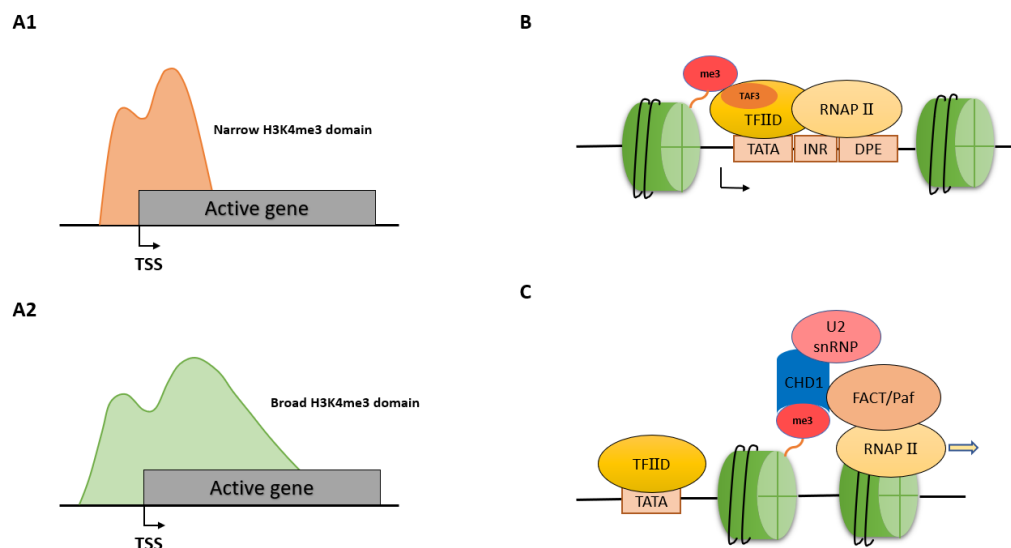


Figure3. (A) The narrow and broad H3K4me3 domains locate at TSS of active genes. (B) Model of H3K4me3 function on transcription initiation. H3K4me3 can improve TFIID and RNAP II recruitment and transcriptional initiation at active gene. (INR: initiator element; DPE: downstream promoter element) (C) Model of H3K4me3 during transcription elongation. After transcriptional activation, trimethylated H3K4 recognizes CHD1 around TSS. Then U2 snRNP is recruited by the SF3a subcomplex of CHD1 and FACT/Paf near the first nucleosome for pre-mRNA and transcription elongation.

2.3 Known Functions of H3K4me3 in Cancer

H3K4 trimethylation is closely related to transcriptional competency and activating, with gene expression maxima close to TSS[46]. In addition, H3K4me3 is linked to different functions in cell nucleus. The ING1 PHD finger is taken an example to recognize trimethylated H3K4 with a high affinity and H3K4me3

binding is required for DNA-damaged repair and cell apoptosis of ING1 (inhibitor of growth 1) function [76]. As trimethylated H3K4 exerts important roles in cell biological processes, it is valid to consider H3K4me3 alteration and its related functions are involved in many human diseases including cancer. Indeed, altered pattern of H3K4me3 has been discovered in various types of tumours, and previous investigations have pointed out that abnormal H3K4me3 in cellular context may well play a part in tumorigenesis. In this section, I utilize deregulated H3K4me3 and mutational effects on H3K4me3 after modification, as informative situations to explain the role of H3K4me3 in oncogenesis and in cancer prognosis.

2.3.1 The Role of H3K4 Trimethylation in Tumorigenesis

According to histone code hypothesis, the levels of (de)methylated histone lysine are precisely mediated respectively by methylating enzymes ("writers") or demethylating enzymes ("erasers") and distinct effector proteins ("readers") [35]. Therefore, miswriting, mis-erasing and misreading of H3K4 trimethylation is able to contribute to tumorigenesis. H3K4 methyltransferase complexes commonly have three structure elements and the catalysed SET domains to methylate H3K4 [36,77]. Snail is deemed a vital epithelial-mesenchymal transition (EMT) inducer, which is a protein encoded by *SNAI1* gene [78]. In prostate cancer cell line, TGF- β 1 can increase *SNAI1* expression by RBBP5 recruitment and H3K4me3 formation near the TSS of *SNAI1* gene during epithelial-mesenchymal transition (EMT) [79]. This result implies that H3K4me3 may be involved in the EMT-associated epithelial cells cancer progression. Histone-lysine N-methyltransferase 2A (KMT2A) is a member of histone methyltransferases (HMTs) and is able to trimethylated H3K4 [80]. Recent evidence indicates that overexpression of KMT2A can increase Cathepsin Z transcription through increasing level of H3K4me3 and performs a vital part in invasion and metastasis of colorectal carcinoma [81].

Mis-regulation of H3K4-specific demethylases is heavily involved in the process of malignancy as well. The jumonji family of lysine demethylases can erase all three methylation and catalyse the removal of H3K4 methylation by the JmiC domain [82]. JARID1B (Lysine-specific demethylase 5B, also called as KDM5B) is an H3K4me3 demethylase, upregulation of KDM5B leads to an obvious reduction of H3K4me3 level in prostate and breast cancers [83,84] which has been shown to be as a transcription suppressor [85]. Additionally, KDM5B directly inhibits the *BRCA1* gene expression by inducing the erasure of H3K4me3, resulting in the increasing the proliferation of the breast cancer cells [84].

2.3.2 Broad H3K4me3 is involved in tumour suppression

The pattern of broad H3K4me3 has been found within hematopoietic stem cells [53] and Wilms tumour [51] in the last decade. However, the biological role of broad H3K4me3 in various cancer cells was expected at that time. About seven years ago, a translational study reported that the broad of H3K4me3 domains was highly involved in transcriptional consistency and cell identity [52]. The enrichment of the widest H3K4me3 domains was observed at genes that participate in cellular specified functions and cell-type identities [52]. To further understand tumour processes, researchers have become more and more interested in the role of broad H3K4me3 in different types of cancers. In 2015, Chen et al. first discovered that broad, highly conserved H3K4me3, whose width is greater than 4kb, was enriched in tumour suppresser genes like *PTEN* and *TP53* (well-known pan-cancer tumour suppresser genes) as an epigenetic signature in human CD4⁺ T cells [53]. These studies also demonstrated that broad H3K4me3 peaks were tightly correlated with improving efficiency of transcriptional elongation and bio-active of enhancers instead of alternative TSSs [53]. It is widely accepted that suppresser genes are inactivated and contribute to the development of carcinogenesis [86]. Therefore, Chen and co-workers extended their study and revealed that narrowness of the widest H3K4me3 could be contributed to the attenuation of transcription elongation and expression of tumour-suppressor genes in cancer cells [53]. These current evidences have suggested that the

width of H3K4me3 has the potential to become an epigenetic signature to discover the unknown tumour suppressor genes in the future.

Three years later, Dhar and co-workers reported the knockdown of KMT2D (Histone-lysine N-methyltransferase 2D, also known as MLL4) in mice resulted in the repression of super enhance signals and broad H3K4me3 at the same time inducing medulloblastoma[87]. Remarkably, H3K4me3 widths and super-enhancers of suppresser genes could be decreased via the knockdown of MLL4 while the interplays of broader H3K4me3 as well as super-enhancers were inhibited at the identical genes[87]. Their results also reported that suppresser genes (for instance Dnmt3a, Bcl6), which had the inhibitory effect on activation of Ras-Raf and Notch-mediated signalling pathway severally, could highly upregulated by MLL4[87]. Taken together, all recent studies implied that broad H3K4me3 domains are highly involved in multiple signal pathways that bring about upregulation of suppresser genes as well as downregulation of oncogenes in multiple cancers.

2.3.3 The Association between H3K4me3 and human cancer prognosis

Cancer is a dynamic and heterogeneous disease[88]. This tumour heterogeneity results in the different clinical prognosis of patients[89]. For most of malignant neoplastic diseases including ovarian cancer, prediction of patient outcomes critically relies on the TNM classification of malignant tumours, what means primary tumour size or direct extent (T), degree of spread to lymph nodes (N) and presence of distant metastases(M)[90]. It supplies a standardized, fundamental prognostic evaluation, treatment and stratification of patients in clinical trials. Disease burden and spread are used to predict the survivals as well as determine of approaches and therapeutic strength for most tumour types[90]. Additionally, tumour grade, histological subtype and patient demographics can dramatically ameliorate the accuracy of outcomes or effectiveness of therapies[90]. Recently, novel molecular biomarkers provide new opportunities to predict outcomes and/or options of therapeutic methods. Alteration of the epigenetic landscape is a hallmark of cancer including histone modifications[91]. The association between changes of histone modification patterns and outcomes of tumours has transpired as a dominant tendency in clinic application and transformative investigations. Some data have presented that alterations of H3K4me3 are correlated with patients' outcomes within various types of cancers[92]. Prior results have found that elevated H3K4me3 levels in nucleus are associated with reduced overall survival of hepatocellular[93] and cervical carcinomas[94]. These are consistent with results in breast[95], and oesophageal cancer[96] that patients possessing elevated level of H3K4me3 had poor 5- and 10-year survival rates respectively. However, conflicting data with respect to correlation of H3K4 trimethylation and cancer survivals have been shown in other studies. For example, He Liu *et al.* suggested that patients with combination of elevated H3K4me3 and Wdr82 levels had a significantly improved outcome in human colorectal cancer[97]. It has also reported that positive staining of H3K4me3 is observed in the medulloblastoma patients with better outcomes[98]. In addition, Ellinger and co-workers have found that the global of H3K4me1-3 is inversely linked to Fuhrman grading, pT (primary tumour) stage, distant metastasis in renal cell carcinoma[99]. The combination of H3K4me1, me2 as well as me3 has seen as an independent factor of progression-free survival[99]. Interestingly, H3K4me3 levels had no relation to prognosis of patients in several types of tumours[100-103], although significant differences of H3K4me3 level were showed between cancer tissue and normal tissue. The basic distinguishing features of the including researches are summed up in Table 1. The objectives of our investigations are to evaluate the prognosis value of H3K4me3 in patients with EOC. Moreover, we assess if alterations of H3K4me3 modification are regulated by the activation of vitamin D receptor and GPER or not

Table 1. The basic features of the including studies about H3K4me3 and prognosis of different cancers

No.	Author/Publication year	Country	Tumour Type	No. of Cases	OS HR (95%CI)	Prognostic Impact
1	Berger <i>et al.</i> (2020)	Germany	Breast cancer	235	n/r	Negative
2	He <i>et al.</i> (2011)	China	Hepatocellular cancer	147	3.592 (2.302-5.605)	Negative
3	Ye <i>et al.</i> (2020)	China	Esophageal cancer	100	2.142 (1.058-4.334)	Negative
4	Beyer <i>et al.</i> (2017)	Germany	Cervical cancer	250	n/r	Negative
5	Dubuc <i>et al.</i> (2013)	Canada	Medulloblastoma	220	n/r	Positive
6	Liu <i>et al.</i> (2018)	China	Colorectal tumor	123	2.988 (1.591-5.612)	Positive
7	Ellinger <i>et al.</i> (2010)	Germany	Renal cell carcinoma	193	0.791 (0.497-1.258)	Positive
8	Schneider <i>et al.</i> (2010)	Germany	Muscle-invasive Bladder tumour	127	1.064 (0.963-1.176)	No Significance
9	Ellinger <i>et al.</i> (2010)	Germany	Prostate tumour	113	n/r	No Significance
10	Zhou <i>et al.</i> (2019)	China	Esophageal carcinoma	129	n/r	No Significance
11	Chen <i>et al.</i> (2013)	China	Oral squamous cell carcinoma	186	n/r	No Significance

CI, confidence interval; HR, hazard ratio; OS, overall survival; Negative: a high level of H3K4me3 is associated with poor prognosis; Positive: a high level of H3K4me3 is associated with favourable prognosis.

2.4 Vitamin D receptor (VDR) and H3K4 trimethylation

The nuclear receptor VDR (Vitamin D receptor) is recognised as a transcriptional factor belonging to the steroid nuclei receptor superfamily [104]. The majority of the biological effects of VDR is exerted by stimulation with VDR ligand $1\alpha,25$ -dihydroxyvitamin D_3 ($1,25(OH)_2D_3$), which is commonly known as calcitriol. Generally, VDR and its ligands were deemed to possess a few various effects on epigenetic events [105]. It has been suggested that $1,25(OH)_2D_3$ is capable of influencing DNA methylation and histone modifications so that it may act as a mediator for the human epigenome [105]. In addition, the stimulation with $1,25(OH)_2D_3$ enhances both the level of chromatin accessibility and VDR binding in the human acute monocytic leukaemia cell line THP-1 [106]. One of the important findings in this previous study is that 550 of 23,000 regions with H3K4me3 are remarkably regulated by $1,25(OH)_2D_3$ treatment [106]. In addition,

treatment with $1,25(\text{OH})_2\text{D}_3$ modulates p21 expression through a mechanism involving in the dynamic enrichment of H3K9ac and H3K4me3 at VDR binding sites on the p21 promoter in the non-malignant prostate cells[107]. Increasing evidence has shown that $1,25(\text{OH})_2\text{D}_3$ has an impact on prevention and survival in human cancers. A previous study reported that $1,25(\text{OH})_2\text{D}_3$ has an anti-proliferative effect on triple-negative breast cancer cells through activation of VDR[108]. Moreover, Goeman *et al.* and co-workers suggested that $1\alpha,25(\text{OH})_2\text{D}_3$ contributes to biological processes such as cell growth, angiogenesis and apoptosis through enhancing the H3K4me3 at different target gene promoters [109]. However, the significance of changed H3K4me3 levels after $1\alpha,25(\text{OH})_2\text{D}_3$ treatment in ovarian cancer cells remains unclear.

2.5 Estrogen Receptors and H3K4 trimethylation

Estrogen receptors (ERs) are known to exhibit different effects in EOC and therefore represent potential promising targets for therapy. At present, three estrogen receptors ($\text{ER}\alpha$, $\text{ER}\beta$ and GPER) have been investigated in relation to EOC [110]. Estrogen receptor alpha ($\text{ER}\alpha$) was identified in the 1960s at first time[111], and estrogen receptor beta ($\text{ER}\beta$) was found in 1990s[112]. $\text{ER}\alpha$ and $\text{ER}\beta$ are two transcription factors of a large family of nuclear receptors[113]. It has demonstrated to mediate the transcription of some oestrogen responsive genes through different estrogenic response elements[114]. Previous study has reported that $\text{ER}\alpha$ action is tightly associated with chromatin structure in cell lines via a key determinant FOXA1[115]. As we know, the epigenetic regulation of chromatin structure has been regarded as a highly complex interplay between multiple histone modifiers and histone modification in the downstream[116]. Moreover, a large body of chromatin modifiers and histone modifications have been described in transcriptional regulation, including $\text{ER}\alpha$ -regulated transcription[117]. As commented earlier, H3K4me3 is one of the best-studied histone marks which is regularly observed enriched at promoter regions[118]. Previous analyses have shown that activated endogenous estrogenic responsive TFF1 gene results in promoter recruitment of MEN-1 (multiple endocrine neoplasia type 1) and in elevated level of H3K4me3[117,119]. H3K4me3 was shown to be enriched after estradiol treatment in breast cancer, accompanied with the recruitment of BAP18 (a novel co-activator of $\text{ER}\alpha$) at the promoter regions of oestrogen-induced genes[120].

Unlike $\text{ER}\alpha$, $\text{ER}\beta$ seemingly plays a different role [121]. Studies in EOC or other tissues suggest that $\text{ER}\beta$ has an inhibitory effect on expression and activity of $\text{ER}\alpha$, thereby contributes to the anti-proliferative effects. In a previous study it was demonstrated that activation of $\text{ER}\beta$ greatly impacted early transcription and mRNA splicing in breast cancer cells[122]. It has also been reported that the accumulation of H3K4me3 is induced on $\text{ER}\alpha$ -suppressed genes at the presence of $\text{ER}\beta$, followed by epigenetic activation of transcription of tumour suppressor p53[123]. All these results have indicated that $\text{ER}\alpha$ and $\text{ER}\beta$ are able to stimulate accumulation of H3K4me3, inducing H3K4me3-induced epigenetic activation of transcription of different genes.

GPER (G protein-coupled estrogen receptor 1, also named as GPER) is a novel membrane-bound the G protein-coupled receptor (GPCR) regulating multiple downstream signals into the cells via its trans-membrane domains[124]. GPER was found by multiple groups in the late 1990s as an orphan G-protein-coupled receptor with seven transmembrane domains[125-127]. In 2007, it was named as G-protein-coupled estrogen receptor 1 (GPER)[124]. GPER is responsible for different early estrogen-induced non-genomic signaling events including cAMP elevation, intracellular calcium mobilization, transactivation of EGFR, activation of PI3K/Akt as well as the MAPK pathway [128-130]. Additionally, ERs are involved in extensive post-translational modifications as acetylation and SUMOylation mediating their functions[131]. Given interactions of $\text{ER}\alpha$, $\text{ER}\beta$ and GPER and their signalling pathways, it suggests that activation of GPER results in a complex interplay of transcriptional and non-transcriptional events. Specific GPER activation with agonist G1 induced arrest of cell cycle in G1/M phase and increased phosphorylated histone H3 and caspase-3-mediated apoptosis, resulting in inhibition of cell growth in breast cancer[132]. In another study,

it has been reported that activation of GPER is able to mimic the actions of 17 β -estradiol on estrogenic related receptor α (ERR α) and enrich histone acetylation at distinct ERR α promoter[133]. However, the interplay of GPER and H3K4me3 in cancer biology has not systematically investigated so far.

3.Publication I



International Journal of
Molecular Sciences



Article

H3K4me3 Is a Potential Mediator for Antiproliferative Effects of Calcitriol ($1\alpha,25(\text{OH})_2\text{D}_3$) in Ovarian Cancer Biology

Nan Han ¹, Udo Jeschke ^{1,2,*} , Christina Kuhn ¹, Anna Hester ¹, Bastian Czogalla ¹ , Sven Mahner ¹, Miriam Rottmann ³, Doris Mayr ⁴, Elisa Schmoeckel ⁴ and Fabian Trillsch ^{1,*} 

¹ Department of Obstetrics and Gynaecology, University Hospital, LMU Munich, Marchioninstr. 15, 81377 Munich, Germany; N.Han@med.uni-muenchen.de (N.H.); christina.kuhn@med.uni-muenchen.de (C.K.); anna.hester@med.uni-muenchen.de (A.H.); bastian.czogalla@med.uni-muenchen.de (B.C.); sven.mahner@med.uni-muenchen.de (S.M.)

² Department of Obstetrics and Gynaecology, University Hospital Augsburg, Stenglinstr. 2, 86156 Augsburg, Germany

³ Munich Cancer Registry (MCR), Bavarian Cancer Registry—Regional Center Munich (LGL), Institute for Medical Information Processing, Biometry and Epidemiology (IBE), Ludwig-Maximilians-University (LMU), 81377 Munich, Germany; rottmann@ibe.med.uni-muenchen.de

⁴ Department of Pathology, LMU Munich, Thalkirchner Str. 36, 80337 Munich, Germany; doris.mayr@med.uni-muenchen.de (D.M.); elisa.schmoeckel@med.uni-muenchen.de (E.S.)

* Correspondence: udo.jeschke@med.uni-muenchen.de (U.J.); Fabian.trillsch@med.uni-muenchen.de (F.T.); Tel.: +49-89-4400-54240 (U.J.); +49-89-4400-76800 (F.T.)

Received: 5 February 2020; Accepted: 18 March 2020; Published: 20 March 2020



Abstract: Posttranslational histone modification plays an important role in tumorigenesis. Histone modification is a dynamic response of chromatin to various signals, such as the exposure to calcitriol ($1\alpha,25(\text{OH})_2\text{D}_3$). Recent studies suggested that histone modification levels could be used to predict patient outcomes in various cancers. Our study evaluated the expression level of histone 3 lysine 4 trimethylation (H3K4me3) in a cohort of 156 epithelial ovarian cancer (EOC) cases by immunohistochemical staining and analyzed its correlation to patient prognosis. The influence of $1\alpha,25(\text{OH})_2\text{D}_3$ on the proliferation of ovarian cancer cells was measured by BrdU proliferation assay in vitro. We could show that higher levels of H3K4me3 were correlated with improved overall survival (median overall survival (OS) not reached vs. 37.0 months, $p = 0.047$) and identified H3K4me3 as a potential prognostic factor for the present cohort. Ovarian cancer cell $1\alpha,25(\text{OH})_2\text{D}_3$ treatment induced H3K4me3 protein expression and exhibited antiproliferative effects. By this, the study suggests a possible impact of H3K4me3 expression on EOC progression as well as its relation to calcitriol ($1\alpha,25(\text{OH})_2\text{D}_3$) treatment. These results may serve as an explanation on how $1\alpha,25(\text{OH})_2\text{D}_3$ mediates its known antiproliferative effects. In addition, they further underline the potential benefit of $1\alpha,25(\text{OH})_2\text{D}_3$ supplementation in context of ovarian cancer care.

Keywords: ovarian cancer; histone 3 lysine 4 trimethylation (H3K4me3); histone modification; calcitriol; $1\alpha,25(\text{OH})_2\text{D}_3$; prognosis; vitamin D receptor; cell proliferation

1. Introduction

Epithelial ovarian cancer (EOC) is one of the most common malignancies in women, with the highest mortality and a five-year survival rate of less than 45% [1,2]. The main reasons for poor prognosis are the lack of effective screening methods and the late clinical manifestation due to asymptomatic tumor progression in most cases. Primary surgical debulking and subsequent

platinum-based chemotherapy is currently the mainstay of treatment with still a curative intention for advanced ovarian cancer. Recently, antiangiogenic treatment and poly (ADP-ribose) polymerase (PARP) inhibitors could be added as targeted therapies to first-line treatment with significant improvement of progression-free survival (PFS) [3]. However, molecular markers are still missing to tailor systemic treatment and reliable predictors from biologic specimens have not yet been fully elucidated.

Global changes in the epigenetic landscape are one important hallmark of cancer. Posttranslational histone modification is considered as a common phenomenon in tumor progression and one of the earliest events in carcinogenesis [4]. Recently, histone modification patterns have been identified as useful in distinguishing subtypes of cancer patients with distinct clinical outcomes, thereby expanding prognostic capabilities [5]. Heterogeneity in cellular (such as global or bulk) levels of histone modifications can be detected by immunohistochemistry (IHC) assay at the level of whole nuclei of cancer cells in tissue specimens [6]. Meanwhile, immunocytochemistry (ICC) is also applied to confirm histone H3 modification expression in normal and cancer cells [5,7]. Former studies have reported that alteration in the histone modification patterns can provide prognostic information for several cancers, including those detected in colon [8,9], kidney [10,11], lung [5,12], stomach [13], pancreas [14,15], ovary [14], and breast [14,16].

Histone H3 tri methyl K4 (H3K4me3) is one of the most extensively studied patterns of histone modifications, which either contributes to transcription activation or is associated with suppressed gene expression [17,18]. Previous studies have proven prognostic value of H3K4me2/3 for colon cancer [8], renal cell carcinoma [10], and lung and kidney cancer [5]. In ovarian cancer biology, prior studies evaluated the expression and role of H3K4me3 protein indirectly via examining gene sets associated with H3K4me3 marks at transcription start sites [19] or via detection of its methyltransferase and demethyltransferase [20,21]. However, the prognostic significance of H3K4 trimethylation and ovarian cancer remains unclear for now.

Gene regulation mediated by nuclear receptors via chromatin remodelling and histone-modifying complexes is one example of how posttranslational changes may influence tumor growth [22]. A well-characterized example of histone modification mediated by nuclear receptors is that $1\alpha,25(\text{OH})_2\text{D}_3$, known as calcitriol or active form of vitamin D, can regulate histone modification and can inhibit cancer progression through the vitamin D receptor (VDR) [23,24]. Recently, it was reported that $1\alpha,25(\text{OH})_2\text{D}_3$ sensitizes the tumor suppressor p16 in kidney cancer cell lines [25]. Another study suggested that $1\alpha,25(\text{OH})_2\text{D}_3$ induces the expression of histone demethylase JMJD3, thus enhancing trimethylated H3K4 elevated by $1\alpha,25(\text{OH})_2\text{D}_3$ at several target gene promoters in breast cancer epithelial cells [26].

As recently reported, different histone modifications are linked with chemotherapy resistance and become an emerging fields of chemotherapeutic targets [27]. However, for EOC, there is only limited evidence of a relation between histone modification expression and development of platinum resistance to date. Prior analyses have demonstrated that the acquired platinum-resistant cell line PEO4 had significantly different H3K4me3 expression compared to the chemosensitive cell line PEO1 [19]. In another report, there was no difference in H3K4me3 expression. However, H3K4me3 proteins could be suppressed by Trichostatin A and 5-aza-CdR in a A2780/A2780cis cisplatin-resistance cell line model [28].

In order to better understand the prognostic value of H3K4me3 for EOC, we correlated H3K4me3 expression in EOC specimens with their clinical course. Alterations in H3K4me3 expression and cell proliferation following $1\alpha,25(\text{OH})_2\text{D}_3$ treatment in ovarian cancer cell lines were also explored to put the $1\alpha,25(\text{OH})_2\text{D}_3$ expression in the biologic context.

2. Results

2.1. H3K4me3 Staining in EOC Patients

Primary EOC specimens from a total of 156 patients with a median age of 64.0 years (range 33–100 years) and a median follow up of 33.5 months were studied. The median of progression-free survival (PFS) was 22.8 months with a corresponding overall survival (OS) of 40.9 months (range: 0–230.0 months). Of this cohort, a total of 91.7% (142 of 156) samples showed nuclear staining of H3K4me3, while the negative cases and missing cases due to technical failure accounted for 3.2% (5 of 156) and 5.1% (8 of 156), respectively. Among all the positive H3K4me3 staining samples, median Immunoreactive Score (IRS) was 6 (23%, 34 of 148). More specifically, 24 (16.2%) samples were identified with strong immunoreactivity (IRS = 9–12), while 24 (16.2%) samples and 95 (64.2%) samples exhibited weak staining (IRS = 2–3) and moderate staining (IRS = 4–8) (Figure 1). No significant correlation of H3K4me3-expression clinical and pathological parameters was detected (Table 1).

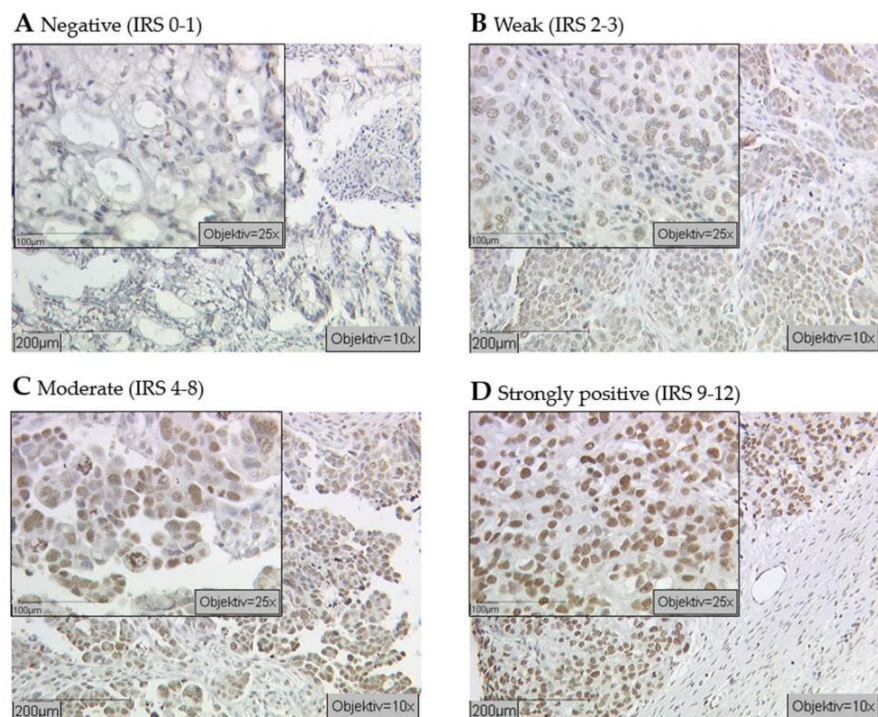


Figure 1. Cellular epigenetic heterogeneity in cancer: Immunohistochemical examination of ovarian cancer tissues with an antibody against histone Histone H3 tri methyl K4 (H3K4me3) revealed different expression levels (indicated by brown staining). Specimens were attributed to negative (A), weak (B), moderate (C), and strongly positive (D) expression levels of H3K4me3 (scale bar 200 µm, small pictures 100 µm).

Table 1. Expression profile of H3K4me3 staining regarding clinical and pathological characteristics.

Parameters	N	H3K4me3 Expression				pValue
		Negative	Weak	Moderate	High	
Histology						
serous	105	2	15	69	19	NS
clear cell	10	0	3	7	1	
endometrioid	20	1	3	7	2	
mucinous	12	2	3	6	2	
Lymph node						
pN0/X	97	5	14	63	15	NS
pN1	51	0	10	32	9	
Overall Survival/months						
<40.9	79	2	16	51	10	NS
≥40.9	69	3	8	44	14	
Grading						
Low	33	3	6	24	5	NS
High	101	2	18	66	15	
FIGO						
I/II	41	3	6	24	8	NS
III/IV	108	2	18	53	16	
Age/years						
<64	70	3	13	42	12	NS
≥64	77	2	11	52	12	

NS = Not significant; FIGO = The International Federation of Gynecology and Obstetrics.

2.2. High H3K4me3 Expression Was Associated with Increased Overall Survival in EOC Patients

We analyzed the correlation between H3K4 trimethylation levels and patient outcomes. As shown in the Kaplan–Meier curve, patients with high expression of H3K4me3 (IRS = 9–12) had improved median overall survival compared to patients with lower levels (median OS not reached vs. 37.0 months, $p = 0.047$, hazard ratio = 0.52, 95% confidence interval = 0.47–0.57) (Figure 2).

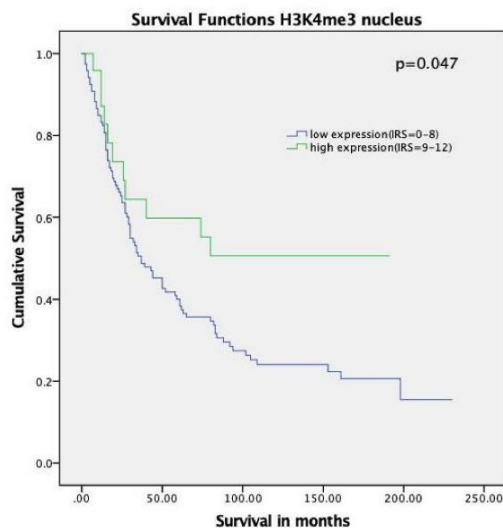


Figure 2. Kaplan–Meier analyses for overall survival: H3K4me3 ($p = 0.047$) with strong expression (Immunoreactive Score (IRS) = 9–12, green) compared to negative, weak, and moderate expression (IRS = 0–8, blue).

2.3. Cox Regression

The multivariate Cox regression analysis of accepted prognostic factors indicated that grading and FIGO stage were independent prognostic factors for the present cohort while H3K4me3 exhibited borderline significance (Table 2).

Table 2. Multivariate analysis.

Covariate	Coefficient (b_i)	HR Exp(b_i)	95% CI for Exp(B)		p Value
			Lower	Upper	
Histology (serous vs. others)	−0.096	0.91	0.70	1.18	0.458
Grade (low vs. high)	1.270	3.56	2.03	6.26	<0.001
FIGO (I, II vs. III, IV)	0.498	1.65	1.03	2.64	0.039
Patients' age (<64 vs. ≥64 years)	−0.108	0.90	0.59	1.37	0.617
H3K4me3 (low vs. high)	−0.623	0.54	0.29	1.00	0.052

CI = confidence interval.

2.4. Co-Expression of VDR and H3K4me3 Protein in Ovarian Cancer Patient Tissue

We further examined the co-expression of VDR and H3K4me3 in ovarian cancer tissues. Double-immunofluorescence in ovarian cancer patients' tissues revealed that H3K4me3 protein is co-localized with VDR. While Histone H3 tri methyl K4 was present in the nuclei, VDR was mainly detected in the cytoplasm (Figure 3).

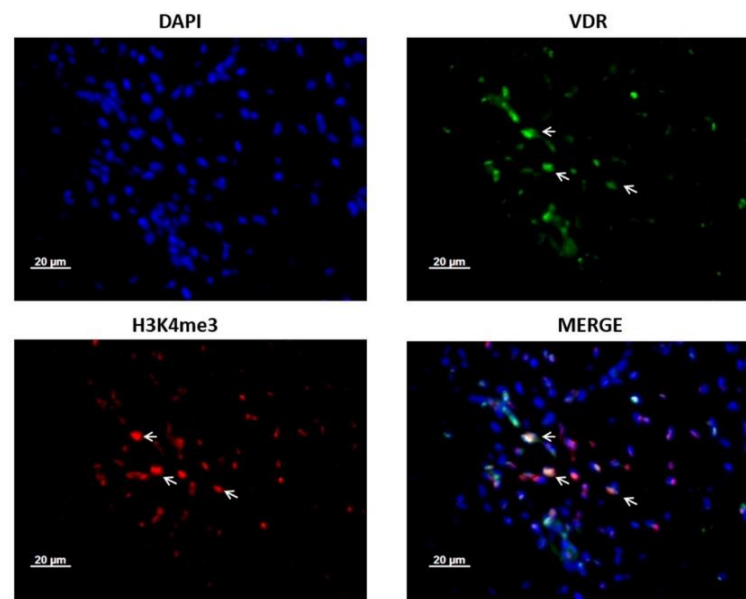


Figure 3. H3K4me3 is co-expressed with vitamin D receptor (VDR) in ovarian cancer patients' tissue. Co-expression of VDR and H3K4me3 proteins is shown with →. Magnification $\times 40$, scale bar = 20 μm . Tissues were co-stained with 4',6-diamino-2-phenylindole (DAPI) (blue), H3K4me3 (red), and VDR (green).

2.5. $1\alpha,25(\text{OH})_2\text{D}_3$ Induced H3K4me3 Expression in A2780 and A2780cis Cell Lines

According to the results of immunocytochemistry (ICC) in epithelial ovarian cancer cell lines, A2780 cells displayed strongly positive immunostaining of H3K4me3 following treatment of 1000 nM $1\alpha,25(\text{OH})_2\text{D}_3$ for 24 h and 48 h (Figure 4A3,B3). The mean optical density (OD) values of nuclear H3K4me3 labeling increased more significantly than in control and lower concentration $1\alpha,25(\text{OH})_2\text{D}_3$ groups ($p < 0.05$ or $p < 0.01$, Figure 4C). Accordingly, staining in A2780 cells (treated by 100 nM $1\alpha,25(\text{OH})_2\text{D}_3$ for 48 h) was higher than in the controls ($p < 0.05$, Figure 4B2,C), but there was no significant change of H3K4me3 expression in the cells treated with 100 nM $1\alpha,25(\text{OH})_2\text{D}_3$ for 24 h (Figure 4A2,C, $p > 0.05$).

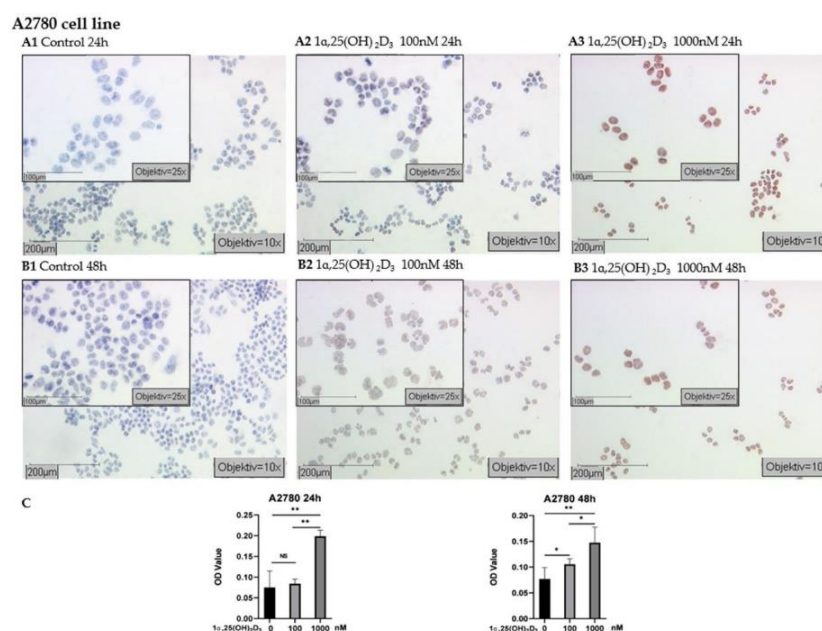


Figure 4. Detection of H3K4me3 with immunocytochemistry in A2780 cell line: (A) representative pictures of H3K4me3 immunocytochemistry staining of A2780 cells treated with $1\alpha,25(\text{OH})_2\text{D}_3$ at different concentrations for 24 h (A1 control; A2 100 nM $1\alpha,25(\text{OH})_2\text{D}_3$; A3 1000 nM $1\alpha,25(\text{OH})_2\text{D}_3$); (B) representative pictures of H3K4me3 immunocytochemistry staining of A2780 cells treated with $1\alpha,25(\text{OH})_2\text{D}_3$ at different concentrations for 48 h (B1 control; B2 100 nM $1\alpha,25(\text{OH})_2\text{D}_3$; B3 1000 nM $1\alpha,25(\text{OH})_2\text{D}_3$) (scale bars 200 μm , small pictures 100 μm); (C) ImageJ-based quantification of immunocytochemistry staining of H3K4me3 in A2780 cell line; NS, no statistical significance ($p > 0.05$); * with statistical significance ($p < 0.05$); ** with statistical significance ($p < 0.01$).

In A2780cis, strongly positive immunostaining was observed in cells treated with 1000 nM $1\alpha,25(\text{OH})_2\text{D}_3$ for 24 h and 48 h (Figure 5A3,B3) and the mean OD value was significantly higher than in the control group (Figure 5C, $p < 0.01$). A2780cis cells receiving 100 nM $1\alpha,25(\text{OH})_2\text{D}_3$ treatment for 48 h displayed no change compared with control (Figure 5C, $p > 0.05$); however, weakly positive staining was visible (Figure 5A2,B2).

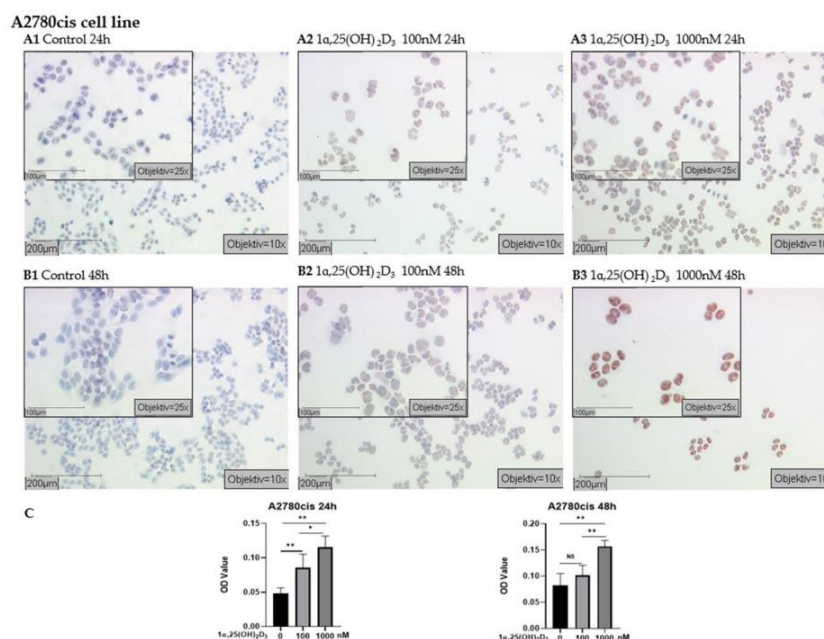


Figure 5. Detection of H3K4me3 with immunocytochemistry in A2780cis cell line: (A) representative pictures of H3K4me3 immunocytochemistry staining of A2780cis cells treated with $1\alpha,25(\text{OH})_2\text{D}_3$ at different concentrations for 24 h (A1 control; A2 100 nM $1\alpha,25(\text{OH})_2\text{D}_3$; A3 1000 nM $1\alpha,25(\text{OH})_2\text{D}_3$); (B) representative pictures of H3K4me3 immunocytochemistry staining of A2780cis cells treated with $1\alpha,25(\text{OH})_2\text{D}_3$ at different concentrations for 48 h (B1 control; B2 100 nM $1\alpha,25(\text{OH})_2\text{D}_3$; B3 1000 nM $1\alpha,25(\text{OH})_2\text{D}_3$) (scale bars 200 μm , small pictures 100 μm); (C) ImageJ-based quantification of immunocytochemistry staining of H3K4me3 in A2780cis cell line; NS, no statistical significance ($p > 0.05$); * with statistical significance ($p < 0.05$); ** with high statistical significance ($p < 0.01$).

2.6. Decreased Proliferation of Ovarian Carcinoma Cells by $1\alpha,25(\text{OH})_2\text{D}_3$

Results of the BrdU assays carried out in $1\alpha,25(\text{OH})_2\text{D}_3$ -treated cells and control cells indicate that the growth of A2780 cells treated with 100 nM $1\alpha,25(\text{OH})_2\text{D}_3$ is inhibited after 48 h ($p < 0.05$), while no significant difference was observed between the untreated control cells and treated cells in the 24 h group ($p = 0.384$). The inhibitory effects on cell proliferation were also observed in the A2780 cell lines exposed to 1000 nM $1\alpha,25(\text{OH})_2\text{D}_3$ (Figure 6, $p \leq 0.005$).

Among the platinum-resistant A2780cis cells treated with 1000 nM $1\alpha,25(\text{OH})_2\text{D}_3$, a growth-promoting effect can be seen in the 24 h group ($p < 0.05$), while the proliferation was inhibited after 48 h ($p < 0.01$). No effects were observed in the A2780cis cells treated with lower concentration (100 nM) of $1\alpha,25(\text{OH})_2\text{D}_3$ (Figure 6, both $p > 0.05$).

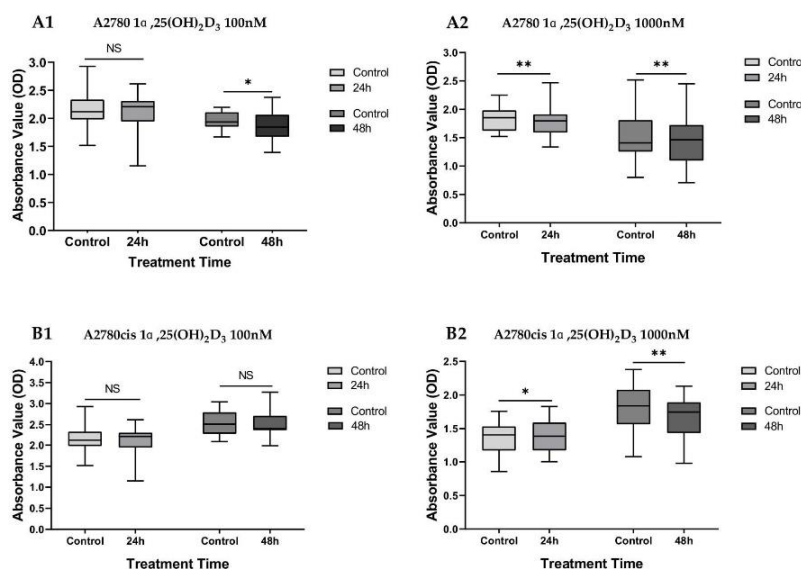


Figure 6. Effects of $1\alpha,25(\text{OH})_2\text{D}_3$ treatment on cell proliferation in A2780 and A2780cis cell lines: Cell proliferation was measured by BrdU incorporation assay (optical density (OD) 450 nm). (A1) A2780 cells treated with 100 nM $1\alpha,25(\text{OH})_2\text{D}_3$ for 24 h and 48 h; (A2) A2780 cells treated with 1000 nM $1\alpha,25(\text{OH})_2\text{D}_3$ for 24 h and 48 h; (B1) A2780cis cells treated with 100 nM $1\alpha,25(\text{OH})_2\text{D}_3$ for 24 h and 48 h; (B2) A2780cis cells treated with 1000 nM $1\alpha,25(\text{OH})_2\text{D}_3$ for 24 h and 48 h. NS, no statistical significance ($p > 0.05$); * with statistical significance ($p < 0.05$); ** with high statistical significance ($p < 0.01$), based on paired-samples T test.

3. Discussion

Within the current analysis, we could demonstrate that a high-level expression of H3K4me3 is associated with better prognosis in EOC patients. In functional studies with ovarian cancer cell lines A2780 and A2780cis, ICC testing revealed that treatment with $1\alpha,25(\text{OH})_2\text{D}_3$ can induce a dose-dependent H3K4me3 expression in ovarian cancer cell lines. Following high-dose $1\alpha,25(\text{OH})_2\text{D}_3$ -treatment, cell proliferation was inhibited in A2780 and A2780cis cell lines underlining the functional significance of this pathway.

Accumulating evidence suggests that histone posttranslational modifications (PTMs) play a crucial role in many key cellular processes including gene transcription, DNA replication, and reparation through alterations in chromatin structure [29] and that aberrant histone modifications could cause various diseases [30,31]. Unlike genetic alterations, changes in histone modifications are reversible and match the dynamic chromatin in nature. According to the “histone code hypothesis”, histone modifications can make considerable impact on chromosome function through distinct mechanisms [32]. For example, histone methyltransferase (classified as “writer”) catalyzes the transfer of methyl groups to lysine and arginine residues of histone proteins and histone demethylase (classified as “eraser”) removes methyl groups from histone protein [33–35]. Some of the modifications like H3K4me2/3, H3K36me, and H3K79 were associated with “open” chromatin and active chromatin, whereas others such as H3K9me, H3K27me, and H4K20me are related to “closed” chromatin and transcriptional repression [36,37]. As a prominent example of the histone modifiers, we have chosen H3K4me3 for the detailed clinical and biologic evaluation in EOC.

The present H3K4me3 expression analysis elucidated that high expression levels are correlated with better clinical outcomes being in agreement with previous observation of the prognostic significance of H3K4me3 in renal cell carcinoma [10]. Kumar et al. reported that H3K4me3 level was significantly decreased in metastasis of renal cell carcinoma and therefore suggested the implication as a biomarker to discriminate metastatic from nonmetastatic tumors [11]. In contrast, other reports suggested that increased H3K4me3 expression was associated with impaired overall survival in various cancers, such as hepatocellular carcinoma [38], cervical cancer [39], and early-stage colon cancer [8]. The discrepancy could be due to the distinct distribution of H3K4me3 expression in various kinds of cancers and even in different stages and histological subtypes of a specific tumor entity. As member of the transcription factor family, VDR can dynamically interact with chromatin components and can therefore potentially mediate the effects of the histone modifications [40]. Therefore, we performed co-immunofluorescence of H3K4me3 and VDR in selected ovarian cancer specimens. Our result displayed obvious co-expression of VDR and H3K4me3 in ovarian cancer. A former study has shown that the level of histone modifications (including H3K4me3) is significantly modulated via enhancing genome-wide the rate of accessible chromatin and vitamin D receptor (VDR) binding by $1,25(\text{OH})_2\text{D}_3$ stimulation [24]. A recent study suggested that the interplay between H3K4 methyltransferase MLL1 and vitamin D pathway could determine cell fate in vitro [41]. Our observation in ovarian cancer patients' tissues coincide with previous studies. Antiproliferative effects of $1,25(\text{OH})_2\text{D}_3$ may involve the mechanisms associated with apoptotic pathway activation and angiogenesis inhibition [42], and the vitamin D receptor was proposed to be crucial for tumor suppression [43]. To further understand the impact of $1,25(\text{OH})_2\text{D}_3$ on the expression of H3K4me3 and cell proliferation, immunocytochemistry and BrdU assay were carried out in ovarian cancer cell lines. Trimethylated H3K4 is a biomarker for transcription initiation and elongation [18]. In the absence of ligands, VDR was shown to interact with corepressor proteins and chromatin-modifying enzymes like histone deacetylase (HDACs) in the deactivation phase [40]. In the activation phase, binding of $1,25(\text{OH})_2\text{D}_3$ leads to alterations in the receptor conformation and access to the binding of co-activators that have histone acetylase activity or are complexed with proteins harboring such activity [40]. Here, we found that $1,25(\text{OH})_2\text{D}_3$ could induce an increased expression of H3K4me3 protein in both the A2780 and A2780cis cell lines and therefore irrespective of the response to platinum treatment.

The Wnt pathway plays an important role in the carcinogenesis of all ovarian cancer subtypes including ovarian cancer stem cells (CSCs) [44] and is considered to promote cancer progression as well as chemoresistance between parental A2780 and platinum-resistant A2780cis cell lines [45,46]. Additionally, some findings indicated that epithelial ovarian cancers may derive from a subpopulation of $\text{CD44}^+\text{CD117}^+$ and that drug-resistant A2780 cells display ovarian CSC properties [47,48]. It has been reported that calcitriol ($1,25(\text{OH})_2\text{D}_3$) can deplete the ovarian CSCs characterized by $\text{CD44}^+\text{CD117}^+$ by targeting the Wnt signaling pathway [49]. In a former study, DACT3 (a negative regulator of Wnt/ β -catenin pathway) could inhibit Wnt/ β -catenin activity although the activating mark H3K4me3 remained at high levels near the DACT3 transcription start site in colorectal cancer cells [50]. Taken together, these findings could partly explain why A2780 as well as A2780cis had a comparable reaction to $1,25(\text{OH})_2\text{D}_3$ treatment with an induced H3K4me3 expression. However, the correlation and the relevance of H3K4me3 to Wnt pathway in ovarian cancer cells will require further research in the future.

Additionally, our results were consistent with findings from Goeman et al., who suggested that $1,25(\text{OH})_2\text{D}_3$ increased the trimethylation of H3K4 at target gene promoters, and the expression of the targeted gene in breast cancer cells was upregulated after treatment with $1,25(\text{OH})_2\text{D}_3$ [26]. Menin, which is a putative tumor suppressor and an integral part of MLL1 and MLL2 histone methyltransferase complexes [51,52], has been suggested to directly interact with VDR and to enhance the transcriptional activity of the receptor [53]. Therefore, histone methyltransferases of H3K4me3 might be absorbed by activated VDR, thus increasing the level of trimethylated H3K4.

Our study indicates that $1\alpha,25(\text{OH})_2\text{D}_3$ has antiproliferative activity on ovarian cancer cells, irrespective from the resistance pattern, mainly at a higher dose for a longer treatment period. This appears in line with the observations found in OVCAR-3 cell line [54], indicating the impact of $1\alpha,25(\text{OH})_2\text{D}_3$ on cell proliferation varied by concentration and treatment time. A high dosage of $1\alpha,25(\text{OH})_2\text{D}_3$ decreased the proliferative activity through G_0/G_1 arrest [55] and upregulation of the cyclin-dependent kinase inhibitor 1A (CDKN1A, known as p21) [56].

In A2780 and A2780cis cells, strongly increased expression of H3K4me3 was accompanied by inhibited activity of $1\alpha,25(\text{OH})_2\text{D}_3$, which is in line with the observation that only upregulated genes after $1\alpha,25(\text{OH})_2\text{D}_3$ treatment show a concurrent significant increase of H3K4me3 at their transcriptional start site [26].

Based on the results of the current study, we assume that H3K4me3 has a pivotal role in mediating the already accepted antiproliferative ability of $1\alpha,25(\text{OH})_2\text{D}_3$ in ovarian cancer biology. The demonstrated relation between H3K4me3 and $1\alpha,25(\text{OH})_2\text{D}_3$ could explain how calcitriol exhibits its effects on tumor suppression and underlines the potential benefit of calcitriol supplementation in context of ovarian cancer care.

4. Materials and Methods

4.1. Patients and Tissue Microarray

The tissue microarray was conducted with 156 EOC tissue specimens obtained from patients who underwent surgery for EOC in the Department of Obstetrics and Gynecology of the Ludwig-Maximilians-University Munich between 1990 and 2002. Clinical data was derived from patient charts and follow-up data was obtained from Munich Cancer Registry. All samples were prepared by formalin fixation and paraffin embedding (FFPE). Three representative tissues were taken from each patient for the microarray analysis to obtain a more accurate image of EOC.

4.2. Ethics Approval

All epithelial ovarian cancer specimens were derived from the archives of the Department Gynecology and Obstetrics in LMU Munich, which were initially applied for pathological diagnostics. In all cases, the diagnostic procedures were completed before the current study was performed. Our study was approved by the Ethics Committee of the Ludwig-Maximilians-University (Date: 30 September 2009; approval number: 227-09; Munich, Germany). All experiments in this study were conducted in accordance with the Declaration of Helsinki. The authors were blind to patient information throughout the trial.

4.3. Immunohistochemistry

The paraffin-embedded and formalin-fixed samples from 156 EOC patients were used to construct a tissue microarray (TMA). Sections of 3 μm were cut from the TMA block and prepared for immunohistochemical (IHC) staining. Deparaffinization was conducted by using xylene, and the samples were rehydrated with ethanol at a descending concentration gradient. Endogenous peroxidase was quenched with 3% hydrogen peroxide in methanol at room temperature. The sections were placed in citrate buffer (pH = 6.0) and heated for 5 min at boiling temperature in a pressure cooker to retrieve the antigen. After cooling for 5 min, the sections were washed with distilled water and phosphate buffered saline solution (PBS) buffer. Appropriate blocking solution was applied to avoid nonspecific binding of immunoglobulins on one side to cell membranes or fatty tissue on the other side due to electrostatic charge. Afterwards, primary antibody H3K4me was applied and incubated overnight at 4 °C.

Growth immunohistochemical staining was performed by using post-block reagent and horse raddish peroxidase (HRP)-polymer, followed by substrate-staining with 3,3'-Diaminobenzidine (DAB). Subsequently, the sections were counterstained with haemalun for 2 min. Table 3 further presented

details with regard to the suitable detective systems and corresponding steps. Ultimately, dehydration of the specimens was performed by using ethanol at an ascending concentration gradient. Tissues retrieved from colon and placenta were used as positive and negative controls in immunohistochemical staining.

Immunoreactive score (IRS) was used to evaluate the immunostaining results, which was calculated by multiplying the intensity of staining reaction (0 = no color reaction; 1 = weak reaction; 2 = moderate reaction; and 3 = intense reaction) by the percentage of positive cells (0 = 0%; 1 = 1–10%; 2 = 11–50%; 3 = 51–80%; and 4 = >80%). The calculated IRS ranged from 0 to 12, among which 0 indicated no expression of histone and 12 suggested strong expression of histone (Table 3). Positive as well as negative controls were included (Figure A1).

Table 3. IRS classification scoring systems.

Intensity of Staining	Percentage of Positive Cells	IRS (0–12)
0 = no color reaction	0 = no positive cells	0–1 = negative
1 = mild reaction	1 = <10% of positive cells	2–3 = weak
2 = moderate reaction	2 = 10–50% positive cells	4–8 = moderate
3 = intense reaction	3 = 51–80% positive cells	9–12 = strong positive
	4 = >80% positive cells	

IRS: Immunoreactive Score.

4.4. Double Immunofluorescence Staining

For the characterization of H3K4me3 and VDR expression in ovarian cancer, double immunofluorescence was applied by same the paraffin-embedded slides ($n = 4$). Paraffin-embedded slides (3 μm thick) were dewaxed in Roticlear for 20 min and washed in a descending ethanol series (100%, 70%, and 50%). Slides were heated in a pressure cooker using sodium citrated buffer (pH = 6.0), including 0.1 M citric acid and 0.1 M sodium citrate in distilled water. After cooling and washing in PBS buffer, slides were blocked with Ultra V Block (Lab Vision, Fremont, CA, USA) for 15 min at room temperature and then incubated with primary antibodies overnight at 4 °C. Both primary antibodies were diluted with a diluting medium (Dako, Hamburg, Germany) according to the following ratios: 1:100 for rabbit anti-Histone H3 tri methyl K4 IgG (Abcam, ab8580) and 1:100 for mouse anti-vitamin D receptor monoclonal IgG2a (Bio-Rad, MCA3543Z). After washing, slides were incubated with Alexa Fluor 488-/Cy3-labeled antibodies (Dianova, Hamburg, Germany) as fluorescent secondary antibodies for 30 min at room temperature in darkness. Alexa Fluor 488- and Cy3-labeled secondary antibodies were at dilutions of 1:100 and 1:500 in Dako, respectively. Finally, the slides were embedded in mounting medium for fluorescence with 4',6-diamino-2-phenylindole (DAPI, Vectastain, Vector Laboratories, Burlingame, CA, USA) for blue staining of the nucleus after washing and drying. Digital photos were taken with a digital camera system (Axiocam; Zeiss CF20DXC; KAPPA Messtechnik, Gleichen, Germany) and digitally saved.

4.5. Cell Lines and Treatment

The human endometrioid ovarian carcinoma cell line A2780 and its platinum-resistant variant A2780cis were obtained from European Collection of Cell Cultures. The A2780 cell line was cultured in RPMI1640 (ThermoFisher Scientific, Waltham, MA, USA) with 10% fetal bovine serum. The A2780cis cells were continuously cultivated in presence of cisplatin at a concentration of 10 mg/mL. All cells were incubated in a humidified incubator at 37 °C and 5% CO₂. Calcitriol was purchased from Cayman Chemical Company (Michigan, USA). Cells were treated with 0.1% Dimethyl sulfoxide (DMSO) as vehicle or calcitriol at indicated concentration in RPMI1640 with fetal bovine serum (FBS) (or with cisplatin).

4.6. Immunocytochemistry

Cells were inoculated into a four-well chamber slide (10^5 cells/well) for immunocytochemistry (ICC) analysis. One day after cell inoculation, the medium was replaced by fresh RPMI1640/10% FBS containing vehicle or $1\alpha,25(\text{OH})_2\text{D}_3$ at different concentrations (100 nM and 1000 nM) and the cells were incubated for indicated time periods (24 h and 48 h). After treatment, the slides were washed with PBS for 5 min and fixed with ice-cold 50%-methanol-50%-ethanol solution for 15 min at room temperature (RT). After the samples were air-dried, blocking solution was added to the slides and the cells were incubated for 5 min at RT, after which the blocking solution was drained away. The samples were incubated with anti-H3K4me3 (Abcam, ab8580) 100 μL /slides (1:500 dilution with PBS) for 16 h at 4 °C. Subsequently, the slides were placed in post-block solution for 20 min and HRP-polymer for 30 min at RT. After each session of incubation, the slides were washed in PBS for 5 min. Substrate-staining was performed with aminoethyl carbazole (AEC) for 4 min at RT, and the reaction was stopped in distilled water (Aqua Dest). Then, the counterstaining was carried out with haemalum for 30 s. Finally, the slides were placed in tap warm water and let sit for 4 min. Five visible fields of each immunocytochemistry staining slide were taken photos under a microscope ($\times 40$), and their optical density (OD value) was measured using Image J software v1.52p (National Institutes of Health, USA).

4.7. Cell Proliferation Assay

Quantification of cell proliferation was determined by the BrdU assay (Roche Applied Science, Mannheim, Germany) based on the measurement of a pyrimidine analogue (BrdU) incorporation during DNA synthesis. The experimental steps were carried out in accordance with the manufacturer's instruction. Briefly, A2780 and A2780cis cell lines were inoculated in triplicate into 96-well flat-bottom plates at a density of 5000 cells/well and were treated with vehicle or $1\alpha,25(\text{OH})_2\text{D}_3$ at indicated concentrations (100 nM and 1000 nM) [57] for different time periods (24 h and 48 h). After treatment, cells were labelled with BrdU and incubated for 2 h at 37 °C. After cell fixation, anti-BrdU-POD (100 μL /well) was applied and incubated for 1.5 h, followed by three times of washing with washing solution. Ten minutes after the substrate solution was added to each well, the reaction was stopped by adding 1 M H_2SO_4 (25 μL /well). The absorbance of the samples at the wavelength of 450 nm was determined by ELISA. All experiments were performed in triplicate.

4.8. Statistical Analysis

The nonparametric Mann–Whitney U test was adopted to assess the correlation between histone H3 tri methyl K4 scores and clinical outcomes. The Cox proportional hazard model was used for the multivariate analyses. The overall survival rate was analyzed by the Kaplan–Meier curve, and the difference in survival rate was tested by log-rank test. Mann–Whitney U test was also employed to calculate the statistical significance of OD values among different groups. Comparison of the absorbance values between the treated cell and controls was evaluated by paired-samples T test. A *p* value less than 0.05 was considered as statistically significant. All the statistical analyses were conducted with IBM SPSS 23 (Armonk, NY, USA), and plotting was completed with Graph-Pad Prism 8.02 (v8, La Jolla, San Diego, CA, USA).

5. Conclusions

In this study, we could demonstrate that high-level H3K4me3 expression is associated with improved outcome in patients with EOC. The results suggest that application of $1\alpha,25(\text{OH})_2\text{D}_3$ increases the expression of H3K4me3 and exerts an inhibitory effect on cell proliferation in ovarian cancer cell lines. Therefore, the results may serve as an explanation on how calcitriol exhibits its effects on tumor suppression and underlines the potential benefit of calcitriol supplementation in context of ovarian cancer care.

Author Contributions: Conceptualization, S.M., F.T., U.J., and E.S.; formal analysis, U.J., M.R. and E.S.; funding acquisition, F.T. and U.J.; investigation, N.H., C.K., B.C., A.H., D.M., U.J., and E.S.; methodology, F.T., J.E., D.M., U.J., and E.S.; project administration, F.T. and U.J.; supervision, S.M., D.M., and U.J.; validation, F.T., S.M., D.M., and U.J.; visualization, N.H.; writing—original draft, N.H. and F.T.; writing—review and editing, B.C., A.H., S.M., D.M., U.J., and E.S. All authors have read and agreed to the published version of the manuscript.

Funding: This research was funded by the LMU Munich Medical Faculty. We further acknowledge financial support by China Scholarship Council (CSC) for Han Nan.

Acknowledgments: The authors would like to thank Simone Hofmann for excellent technical support. We further thank Sabina K. Page for proofreading the manuscript as a native speaker of the English language.

Conflicts of Interest: Sven Mahner reports grants and personal fees from AstraZeneca, Clovis, Medac, MSD, PharmaMar, Roche, Sensor Kinesis, Tesaro, and Teva outside the submitted work. Fabian Trillsch has received grants and personal fees from AstraZeneca, Clovis, Medac, PharmaMar, Roche, and Tesaro outside the submitted work. The other authors declare no conflict of interest.

Appendix A

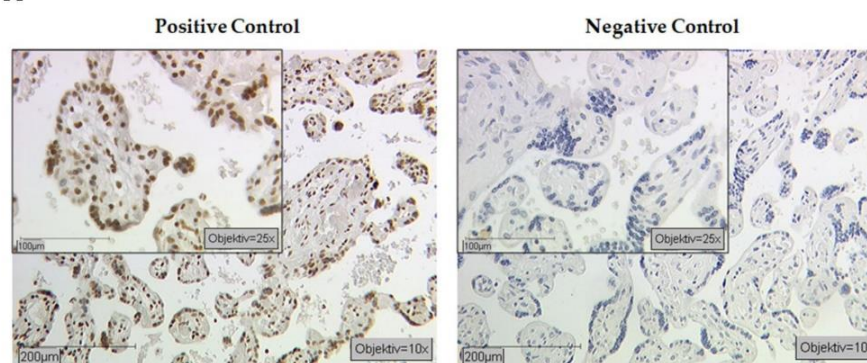


Figure A1. Positive and negative controls of H3K4me3 staining: We used the term placental villous tissue for positive and negative controls.

References

1. Ng, J.S.; Low, J.J.; Ilancheran, A. Epithelial ovarian cancer. *Best Pract. Res. Clin. Obstet. Gynaecol.* **2012**, *26*, 337–345. [[CrossRef](#)] [[PubMed](#)]
2. Webb, P.M.; Jordan, S.J. Epidemiology of epithelial ovarian cancer. *Best Pract. Res. Clin. Obstet. Gynaecol.* **2017**, *41*, 3–14. [[CrossRef](#)] [[PubMed](#)]
3. Schmid, B.C.; Oehler, M.K. Improvements in progression-free and overall survival due to the use of anti-angiogenic agents in gynecologic cancers. *Curr. Treat. Options Oncol.* **2015**, *16*, 2. [[CrossRef](#)] [[PubMed](#)]
4. Jones, P.A.; Baylin, S.B. The fundamental role of epigenetic events in cancer. *Nat. Rev. Genet.* **2002**, *3*, 415–428. [[CrossRef](#)]
5. Seligson, D.B.; Horvath, S.; McBrien, M.A.; Mah, V.; Yu, H.; Tze, S.; Wang, Q.; Chia, D.; Goodglick, L.; Kurdistani, S.K. Global levels of histone modifications predict prognosis in different cancers. *Am. J. Pathol.* **2009**, *174*, 1619–1628. [[CrossRef](#)]
6. Seligson, D.B.; Horvath, S.; Shi, T.; Yu, H.; Tze, S.; Grunstein, M.; Kurdistani, S.K. Global histone modification patterns predict risk of prostate cancer recurrence. *Nature* **2005**, *435*, 1262–1266. [[CrossRef](#)]
7. Crosio, C.; Heitz, E.; Allis, C.D.; Borrelli, E.; Sassone-Corsi, P. Chromatin remodeling and neuronal response: Multiple signaling pathways induce specific histone H3 modifications and early gene expression in hippocampal neurons. *J. Cell Sci.* **2003**, *116*, 4905–4914. [[CrossRef](#)]
8. Benard, A.; Goossens-Beumer, I.J.; van Hoesel, A.Q.; de Graaf, W.; Horati, H.; Putter, H.; Zeebstraten, E.C.; van de Velde, C.J.; Kuppen, P.J. Histone trimethylation at H3K4, H3K9 and H4K20 correlates with patient survival and tumor recurrence in early-stage colon cancer. *BMC Cancer* **2014**, *14*, 531. [[CrossRef](#)]

9. Tamagawa, H.; Oshima, T.; Shiozawa, M.; Morinaga, S.; Nakamura, Y.; Yoshihara, M.; Sakuma, Y.; Kameda, Y.; Akaike, M.; Masuda, M.; et al. The global histone modification pattern correlates with overall survival in metachronous liver metastasis of colorectal cancer. *Oncol. Rep.* **2012**, *27*, 637–642. [[CrossRef](#)]
10. Ellinger, J.; Kahl, P.; Mertens, C.; Rogenhofer, S.; Hauser, S.; Hartmann, W.; Bastian, P.J.; Buttner, R.; Muller, S.C.; von Ruecker, A. Prognostic relevance of global histone H3 lysine 4 (H3K4) methylation in renal cell carcinoma. *Int. J. Cancer* **2010**, *127*, 2360–2366. [[CrossRef](#)]
11. Kumar, A.; Kumari, N.; Sharma, U.; Ram, S.; Singh, S.K.; Kakkar, N.; Kaushal, K.; Prasad, R. Reduction in H3K4me patterns due to aberrant expression of methyltransferases and demethylases in renal cell carcinoma: Prognostic and therapeutic implications. *Sci. Rep.* **2019**, *9*, 8189. [[CrossRef](#)]
12. Barlesi, F.; Giaccone, G.; Gallegos-Ruiz, M.I.; Loundou, A.; Span, S.W.; Lefevre, P.; Kruyt, F.A.; Rodriguez, J.A. Global histone modifications predict prognosis of resected non small-cell lung cancer. *J. Clin. Oncol.* **2007**, *25*, 4358–4364. [[CrossRef](#)] [[PubMed](#)]
13. Park, Y.S.; Jin, M.Y.; Kim, Y.J.; Yook, J.H.; Kim, B.S.; Jang, S.J. The global histone modification pattern correlates with cancer recurrence and overall survival in gastric adenocarcinoma. *Ann. Surg. Oncol.* **2008**, *15*, 1968–1976. [[CrossRef](#)] [[PubMed](#)]
14. Wei, Y.; Xia, W.; Zhang, Z.; Liu, J.; Wang, H.; Adsay, N.V.; Albarracin, C.; Yu, D.; Abbruzzese, J.L.; Mills, G.B.; et al. Loss of trimethylation at lysine 27 of histone H3 is a predictor of poor outcome in breast, ovarian, and pancreatic cancers. *Mol. Carcinog.* **2008**, *47*, 701–706. [[CrossRef](#)] [[PubMed](#)]
15. Manuyakorn, A.; Paulus, R.; Farrell, J.; Dawson, N.A.; Tze, S.; Cheung-Lau, G.; Hines, O.J.; Reber, H.; Seligson, D.B.; Horvath, S.; et al. Cellular histone modification patterns predict prognosis and treatment response in resectable pancreatic adenocarcinoma: Results from RTOG 9704. *J. Clin. Oncol.* **2010**, *28*, 1358–1365. [[CrossRef](#)] [[PubMed](#)]
16. Elsheikh, S.E.; Green, A.R.; Rakha, E.A.; Powe, D.G.; Ahmed, R.A.; Collins, H.M.; Soria, D.; Garibaldi, J.M.; Paish, C.E.; Liber, D.; et al. Global histone modifications in breast cancer correlate with tumor phenotypes, prognostic factors, and patient outcome. *Cancer Res.* **2009**, *69*, 3802–3809. [[CrossRef](#)]
17. Pinskaya, M.; Morillon, A. Histone H3 lysine 4 di-methylation: A novel mark for transcriptional fidelity? *Epigenetics* **2009**, *4*, 302–306. [[CrossRef](#)]
18. Kusch, T. Histone H3 lysine 4 methylation revisited. *Transcription* **2012**, *3*, 310–314. [[CrossRef](#)]
19. Chapman-Rothe, N.; Curry, E. Zellerhistone marks define gene sets in high-grade serous ovarian cancer that distinguish malignant, tumour-sustaining and chemo-resistant ovarian tumour cells. *Oncogene* **2013**, *32*, 4586–4592. [[CrossRef](#)]
20. Jiang, Y.; Lyu, T.; Che, X.; Jia, N.; Li, Q.; Feng, W. Overexpression of SMYD3 in ovarian cancer is associated with ovarian cancer proliferation and apoptosis via methylating H3K4 and H4K20. *J. Cancer* **2019**, *10*, 4072–4084. [[CrossRef](#)]
21. Kuang, Y.; Lu, F.; Guo, J.; Xu, H.; Wang, Q.; Xu, C.; Zeng, L.; Yi, S. Histone demethylase KDM2B upregulates histone methyltransferase EZH2 expression and contributes to the progression of ovarian cancer in vitro and in vivo. *Oncotargets Ther.* **2017**, *10*, 3131–3144. [[CrossRef](#)] [[PubMed](#)]
22. Kishimoto, M.; Fujiki, R.; Takezawa, S.; Sasaki, Y.; Nakamura, T.; Yamaoka, H.; Kato, S. Nuclear receptor mediated gene regulation through chromatin remodeling and histone modifications. *Endocr. J.* **2006**, *53*, 157–172. [[CrossRef](#)] [[PubMed](#)]
23. Thorne, J.L.; Maguire, O.; Doig, C.L.; Battaglia, S.; Fehr, L.; Sucheston, L.E.; Heinaniemi, M.; O'Neill, L.P.; McCabe, C.J.; Turner, B.M.; et al. Epigenetic control of a VDR-governed feed-forward loop that regulates p21(waf1/cip1) expression and function in non-malignant prostate cells. *Nucleic Acids Res.* **2011**, *39*, 2045–2056. [[CrossRef](#)] [[PubMed](#)]
24. Nurminen, V.; Neme, A.; Seuter, S.; Carlberg, C. The impact of the vitamin D-modulated epigenome on VDR target gene regulation. *Biochim. Biophys. Acta Gene Regul. Mech.* **2018**, *1861*, 697–705. [[CrossRef](#)]
25. Shen, Y.; Yu, D.; Qi, P.; Wang, X.; Guo, X.; Zhang, A. Calcitriol induces cell senescence of kidney cancer through JMJD3 mediated histone demethylation. *Oncotarget* **2017**, *8*, 100187–100195. [[CrossRef](#)]
26. Goeman, F.; De Nicola, F.; D'Onorio De Meo, P.; Pallocca, M.; Elmi, B.; Castrignano, T.; Pesole, G.; Strano, S.; Blandino, G.; Fanciulli, M.; et al. VDR primary targets by genome-wide transcriptional profiling. *J. Steroid Biochem. Mol. Biol.* **2014**, *143*, 348–356. [[CrossRef](#)]
27. Borley, J.; Brown, R. Epigenetic mechanisms and therapeutic targets of chemotherapy resistance in epithelial ovarian cancer. *Ann. Med.* **2015**, *47*, 359–369. [[CrossRef](#)]

28. Meng, F.; Sun, G.; Zhong, M.; Yu, Y.; Brewer, M.A. Anticancer efficacy of cisplatin and trichostatin A or 5-aza-2'-deoxycytidine on ovarian cancer. *Br. J. Cancer* **2013**, *108*, 579–586. [[CrossRef](#)]
29. Kouzarides, T. Chromatin modifications and their function. *Cell* **2007**, *128*, 693–705. [[CrossRef](#)]
30. Berdasco, M.; Esteller, M. Aberrant epigenetic landscape in cancer: How cellular identity goes awry. *Dev. Cell* **2010**, *19*, 698–711. [[CrossRef](#)]
31. Füllgrabe, J.; Kavanagh, E.; Joseph, B. Histone onco-modifications. *Oncogene* **2011**, *30*, 3391–3403. [[CrossRef](#)] [[PubMed](#)]
32. Chi, P.; Allis, C.D.; Wang, G.G. Covalent histone modifications—Miswritten, misinterpreted and mis-erased in human cancers. *Nat. Rev. Cancer* **2010**, *10*, 457–469. [[CrossRef](#)] [[PubMed](#)]
33. Strahl, B.D.; Allis, C.D. The language of covalent histone modifications. *Nature* **2000**, *403*, 41–45. [[CrossRef](#)] [[PubMed](#)]
34. Jenuwein, T.; Allis, C.D. Translating the histone code. *Science* **2001**, *293*, 1074–1080. [[CrossRef](#)] [[PubMed](#)]
35. Ruthenburg, A.J.; Allis, C.D.; Wysocka, J. Methylation of lysine 4 on histone H3: Intricacy of writing and reading a single epigenetic mark. *Mol. Cell* **2007**, *25*, 15–30. [[CrossRef](#)]
36. Dawson, M.A.; Kouzarides, T. Cancer epigenetics: From mechanism to therapy. *Cell* **2012**, *150*, 12–27. [[CrossRef](#)]
37. Barski, A.; Cuddapah, S.; Cui, K.; Roh, T.-Y.; Schones, D.E.; Wang, Z.; Wei, G.; Chepelev, I.; Zhao, K. High-resolution profiling of histone methylations in the human genome. *Cell* **2007**, *129*, 823–837. [[CrossRef](#)]
38. He, C.; Xu, J.; Zhang, J.; Xie, D.; Ye, H.; Xiao, Z.; Cai, M.; Xu, K.; Zeng, Y.; Li, H.; et al. High expression of trimethylated histone H3 lysine 4 is associated with poor prognosis in hepatocellular carcinoma. *Hum. Pathol.* **2012**, *43*, 1425–1435. [[CrossRef](#)]
39. Beyer, S.; Zhu, J.; Mayr, D.; Kuhn, C.; Schulze, S.; Hofmann, S.; Dannecker, C.; Jeschke, U.; Kost, B.P. Histone H3 acetyl K9 and histone H3 Tri methyl K4 as prognostic markers for patients with cervical cancer. *Int. J. Mol. Sci.* **2017**, *18*, 477. [[CrossRef](#)]
40. Carlberg, C.; Campbell, M.J. Vitamin D receptor signaling mechanisms: Integrated actions of a well-defined transcription factor. *Steroids* **2013**, *78*, 127–136. [[CrossRef](#)]
41. Zhang, H.; Khoa, L.T.P.; Mao, F.; Xu, H.; Zhou, B.; Han, Y.; O'Leary, M.; Nusrat, A.; Wang, L.; Saunders, T.L.; et al. MLL1 inhibition and vitamin D signaling cooperate to facilitate the expanded pluripotency state. *Cell Rep.* **2019**, *29*, 2659–2671. [[CrossRef](#)] [[PubMed](#)]
42. Deeb, K.K.; Trump, D.L.; Johnson, C.S. Vitamin D signalling pathways in cancer: Potential for anticancer therapeutics. *Nat. Rev. Cancer* **2007**, *7*, 684–700. [[CrossRef](#)] [[PubMed](#)]
43. Thorne, J.; Campbell, M.J. The vitamin D receptor in cancer. *Proc. Nutr. Soc.* **2008**, *67*, 115–127. [[CrossRef](#)] [[PubMed](#)]
44. Arend, R.C.; Londoño-Joshi, A.I.; Straughn, J.M.; Buchsbaum, D.J. The Wnt/ β -catenin pathway in ovarian cancer: A review. *Gynecol. Oncol.* **2013**, *131*, 772–779. [[CrossRef](#)] [[PubMed](#)]
45. Pfanckuchen, D.B.; Baltés, F.; Batoool, T.; Li, J.-P.; Schlesinger, M.; Bendas, G. Heparin antagonizes cisplatin resistance of A2780 ovarian cancer cells by affecting the Wnt signaling pathway. *Oncotarget* **2017**, *8*. [[CrossRef](#)]
46. Trillsch, F.; Preinfalk, V.; Rahmeh, M.; Vogel, M.; Czogalla, B.; Burges, A.; Jeschke, U.; Mahner, S. Inhibition of Wnt signaling as therapeutic option in platinum-resistant ovarian cancer. *J. Clin. Oncol.* **2017**, *35*, e17050. [[CrossRef](#)]
47. Zhang, S.; Balch, C.; Chan, M.W.; Lai, H.C.; Matei, D.; Schilder, J.M.; Yan, P.S.; Huang, T.H.M.; Nephew, K.P. Identification and characterization of ovarian cancer-initiating cells from primary human tumors. *Cancer Res.* **2008**, *68*, 4311–4320. [[CrossRef](#)]
48. Han, X.; Du, F.; Jiang, L.L.; Zhu, Y.; Chen, Z.; Liu, Y.; Hong, T.; Wang, T.; Mao, Y.; Wu, X.; et al. A2780 human ovarian cancer cells with acquired paclitaxel resistance display cancer stem cell properties. *Oncol. Lett.* **2013**, *6*, 1295–1298. [[CrossRef](#)]
49. Srivastava, A.K.; Rizvi, A.; Cui, T.; Han, C.; Banerjee, A.; Naseem, I.; Zheng, Y.; Wani, A.A.; Wang, Q.-E. Depleting ovarian cancer stem cells with calcitriol. *Oncotarget* **2018**, *9*. [[CrossRef](#)]
50. Jiang, X.; Tan, J.; Li, J.; Kivimäe, S.; Yang, X.; Zhuang, L.; Lee, P.L.; Chan, M.T.W.; Stanton, L.W.; Liu, E.T.; et al. DACT3 is an epigenetic regulator of Wnt/ β -catenin signaling in colorectal cancer and is a therapeutic target of histone modifications. *Cancer Cell* **2008**, *13*, 529–541. [[CrossRef](#)]

51. Dreijerink, K.M.A.; Mulder, K.W.; Winkler, G.S.; Höppener, J.W.M.; Lips, C.J.M.; Timmers, H.T.M. Menin links estrogen receptor activation to histone H3K4 trimethylation. *Cancer Res.* **2006**, *66*, 4929–4935. [[CrossRef](#)] [[PubMed](#)]
52. Thakker, R.V. Multiple endocrine neoplasia type 1 (MEN1). *Best Pract. Res. Clin. Endocrinol. Metab.* **2010**, *24*, 355–370. [[CrossRef](#)] [[PubMed](#)]
53. Dreijerink, K.M.A.; Varier, R.A.; van Nuland, R.; Broekhuizen, R.; Valk, G.D.; van der Wal, J.E.; Lips, C.J.M.; Kummer, J.A.; Timmers, H.T.M. Regulation of vitamin D receptor function in MEN1-related parathyroid adenomas. *Mol. Cell. Endocrinol.* **2009**, *313*, 1–8. [[CrossRef](#)] [[PubMed](#)]
54. Ahonen, M.H.; Zhuang, Y.-H.; Aine, R.; Ylikomi, T.; Tuohimaa, P. Androgen receptor and vitamin D receptor in human ovarian cancer: Growth stimulation and inhibition by ligands. *Int. J. Cancer* **2000**, *86*, 40–46. [[CrossRef](#)]
55. Carlberg, C.; Seuter, S. The vitamin D receptor. *Dermatol. Clin.* **2007**, *25*, 515–523. [[CrossRef](#)]
56. Liu, M.; Lee, M.H.; Cohen, M.; Bommakanti, M.; Freedman, L.P. Transcriptional activation of the Cdk inhibitor p21 by vitamin D3 leads to the induced differentiation of the myelomonocytic cell line U937. *Genes Dev.* **1996**, *10*, 142–153. [[CrossRef](#)]
57. Abdelbaset-Ismail, A.; Pedziwiatr, D.; Suszynska, E.; Sluczanska-Glabowska, S.; Schneider, G.; Kakar, S.S.; Ratajczak, M.Z. Vitamin D3 stimulates embryonic stem cells but inhibits migration and growth of ovarian cancer and teratocarcinoma cell lines. *J. Ovarian Res.* **2016**, *9*, 26. [[CrossRef](#)]



© 2020 by the authors. Licensee MDPI, Basel, Switzerland. This article is an open access article distributed under the terms and conditions of the Creative Commons Attribution (CC BY) license (<http://creativecommons.org/licenses/by/4.0/>).

4.Publication II



Article

The G-Protein-Coupled Estrogen Receptor (GPER) Regulates Trimethylation of Histone H3 at Lysine 4 and Represses Migration and Proliferation of Ovarian Cancer Cells In Vitro

Nan Han ¹, Sabine Heublein ^{1,2}, Udo Jeschke ^{1,3,*} , Christina Kuhn ^{1,3}, Anna Hester ¹, Bastian Czogalla ¹ , Sven Mahner ¹, Miriam Rottmann ⁴, Doris Mayr ⁵, Elisa Schmoeckel ⁵ and Fabian Trillsch ^{1,*}

- ¹ Department of Obstetrics and Gynaecology, University Hospital, LMU Munich, Marchioninstr. 15, 81377 Munich, Germany; nanh14162@gmail.com (N.H.); sabine.heublein@med.uni-heidelberg.de (S.H.); christina.kuhn@uk-augsburg.de (C.K.); anna.hester@med.uni-muenchen.de (A.H.); bastian.czogalla@med.uni-muenchen.de (B.C.); sven.mahner@med.uni-muenchen.de (S.M.)
- ² Department of Obstetrics and Gynaecology, Heidelberg University Hospital, Im Neuenheimer Feld 440, 69120 Heidelberg, Germany
- ³ Department of Obstetrics and Gynaecology, University Hospital Augsburg, Stenglinstr. 2, 86156 Augsburg, Germany
- ⁴ Munich Cancer Registry (MCR), Bavarian Cancer Registry—Regional Center Munich (LGL), Institute for Medical Information Processing, Biometry and Epidemiology (IBE), Ludwig-Maximilians-University (LMU), 81377 Munich, Germany; rottmann@ibe.med.uni-muenchen.de
- ⁵ Department of Pathology, LMU Munich, Thalkirchner Str. 36, 80337 Munich, Germany; doris.mayr@med.uni-muenchen.de (D.M.); elisa.schmoeckel@med.uni-muenchen.de (E.S.)
- * Correspondence: Udo.Jeschke@med.uni-muenchen.de (U.J.); fabian.trillsch@med.uni-muenchen.de (F.T.); Tel.: +49-89-4400-54240 (U.J.); +49-89-4400-76800 (F.T.)



Citation: Han, N.; Heublein, S.; Jeschke, U.; Kuhn, C.; Hester, A.; Czogalla, B.; Mahner, S.; Rottmann, M.; Mayr, D.; Schmoeckel, E.; et al. The G-Protein-Coupled Estrogen Receptor (GPER) Regulates Trimethylation of Histone H3 at Lysine 4 and Represses Migration and Proliferation of Ovarian Cancer Cells In Vitro. *Cells* **2021**, *10*, 619. <https://doi.org/10.3390/cells10030619>

Academic Editor: Ritva Tikkanen

Received: 17 February 2021

Accepted: 9 March 2021

Published: 11 March 2021

Publisher's Note: MDPI stays neutral with regard to jurisdictional claims in published maps and institutional affiliations.



Copyright: © 2021 by the authors. Licensee MDPI, Basel, Switzerland. This article is an open access article distributed under the terms and conditions of the Creative Commons Attribution (CC BY) license (<https://creativecommons.org/licenses/by/4.0/>).

Abstract: Histone H3 lysine 4 trimethylation (H3K4me3) is one of the most recognized epigenetic regulators of transcriptional activity representing, an epigenetic modification of Histone H3. Previous reports have suggested that the broad H3K4me3 domain can be considered as an epigenetic signature for tumor-suppressor genes in human cells. G-protein-coupled estrogen receptor (GPER), a new membrane-bound estrogen receptor, acts as an inhibitor on cell growth via epigenetic regulation in breast and ovarian cancer cells. This study was conducted to evaluate the relationship of GPER and H3K4me3 in ovarian cancer tissue samples as well as in two different cell lines (Caov3 and Caov4). Silencing of GPER by a specific siRNA and two selective regulators with agonistic (G1) and antagonistic (G15) activity were applied for consecutive in vitro studies to investigate their impacts on tumor cell growth and the changes in phosphorylated ERK1/2 (p-ERK1/2) and H3K4me3. We found a positive correlation between GPER and H3K4me3 expression in ovarian cancer patients. Patients overexpressing GPER as well as H3K4me3 had significantly improved overall survival. Increased H3K4me3 and p-ERK1/2 levels and attenuated cell proliferation and migration were observed in Caov3 and Caov4 cells via activation of GPER by G1. Conversely, antagonizing GPER activity by G15 resulted in opposite effects in the Caov4 cell line. In conclusion, interaction of GPER and H3K4me3 appears to be of prognostic significance for ovarian cancer patients. The results of the in vitro analyses confirm the biological rationale for their interplay and identify GPER agonists, such as G1, as a potential therapeutic approach for future investigations.

Keywords: GPER; H3K4me3; GPER agonist G1; G15; ovarian cancer; cell migration and proliferation; p-ERK1/2

1. Introduction

Epithelial ovarian cancer (EOC) is the fifth leading cause of female cancer-associated death in Western countries [1]. One of the main reasons for the high mortality is delayed diagnosis in the advanced stage, when the cancer is already disseminated within the

abdomen [2]. Given the heterogeneity of ovarian cancer, novel molecular drug targets need to be identified to tailor innovative personalized treatment approaches [3].

Estradiol (E2) is an important determinant of gynecologic malignancies, including ovarian cancer [4,5]. In this context, G-protein-coupled estrogen receptor (GPER) is a new member of the G-protein-coupled receptor (GPCR) family, mediating signals into the cells via its trans-membrane domains [6]. In 2000, a study reported that rapid 17β -estradiol-mediated activation of extracellular signal-regulated kinases (ERKs) was dependent on the protein of an orphan G-protein-coupled receptor with seven transmembrane domains [7]. In 2007, it was named as G-protein-coupled estrogen receptor 1 (GPER) [6]. GPER can initiate many early non-genomic signaling events of estrogen, such as enrichment of cAMP production, intracellular calcium mobilization, transactivation of EGFR and activation of PI3K/Akt as well as the MAPK pathway [8–10]. In GPER- and ER α -positive ovarian cancer cells, EGFR/ERK signaling is activated by 17β -estradiol and the selective GPER ligand G1, respectively; in contrast, however, the progesterone receptor only responds to E2 [11]. It has suggested that a functional interaction between GPER and ER α may exist in tumor cells [12].

Previous studies have demonstrated that activation of GPER inhibits proliferation and migration in different human cancer cell lines [13–15]. Activation of GPER could inhibit the growth of colorectal cancer cells in vivo via sustained ERK1/2 activation [15]. A similar result has been obtained in prostate cancer PC-3 cells, in that activation of GPER maintains phosphorylation of the ERK1/2 level, resulting in the arrest of PC-3 growth [14]. However, controversial results have been reported regarding the role of GPER in ovarian carcinogenesis [16–18]. Previous findings established that GPER stimulated the proliferation, migration and invasion in a ligand-independent manner in ovarian cancer SKOV3 cells [17]. Ignatov et al. elucidated that activation of GPER by G1 (1-[4-(6-bromobenzo [1,3]dioxol-5-yl)-3a,4,5,9b-tetrahydro-3H-cyclopenta[c]quinolin-8-yl]-ethanone), the selective synthetic agonist of GPER, suppressed proliferation of SKOV3 and OVCAR3 cells by inducing cell apoptosis and partially cell cycle arrest and was associated with increased phosphorylation of H3 [19]. The results imply that activated GPER may alter histone modifications in ovarian cancer. Moreover, the GPER selective antagonist G15, with a similar structure to G1, was identified in 2009 [20]. G15 is effective in inhibiting all G1-induced effects tested to date and many 17β -estradiol-mediated effects [6].

In contrast to the phosphorylation, histone H3 trimethylation at lysine 4 (H3K4me3) is a marker for trimethylation at the 4th lysine residue of the histone H3 protein, representing one of the best studied post-translational histone modifications [21]. The H3K4me3 modification is strongly associated with transcriptional initiation and elongation [22]. Different H3K4me3 profiles between cell lines link with transcriptional differences between the cell lines [23]. H3K4me3 is widely recognized as an active promoter that is positively correlated with gene expression [24] and closely involved in the tumor suppressor genes, treatment and prognostic outcome of cancer patients [25–27]. It has been demonstrated that NEK2 promotes proliferation, migration and tumor growth of gastric cancer cells through regulating the level of H3K4me3 [28]. Another study has demonstrated that broad H3K4me3 domains catalyzed by MLL4 (a COMPASS-like enzyme) are linked to transcriptional activation by interacting with super-enhancers at the tumor-suppressor genes in brain cancer cells [29]. Our own data suggests that $1\alpha, 25(\text{OH})_2\text{D}_3$ (calcitriol) is able to induce H3K4me3 expression via vitamin D receptor in ovarian cancer [30]. In addition, an association of H3K4me3 with estrogen receptor α (ER α)-regulated gene transcription has been described [31]. Accumulation of H3K4me3 during ER α -activated transcription has been noted [32], while further studies point out that H3K4me3 expression is increased by ER β stimulation [33]. According to the existing evidence, GPER is considered as a non-classical estrogen receptor [6], which is associated with 17β -estradiol-mediated rapid signaling events and transcriptional regulation [6,12]. However, the interplay of GPER and H3K4me3 in cancer biology has not been systematically investigated so far.

To study the relationship of GPER and H3K4me3 in ovarian cancer, we examined the expression levels of H3K4me3 in ovarian cancer specimens by immunohistochemistry, and followed these results in vitro by thoroughly investigating the effect of GPER in ovarian cancer cells via its specific agonist G1, antagonist G15 and knockdown of GPER expression.

2. Materials and Methods

2.1. Ethics Approval

All epithelial ovarian cancer specimens were derived from the archives of the Department Gynaecology and Obstetrics in LMU Munich, which were initially applied for pathological diagnostics. In all cases, the diagnostic procedures were completed before the current study was performed. Our study was approved by the Ethics Committee of the Ludwig-Maximilians-University (Date: 30 September 2009; approval number: 227-09; Munich, Germany). All experiments in this study were conducted in accordance with the Declaration of Helsinki. The authors were blinded to the patient data throughout the experimental analysis.

2.2. Patients and Tissue Microarray

The tissue microarray was conducted with 156 EOC tissue specimens obtained from patients who underwent surgery for EOC in the Department of Obstetrics and Gynecology of the Ludwig-Maximilians-University Munich between 1990 and 2002. Clinical data was derived from patient charts and follow-up data were obtained from the Munich Cancer Registry. All samples were prepared by formalin fixation and paraffin embedding (FFPE). Three representative tissues were taken from each patient for the microarray analysis to obtain a more accurate image of EOC [34].

2.3. Immunohistochemistry

The paraffin-embedded and formalin-fixed samples from 156 EOC patients were used to construct a tissue microarray (TMA). Sections of 3 μm were cut from the TMA block and immunohistochemical (IHC) staining for GPER and H3K4me3 was performed as previously described [30,35]. The intensity of the expression was evaluated by the immunoreactive score (IRS).

2.4. Chemicals and Cell Culture

G1 (selective GPER agonist, Catalog No.: 3577) and G15 (selective GPER antagonist, Catalog No.: 3678) were purchased from Tocris. Both of them were dissolved with DMSO and stored at $-20\text{ }^{\circ}\text{C}$ according to company protocol.

The human ovarian cancer cell lines Caov3 and Caov-4 were purchased from the American Tissue Culture Collection (ATCC, Wesel, Germany). While Caov-4 is derived from a metastatic site of a 45-year-old female with high-grade serous histology, Caov3 is from the primary tumor of a 54-year-old Caucasian female with adenocarcinoma of the ovary. Both cell lines were routinely cultured in RPMI1640 (ThermoFisher Scientific, Waltham, MA, USA) supplemented with 10% fetal bovine serum (FBS) at $37\text{ }^{\circ}\text{C}$ in a humidified 5% CO_2 air. The medium was changed into phenol red-free RPMI1640 (ThermoFisher Scientific) plus 10% charcoal stripped FBS (Gibco, New York, NY, USA) 24 h before all experiments. Cells were treated with 0.1% (*v/v*) dimethyl sulfoxide (DMSO) as the vehicle.

2.5. MTT Assay

Cell viability was assessed by doing a 3-(4,5-dimethylthiazol-2-yl)-2,5-diphenyltetrazolium-bromide assay (MTT assay). Cells were seeded into 96-well plates at a density of 5.0×10^3 /well in triplicates and incubated for 24 h. After this, cells were treated by a concentration gradient of G1 for 24 h in the incubator, followed by the addition of 20 μL of 5 mg/mL MTT (Sigma-Aldrich Co., St. Louis, MO, USA) to each well for 90 min at $37\text{ }^{\circ}\text{C}$. The culture medium with MTT was

removed. Purple formazan crystals were dissolved in 200 μ L DMSO/well and then mixed thoroughly on the shaker for 5 min at room temperature. The optical density (OD) was read at 595 nm using an Elx800 universal Microplate Reader. The experiments were repeated three times at least. The IC50 values were calculated by GraphPad Prism 8 software.

2.6. siRNA Transfection

Caov3 and Caov4 cells were seeded into 6-well plates until 60–80% confluence before transfection. GPER-specific siRNA (QIAGEN Sciences, Cat.No.1027416, Germantown, MD, USA) or non-specific control siRNA (QIAGEN, Cat.No.1027280) were transiently transfected using Lipofectamin RNAiMAX reagent (Invitrogen, Carlsbad, CA, USA) according to the manufacturer's instructions. The level of GPER protein in transfected cells was analyzed by Western blotting to verify the effect of transfection after 48 h.

2.7. Preparation of Cell Lysates and Western Blot

Western blot analysis was performed with the cell lysates of different groups of treated cells or untreated cells. Then cells were harvested and lysed by RIPA buffer (Sigma-Aldrich, Steinheim, Germany). The protein concentration of the supernatant was determined by Bradford assay. Proteins were separated by electrophoresis in 10% or 12% SDS-PAGE gels and transferred to PVDF membranes. The membranes were incubated overnight at -4 °C with a 1:2000 dilution of GPER antibody (LS-C203019, Lifespan Biosciences, Seattle, WA, USA), 1:1000 dilution of ER α antibody (ab79413, Abcam, Cambridge, UK), 1:200 dilution of ER β antibody (53472, Anaspec, Fremont, CA, USA), 1 μ g/mL dilution H3K4me3 antibody (ab8580, Abcam), 1:2000 dilution of Histone 3 antibody (#4499, Cell Signaling Technology, Danvers, MA, USA), 1:500 dilution of p-ERK1/2 (ab47339, Abcam) or 1:1000 dilution of β -actin antibody (A5441, Sigma, Kawasaki, Japan). Since the Caov3 cell line has been previously published to produce GPER by our institution [35], it was also used as a positive control of GPER in our study. In addition, we utilized the same antibody of GPER as our previous studies [35–38]. Afterwards, the membranes were washed three times and incubated for 2 h with a 1:1000 dilution of the corresponding alkaline phosphatase-conjugated secondary antibodies. Blotting was detected and visualized by BCIP/NBT Color Development Substrate (Promega, Madison, WI, USA).

Images were analyzed by an image analyzer (Molecular Imager[®] Gel DocTM XR+, Bio-rad) using software Quantity One 4.6.7 (Bio-Rad, Munich, Germany). β -actin was used as an endogenous control. Results shown are representative of at least three biological replicates.

2.8. Wound Healing (Scratch) Assay

The wound healing assay was used to evaluate the cell migration of two ovarian cancer cell lines upon treatment. The cells (1×10^6 /well) and siRNA-transfected cells were seeded into 24-well plates, allowed to form a confluent monolayer and serum-starved overnight. A scratch was made by a sterile 200 μ L pipette tip in order to create a denuded gap of constant width. Each well was rinsed once with PBS to remove the detached cells. Cells were exposed to different reagents (serum-free culture medium), including the control with the vehicle, 1 μ M G1, 1 μ M G15, 1 μ M G1 with 1 μ M G15, GPER siRNA with vehicle and GPER siRNA with 1 μ M G1. Cells were incubated at 37 °C in the presence of 5% CO₂. The migrations of the cell lines were monitored at different time points (0 h and 48 h), using an inverse phase-contrast microscope (Leica Dmi1, Leica, Wetzlar, Germany) with a camera (LEICA MC120 HD, Leica, Wetzlar, Germany). The experiments were repeated three times. Finally, an image of the wound area was measured by Image J software. The migration of cells toward the wound was expressed as a percentage of wound closure:

$$\text{The percentage (\%)} \text{ wound closure} = ((A_t = 0 \text{ h} - A_t = \Delta \text{ h}) / A_t = 0 \text{ h}) \times 100\% \quad (1)$$

In our study, $A_t = 0$ h means the area of wound measured immediately after a scratch, and $A_t = \Delta$ h means the area of wound measured 48 h after a scratch.

2.9. BrdU Assay

Cell proliferation was determined by BrdU assay (Roche Applied Science, Mannheim, Germany) based on the measurement of a pyrimidine analogue (BrdU) incorporation during DNA synthesis. The experiments were performed in accordance with the manufacturer's instruction. Briefly, the Caov3 and Caov-4 cell lines were planted in triplicate in 96-well plates (5×10^3 cells/well) and incubated for 24 h in the incubator. To detect the effect of the GPER on the Caov3 and Caov4 cells, GPER-knockdown cells (5×10^3 cells/well) were seeded in triplicate in 96-well plates simultaneously. Cells were treated with different reagents, including the control with the vehicle, 1 μ M G1, 1 μ M G15, 1 μ M G1 with 1 μ M G15, GPER siRNA with vehicle and GPER siRNA with 1 μ M G1. After 24-h of treatment, the cells were labelled with BrdU and incubated for 2 h at 37 °C. Anti-BrdU-POD (100 μ L/well) was added and remained for 90 min at room temperature after cell fixation, followed by washing three times. A total of 8 min after the substrate solution was added to each well, the reaction was stopped by adding 1M H_2SO_4 (25 μ L/well). The absorbance of the samples at 450 nm was measured using an Elx800 universal Microplate Reader. All experiments were repeated in triplicate.

2.10. Statistical Analysis

A Spearman rank test was performed for correlations between the continuous variables. Survival times were compared using the Kaplan–Meier (log-rank) test method. The ROC curve and Youdan index were used to identify an appropriate cut-off [39,40]. All values in vitro were reported as the mean \pm SEM of three independent experiments. Data were analyzed by a two-tailed student's *t*-test between two groups and one-way ANOVA in multiple groups. The statistical analyses were performed using SPSS version 25.0 (IBM, Armonk, NY, USA). A *p*-value of <0.05 was considered to be statistically significant for all analyses.

3. Results

3.1. H3K4me3 Correlates with GPER Expression in EOC

The combination of both GPER and H3K4me3 stainings was technically feasible in 146 of 156 cases (93.6%), including serous (103 of 146 cases, 70%), clear cell (11 of 146 cases, 8%), endometrioid (20 of 146 cases, 14%) and mucinous carcinomas (12 of 146 cases, 8%). Of this cohort, missing cases due to technical failure accounted for 6.4% (10 of 156). According to previous studies of GPER and H3K4me3 localization, GPER staining was predominantly observed in the cytoplasm and membrane in ovarian cancer specimens, while H3K4me3 staining primarily localized within the nuclei of EOC cells (Figure 1). Detailed information of the GPER and H3K4me3 immunoreactive score (IRS) regarding clinical and pathological characteristics have already been reported in recently published data by our group [30,35]. Analyses show that a nuclear H3K4me3 expression is positively correlated with GPER expression ($Rho = 0.177$; $p = 0.033$). Representative staining of GPER and H3K4me3, from the same patient, is shown in Figure 1.

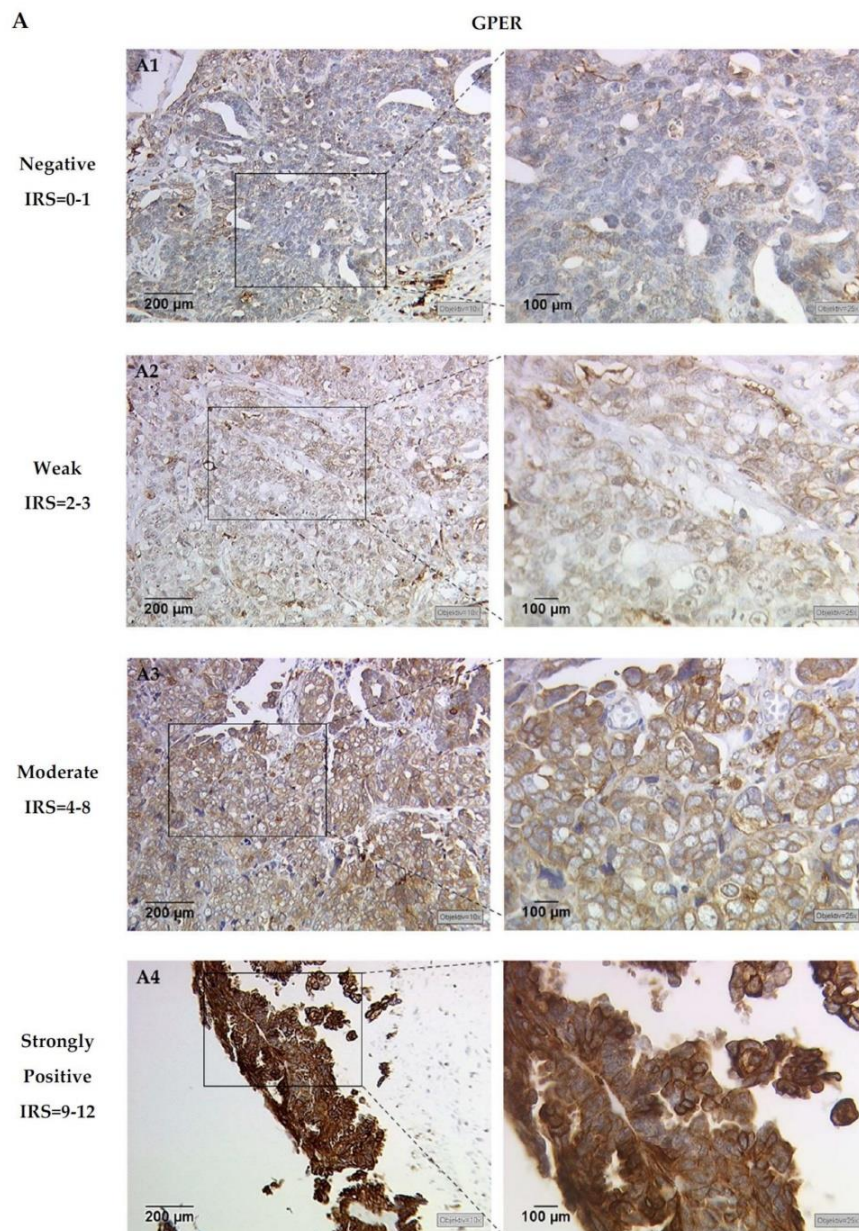


Figure 1. Cont.

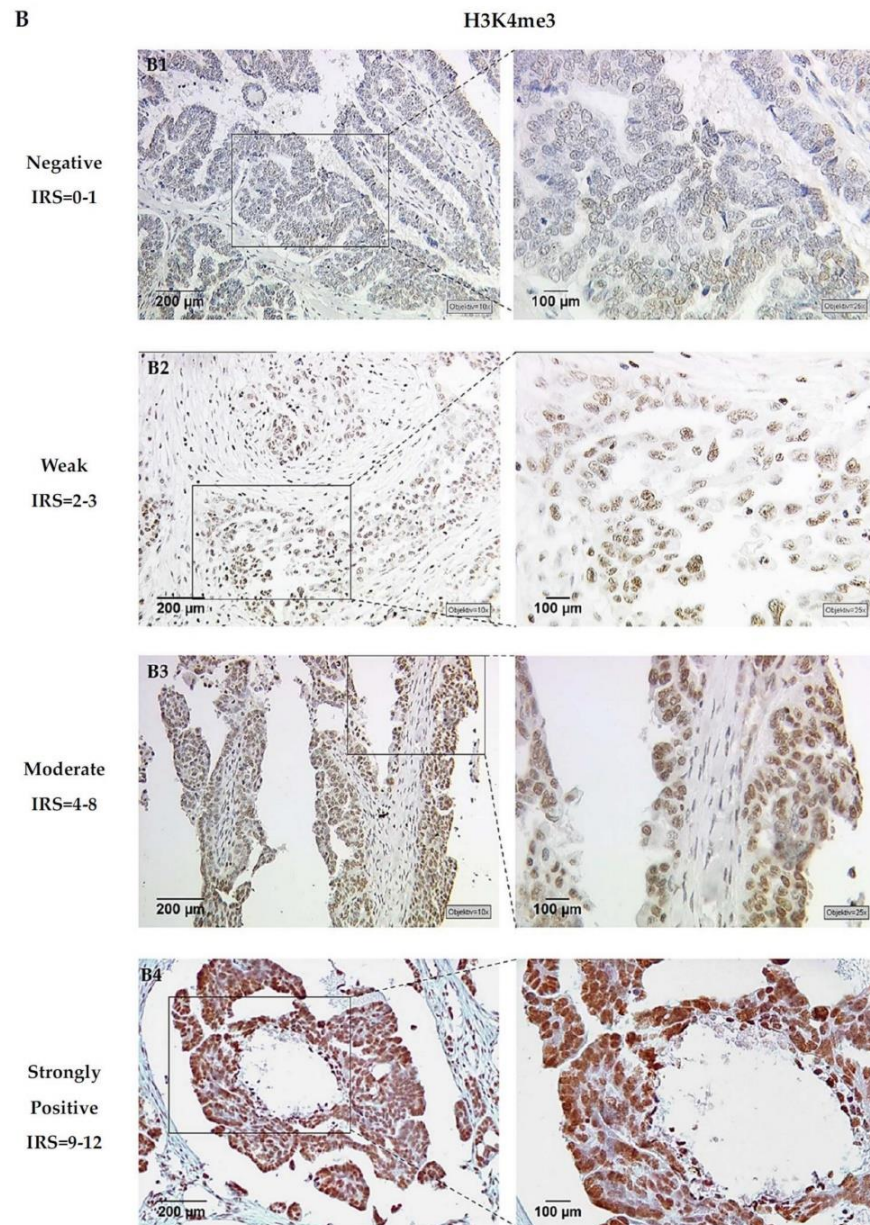


Figure 1. Representative microphotographs of (A) G-protein-coupled estrogen receptor (GPER) and (B) H3K4me3 expression, in the same ovarian cancer patient, are presented. A1 and B1 represent the same patient, and so forth. GPER immunohistochemical staining displays cytoplasm and membranes, while H3K4me3 shows a nucleic staining pattern in ovarian cancer specimens. Specimens were attributed to negative (IRS = 0–1, A1 and B1), weak (IRS = 2–3, A2 and B2), moderate (IRS = 4–8, A3 and B3) and strongly positive (IRS = 9–12, A4 and B4) expression levels of GPER and H3K4me3 (left panel: scale bar = 200 μm; right panel: scale bar = 100 μm).

3.2. H3K4me3 Expression Has Prognostic Impact in GPER Positive EOC Patients

In our previous work, we demonstrated no significant difference in prognosis for EOC patients whether whose tumors expressed GPER or not [35]. To examine the clinical significance of tumors expressing both H3K4me3 and GPER, survival analyses were conducted by the Kaplan–Meier curves with a log-rank test. When cases with higher expression of GPER (IRS = 6–12) were evaluated, strong expression of H3K4me3 (IRS = 9–12) was associated with a favorable prognosis (median overall survival not reached vs. 39.0 months, $p = 0.037$, Figure 2).

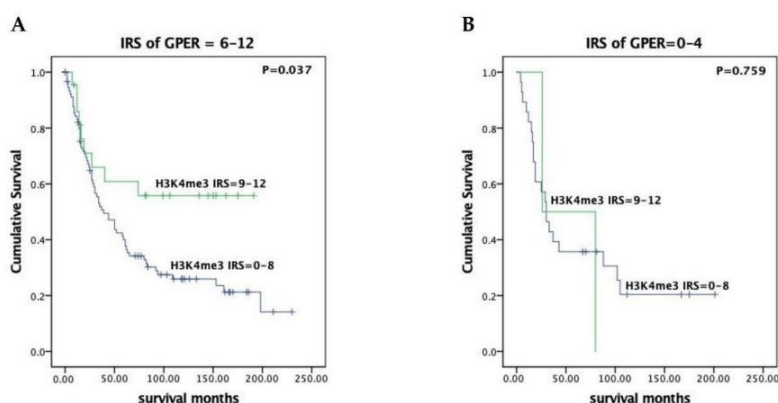


Figure 2. H3K4me3 associated with favorable outcome in higher GPER-expressing (IRS = 6–12) EOC patients. The prognostic significance of H3K4me3 was evaluated in subgroups of patients with high- (IRS = 6–12, (A)) compared to low-level (IRS = 0–4, (B)) GPER expression. Survival of patients with high levels of H3K4me3 expression (IRS = 9–12) (green lines) was compared to those with lower H3K4me3 expression (IRS = 0–8) (blue lines) by the log-rank test and Kaplan–Meier survival analysis. Notably, H3K4me3 predicts significantly better outcome in the subgroup classified as high-level GPER expression (left, (A)) compared to low-level GPER expression (right, (B)).

3.3. Expressions of GPER, ER α and ER β in Caov3 and Caov4 Cell Lines

First of all, we detected the expressions of GPER, ER α and ER β in the Caov3 and Caov4 cell lines by Western blot (Figure 3). MCF-7 breast cancer cells were used as a positive control of ER α and ER β . GPER expression was observed in both of the Caov3 and Caov4 cell lines. Compared with the Caov3 cell line, Caov4 cells expressed a stronger GPER protein (Figure 3C, ** $p < 0.01$). Our result showed that the Caov4 cells expressed strongly the ER α protein; however, the expression of ER α was negative in Caov3 cells (Figure 3B,D). In addition, ER β was not expressed in either of the Caov3 and Caov4 cell lines (Figure 3B).

To confirm that GPER was involved in the G1-induced proliferation and migration of ovarian cancer cells, and in relationship with other protein expressions, we knocked down GPER expression with GPER siRNA. Western blot results showed obvious decreases in GPER expression in the GPER siRNA-transfected groups compared with that of the control groups (Figure 4, ** $p < 0.01$). An increasing level of GPER expression and the decreasing level of GPER expression were found, respectively, after 1 μ M G1 and 1 μ M G15 treatment for 24 h in the Caov3 and Caov4 cell lines (Figure S2).

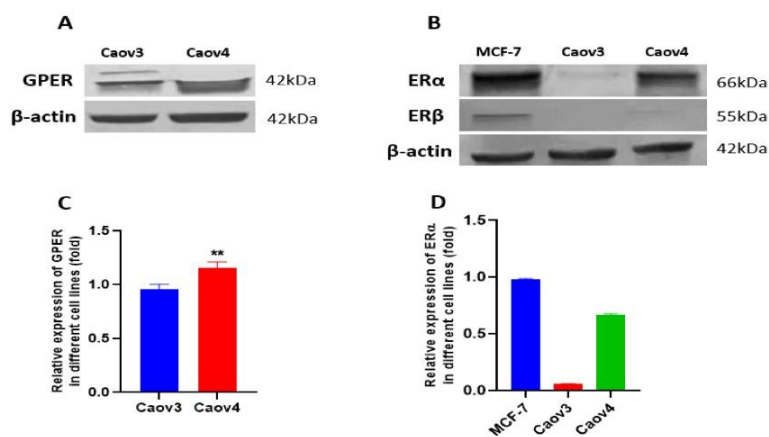


Figure 3. The expressions of GPER, ER α and ER β in Caov3 and Caov4 cell lines. The protein levels of GPER and ER α were detected by Western blot analysis. (A) Representative example of GPER protein expression in Caov3 and Caov4 cells. (B) The ER α and ER β expression in MCF-7 breast cancer cells and in Caov3 and Caov4 ovarian cancer cells. The MCF-7 cell line was seen a positive control of ER α and ER β expressions. (C,D) Histograms represent the ratio of GPER and ER α to β -actin, respectively, as assessed with pooled densitometric data. β -actin was used as a loading control. Each experiment was repeated at least three times. The results are shown as the mean \pm SEM (** $p < 0.01$).

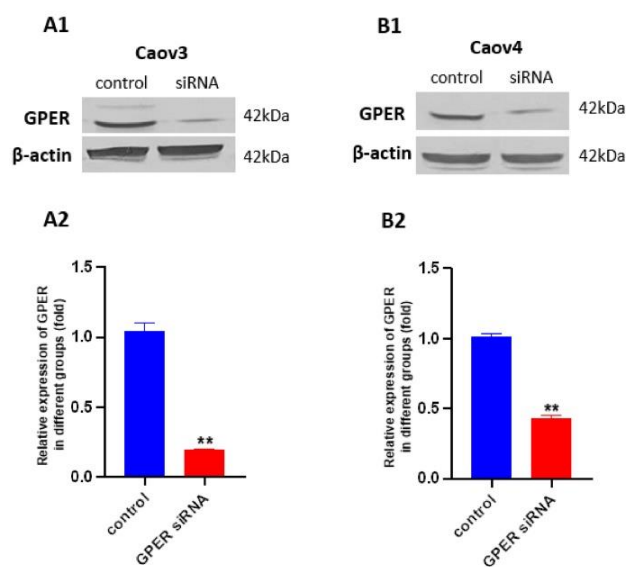


Figure 4. Knockdown of GPER expression with GPER siRNA in Caov3 and Caov4 cell lines. Western blot was used to analysed GPER protein levels after transfection (72 h) with or without GPER siRNA. (A1) Caov3; (B1) Caov4. Histograms compares the presence of GPER expression between control and GPER siRNA groups in Caov3 (A2) and Caov4 (B2) cell lines. Results were from one of three representative experiments and showed as mean \pm SEM (** $p < 0.01$ control group vs. GPER siRNA group).

3.4. IC₅₀ of G1 in Ovarian Cancer Cells

To investigate whether GPER could influence the growth of ovarian cancer cells, Caov3 and Caov4 cells were incubated with increasing concentrations of the GPER-specific agonist G1 for 24 h. A concentration-dependent inhibition of cell viability was observed (Figure 5). The estimated IC₅₀ value was 2.25 μ M and 2.29 μ M for Caov3 and Caov4, respectively. In addition, we also extended our experiments using G36, a newly discovered GPER antagonist, to treat Caov3 and Caov4 cells for 24 h. The results showed that only a very high concentration of G36 could suppress cell viability in Caov3; however, G36 was not able to influence the growth of Caov4 cells (Figure S1). Therefore, 1 μ M was used as an exposure concentration of G1 and G15 (a selective GPER antagonist) to carry out the next experiments of our research.

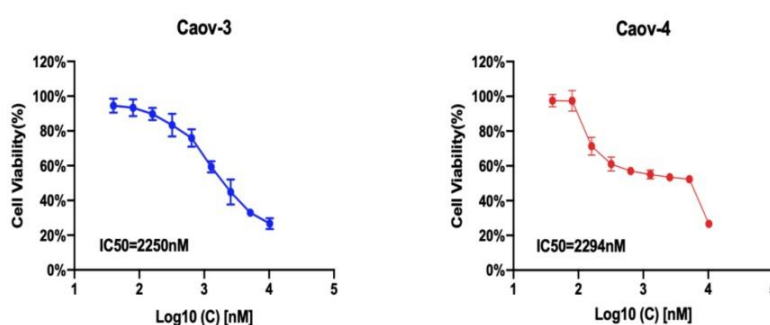


Figure 5. The IC₅₀ value of G1 in different ovarian cancer cell lines. Caov3 and Caov4 cells were treated with gradient concentration of G1 for 24 h and cell viability was detected using an MTT assay. Each experiment was repeated six times ($n = 6$). The results are displayed as the means \pm SD.

3.5. The Selective GPER Agonist G1 Inhibits Cell Proliferation via Activation of GPER in Caov3 and Caov4 Cell Lines

To explore the function of GPER in ovarian cancer cells, we administered 1 μ M G1, 1 μ M G15 and 1 μ M G1 with 1 μ M G15 to ovarian cancer cells and the treatment time was 24 h. Then cell proliferation was detected by using a BrdU assay. Obvious suppression of cell proliferation was observed in Caov3 and Caov4 cell lines after 1 μ M G1 treatment for 24 h (Figure 6, $*** p < 0.001$ vs. control group). Additionally, 1 μ M G15 treatment for 24 h was able to increase cell proliferation of Caov4 cells (Figure 6B, $** p < 0.01$ G15 group vs. control group). G15 had no effect on the Caov3 cell line alone (Figure 6A, $p > 0.05$). Our findings also suggested that G15 played an opposing role on proliferation of Caov4 cells as compared to G1 treatment (Figure 6B, $### p < 0.001$ G1 + G15 group vs. G1 group; $^{\$} p < 0.05$, G15 group vs. G1 + G15 group). In the Caov3 cell line, we did not obtain a significant difference between the G15 group and G1 + G15 group; however, remarkable differences were found between the G1 group and G1 + G15 group (Figure 6A, $## p < 0.01$, G1 group vs. G1 + G15 group). All the results suggested that G15, the selective GPER antagonist, could block the inhibitory action of G1 to cell proliferation in the Caov3 and Caov4 cell lines.

To further explore the involvement of GPER activation in the inhibitory effect of G1 on ovarian cancer cells, we extended our experiments by knockdown of GPER and stimulation of G1 together. We knocked-down GPER with GPER siRNA and then treated the GPER-knockdown cells with 1 μ M G1 for 24 h. There were no statistical discrepancies between the control groups and GPER siRNA-transfected groups in Caov3 and Caov4 cells (Figure 6, $p > 0.05$). It indicated that the GPER-knockdown of Caov3 and Caov4 cells could not inhibit cell proliferation. Significant differences were observed between the G1 groups and GPER siRNA with the G1 groups in both Caov3 and Caov4 cell lines (Figure 6, $## p < 0.01$ and $### p < 0.001$ vs. G1 group, respectively). In addition, there were no

differences between the GPER siRNA groups and GPER siRNA + G1 groups (Figure 6A,B, $p > 0.05$). These results showed that G1 was not able to exert its inhibitory action onto the GPER-knockdown Caov3 and Caov4 cells. Taken together, our results suggest that GPER activation is involved in the G1-induced inhibitory effect on Caov3 and Caov4 cells.

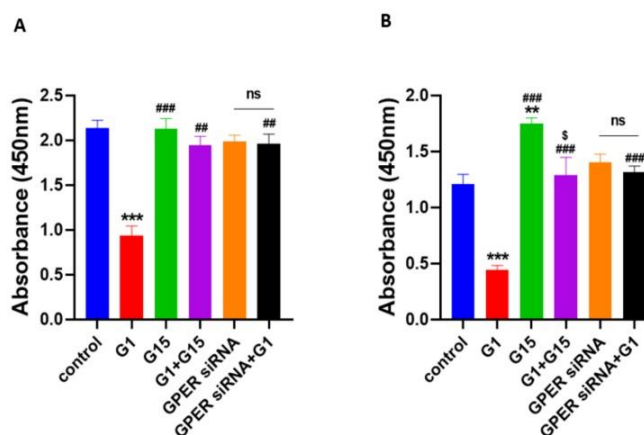


Figure 6. Effects of G1 and G15 treatment on cell proliferation in ovarian cancer cells. Cell proliferation was detected by the BrdU assay. Cells were treated with 1 μ M G1, 1 μ M G15, 1 μ M G1 + 1 μ M G15 and GPER-knockdown cells with the vehicle and GPER siRNA cells with 1 μ M G1 for 24 h. The result was presented as effective absorbance at 450 nm. The histograms are displayed: (A) Caov3, and (B) Caov4. Six study groups in each ovarian cancer cell line were studied: control, 1 μ M G1, 1 μ M G15, 1 μ M G1 + 1 μ M G15, GPER siRNA and GPER siRNA + 1 μ M G1. Each experiment was independently performed at least four times in multiple cultures. The data are represented by the mean \pm SEM. Statistical analyses were performed by one-way ANOVA tests (ns $p > 0.05$, ** $p < 0.01$, *** $p < 0.001$ vs. control; ### $p < 0.01$, ### $p < 0.001$ vs. G1 group; \$ $p < 0.05$ vs. G15 group).

3.6. G1 Suppresses Cell Migration through Activation of GPER in Caov3 and Caov4 Cell Lines

We observed the effects of activated GPER by G1 on cell migration of ovarian cancer cells by the wound healing assay. The M30 apoptosis assay was first carried out to verify that G1-induced alteration of cell migration was not because G1 caused significant cell death. There were no differences found in the Caov3 and Caov4 cell lines (Figure S3). Our data of the wound healing assay demonstrated that 48 h treatment with 1 μ M G1 decreased the migration intensity of the Caov3 and Caov4 cells considerably (Figure 7). To confirm that GPER took part in the regulation of cell migration caused by G1, we knocked down the GPER protein with GPER siRNA and then treated the GPER-siRNA cells with 1 μ M G1 for 48 h. Knocking down the GPER protein of Caov3 and Caov4 cells could not influence their cell migration (Figure 7, $p > 0.05$ vs. control group). Our data displayed that the percentage of wound closure of GPER siRNA with G1 treatment groups were significantly higher than that of the G1 groups in Caov3 (Figure 7A,C, ## $p < 0.01$ G1 group vs. GPER siRNA + G1 group) and Caov4 (Figure 7B,D, ## $p < 0.01$ G1 group vs. GPER siRNA + G1 group) cells. Moreover, no obvious differences between the GPER siRNA groups and GPER + G1 groups were found in the Caov3 and Caov4 cell lines (Figure 7, $p > 0.05$). Our data indicated that 1 μ M G1 led to the inhibition of cell migration via the activation of GPER in Caov3 and Caov4 cells.

We extended our research by using 1 μ M G15 to block the action of G1. No notable differences were found between the control group and G15 group in the Caov3 cell line (Figure 7A,C, $p > 0.05$). In addition, G15 was not able to block the action of G1 in Caov3 cells ($p > 0.05$, G1 group vs. G1 + G15 group). However, 1 μ M G15 caused a great increased

capacity of cell migration in the Caov4 cell line (Figure 7B,D, * $p < 0.05$). Additionally, 1 μM G15 was capable of counteracting the action of G1 in cell migration in Caov4 (Figure 7B,D, ## $p < 0.01$ G1 group vs. G1 + G15 group and \$\$ $p < 0.01$ G15 group vs. G1 + G15 group).

3.7. G1 Treatment Elevates the Levels of ERK1/2 Phosphorylation and H3K4me3 via Activation of GPER

A previous study has reported that phosphorylated ERK1/2 is frequently a common endpoint of activation of GPER [41]. Therefore, we investigated the levels of phosphorylated ERK 1/2 (p-ERK1/2) and H3K4me3 after G1 treatment for the indicated times in order to confirm the GPER pathway was activated by G1. In this study, we found that G1 treatment (30–60 min) was able to rapidly increase the phosphorylation of the ERK1/2 and H3K4me3 levels (Figure 8). The phosphorylation of ERK1/2 and H3K4me3 were maintained for 24 h in both the Caov3 and Caov4 cells (Figure 8).

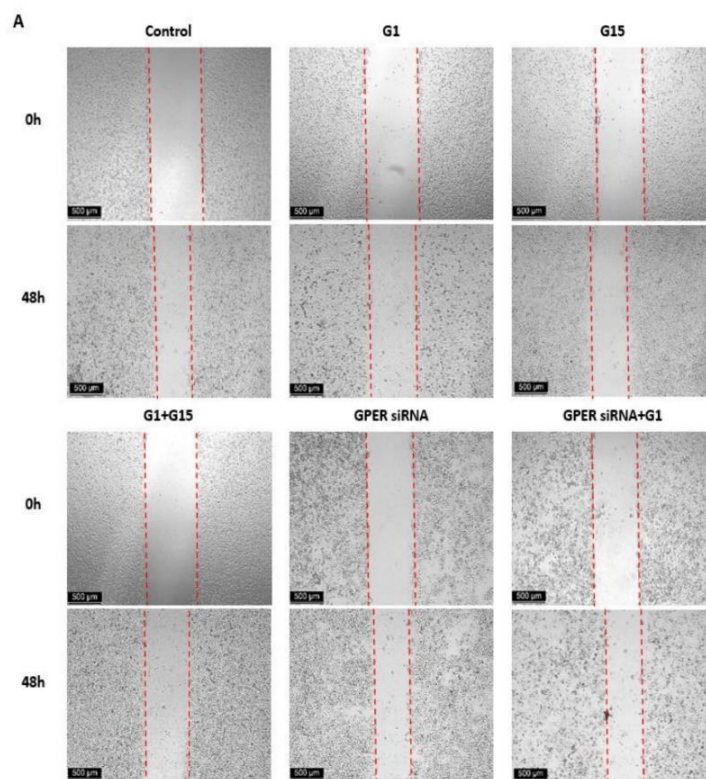


Figure 7. Cont.

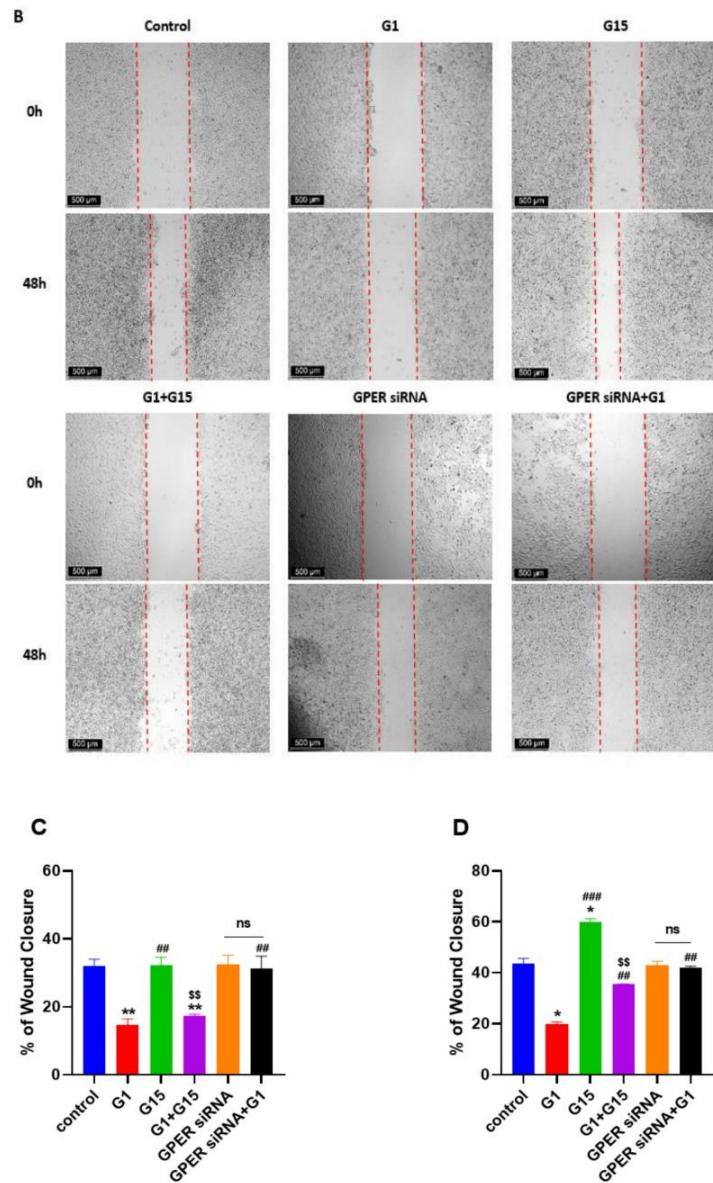


Figure 7. Results of wound healing scratch assay using (A) the Caov3 cell line and (B) the Caov4 cell line. The microscopy images of the wound healing assay at 0 h and 48 h. Six study groups in each ovarian cancer cell line were observed: control, 1 μ M G1, 1 μ M G15, 1 μ M G1 + 1 μ M G15, GPER siRNA group and GPER siRNA + 1 μ M G1. The scale bar at the left lower corner is 500 μ m. Histograms compares the presence of wound closure among the different groups in the Caov3 (C) and Caov4 (D) cell lines. Data were analyzed by ANOVA and a Tukey post-hoc test (* $p < 0.05$, ** $p < 0.01$ vs. control; ## $p < 0.01$, ### $p < 0.001$ vs. G1 group; \$\$ $p < 0.01$ vs. G15 group). The results are presented as the mean \pm SEM of three separate experiments ($n = 3$).

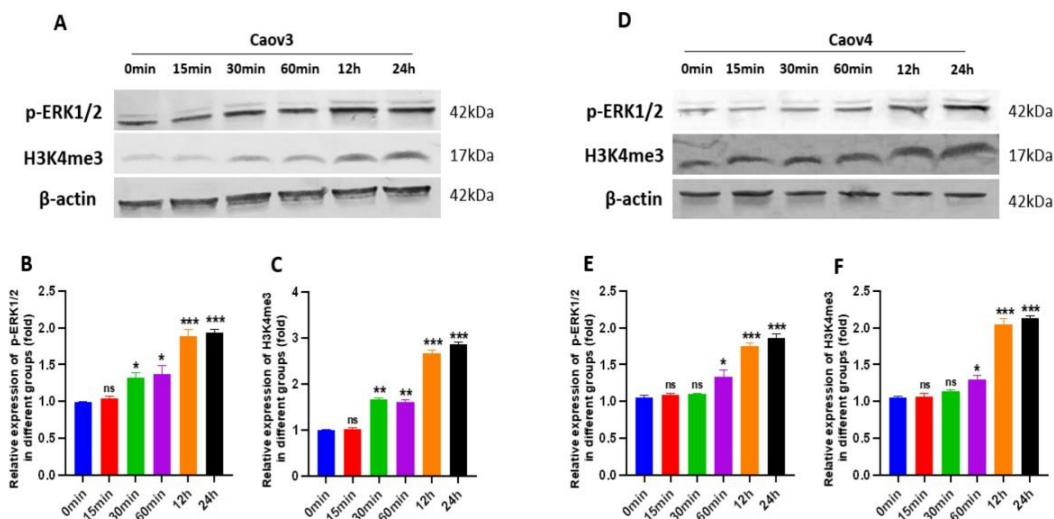


Figure 8. The levels of phosphorylated ERK 1/2 (p-ERK1/2) and H3K4me3 protein were shown. The levels of p-ERK1/2 and H3K4me3 were determined using Western blot analysis. (A–C) Caov3 cells were treated with 1 μM G1 for the indicated times. (D–F) Caov4 cells were treated with 1 μM G1 for the indicated times. β-actin was used as the loading control. The results are presented as the mean ± SEM of three independent experiments ($n = 3$). Data were calculated by an independent *t* test (ns $p > 0.05$, * $p < 0.05$, ** $p < 0.01$ and *** $p < 0.001$).

To confirm GPER was involved in regulation of p-ERK1/2 and H3K4me3, the GPER-specific antagonist G15, G1 + G15, siRNA-specific targeting to GPER and GPER siRNA with G1 were utilized. The levels of p-ERK1/2 and H3K4me3 proteins were investigated by Western blot assay. As shown in Figures 9 and 10, G1 treatment activated p-ERK1/2, as seen by the increased levels of the phosphorylation status. Meanwhile, increasing levels of H3K4me3 protein were found after G1 treatment for 24 h in both cell lines. Knockdown of GPER significantly attenuated phosphorylated ERK1/2, as shown by a significant decrease (Figures 9 and 10, * $p < 0.05$ or ** $p < 0.01$, GPER siRNA group vs. control group). No remarkable differences of p-ERK1/2 and H3K4me3 levels were found between the GPER siRNA and GPER siRNA+G1 group of Caov3 (Figure 9, $p > 0.05$) and Caov4 cells (Figure 10, $p > 0.05$). Furthermore, 1 μM G1 treatment for 24 h was not able to enhance phosphorylated ERK1/2 and H3K4me3 protein of GPER-knockdown Caov3 and Caov4 cells (Figures 9 and 10, ## $p < 0.01$ or ### $p < 0.001$ G1 group vs. GPER siRNA + G1 group). All the results suggested that G1 treatment activated ERK1/2 rapidly and maintained the phosphorylated status for 24 h. At the same time, activation of GPER by G1 elevated the levels of p-ERK1/2 and H3K4me3 in Caov3 and Caov4 cells.

We also used 1 μM G15 and 1 μM G1 + 1 μM G15 to treat ovarian cancer cells for 24 h, respectively, to extend our study. Obviously reduced levels of p-ERK1/2 and H3K4me3 were observed after G15 treatment in Caov4 cells (Figure 10, * $p < 0.05$ or *** $p < 0.001$ vs. control group). G15 had no effect on regulation of p-ERK1/2 and H3K4me3 proteins in the Caov3 cell line. In addition, G15 blocked the enhancement of the p-ERK1/2 and H3K4me4 levels in Caov3 cells (Figure 9A–C) and Caov4 cells (Figure 10A–C). The alteration of H3K4me3 staining was displayed after G1 or G15 treatment for 24 h in Caov3 and Caov4 cells (Figure S4).

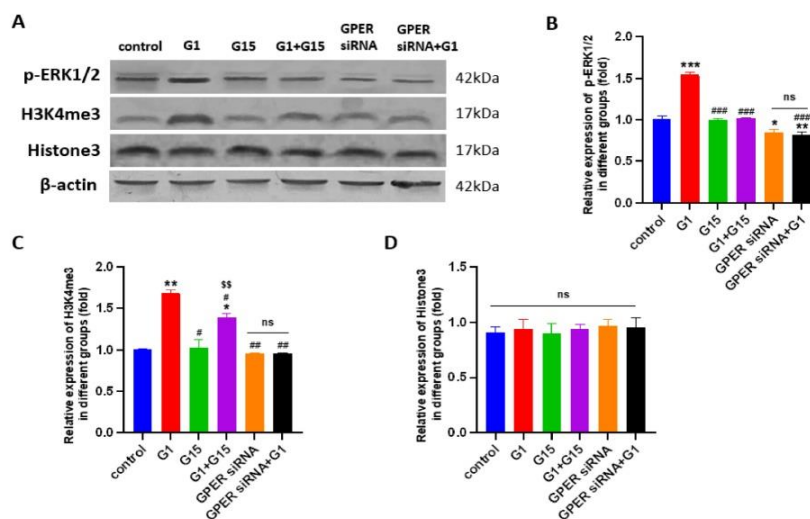


Figure 9. The levels of p-ERK1/2 and H3K4me3 and Histone 3 in Caov3 were detected by Western blot analysis. (A) The Caov3 cells were treated by 1 μ M G1, 1 μ M G15, 1 μ M G1 + 1 μ M G15, GPES siRNA with vehicle and GPES siRNA + G1 for 24 h. Histograms illustrate the ratio of (B) p-ERK1/2, (C) H3K4me3 and (D) Histone3. β -actin was used as the loading control. The results are presented as the mean \pm SEM of three independent experiments ($n = 3$). Data were calculated by one-way ANOVA (ns $p > 0.05$, * $p < 0.05$, ** $p < 0.01$, *** $p < 0.001$ vs. control; # $p < 0.05$, ## $p < 0.01$, ### $p < 0.001$ vs. G1 group; §§ $p < 0.01$ vs. G15 group).

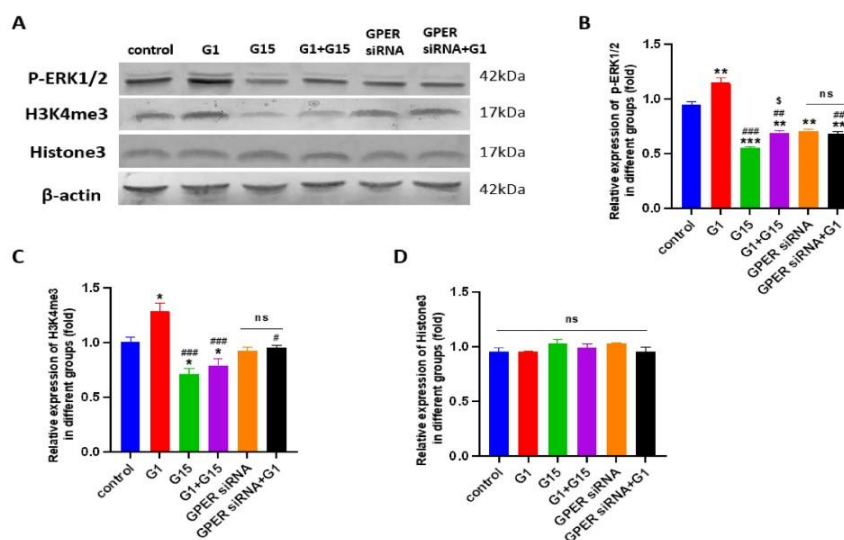


Figure 10. The levels of p-ERK1/2 and H3K4me3 and Histone 3 in the Caov4 cell line were detected by Western blot analysis. (A) The Caov4 cells were treated by 1 μ M G1, 1 μ M G15, 1 μ M G1 + 1 μ M G15, GPES siRNA with vehicle and GPES siRNA + G1 for 24 h. Histograms illustrate the ratio of (B) p-ERK1/2, (C) H3K4me3 and (D) Histone3. β -actin was used as the loading control. The results are presented as the mean \pm SEM of three independent experiments ($n = 3$). Data were calculated by one-way ANOVA (ns $p > 0.05$, * $p < 0.05$, ** $p < 0.01$, *** $p < 0.001$ vs. control; # $p < 0.05$, ## $p < 0.01$, ### $p < 0.001$ vs. G1 group; § $p < 0.05$ vs. G15 group).

4. Discussion

In our study, we elucidated a positive correlation between GPER and H3K4me3 in EOC patients. High expression of both GPER and H3K4me3 was associated with a favorable prognosis. Using *in vitro* experimental models, we demonstrated that the G1 treatment significantly inhibited the proliferation and migration of Caov3 and Caov4 cells, and increased the levels of p-ERK1/2 and H3K4me3 proteins via activation of GPER (Figure 11). Conversely, GPER antagonist G15 was able to block the inhibitory effect of G1 on cell proliferation and migration and induce the attenuation of H3K4me3 protein in the Caov4 cell line. We therefore proposed that activated GPER induced H3K4me3 expression and therapeutic approaches addressing this interplay might have the potential to reduce of migration and growth of ovarian cancer cells impacting the clinical behavior of the disease.

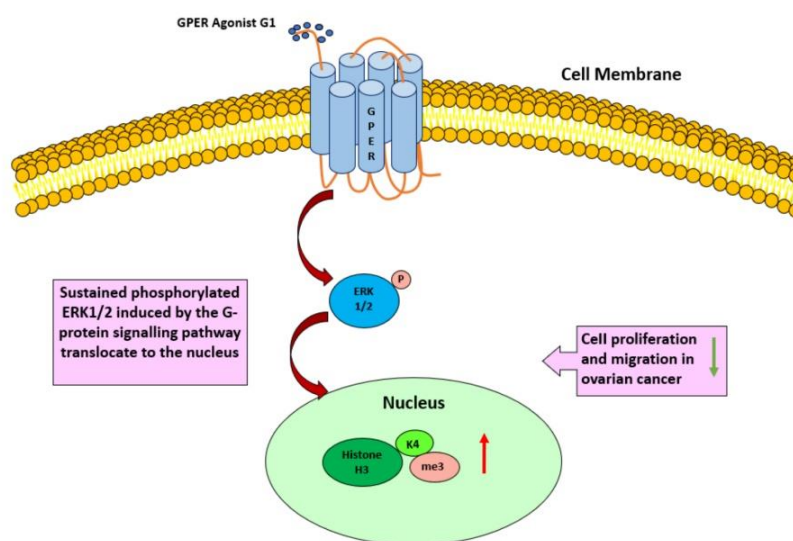


Figure 11. A proposed model to illustrate that activation of GPER by the selective agonist G1 regulates the level of p-ERK1/2 and H3K4me3, along with inhibition of cell proliferation and migration in ovarian cancer cells.

At present there have been several reports about GPER and clinical outcomes of ovarian cancer patients, providing very confusing and controversial results. Smith and co-workers found that the GPER expression was linked to lower survival rates in ovarian cancer [42]. However, the contrary result was observed in another study, which suggested a loss of GPER expression during ovarian tumorigenesis and that GPER expression was associated with a favorable clinical outcome [19]. A previous study in our institution reported that, in EOC tissue, GPER was related to prolonged overall survival in FSHR (follicle stimulating hormone receptor)/LHCGR (luteinizing hormone receptor)-negative patients [35]. Trimethylation of histone H3 lysine 4 (H3K4me3) is a well-known modification linked to gene transcription and enriched in gene promoters [22]. The prognostic relevance of H3K4me3 modification has been reported by others in different human cancers. Recent studies demonstrated that the increased expression of H3K4me3 was associated with an improved prognosis in bladder and renal cell carcinomas [43,44]. The opposite results were also reported, in that a higher level of H3K4me3 was correlated with a worse prognosis in hepatocellular cancer [45] and breast cancer [46]. In our study, our data revealed the first time that GPER was positively related with H3K4me3 expression and a higher level of H3K4me3 in combination with GPER was associated with a better prognosis outcome.

Our result was partly consistent with the previous results. These discrepancies might be explained by different patterns of GPER and H3K4me3 in different types of cancers and in various histologic types of some cancers. The heterogeneity of H3K4me3 was also proved in different cell lines, as colorectal cancer cells expressed obviously lower levels of H3K4me3 than normal cells [47], whereas gain of H3K4me3 was remarkably collected with late-stage breast cancer cells [46]. A previous study showed that the low level of H3K4me3 was associated with adverse clinical-pathological parameters and correlated with patients' outcome in renal cell carcinoma [44]. Moreover, a recent study suggested that broad H3K4me3 was able to result in activation of tumor suppressor genes and repression of oncogenes [25]. Therefore, we assumed that activation of GPER might increase the level of H3K4me3 and, in the meanwhile, suppress the growth of ovarian cancer cells.

In agreement with the expression analyses, controversial results regarding the role of GPER were shown in different cancer cell lines. Our results in demonstrating the inhibitory effects of G1 on cell proliferation and migration of Caov3 and Caov4 cells (Figure 5) are consistent with the observations released in other ovarian cancer models; however, they are inconsistent with other studies that reported GPER promoted growth of the SKOV3 [17] and OVCAR5 [18] cell lines. The contradictory results might be due to the utilization of agonists or antagonist of different specificities, such as estrogen and 1,3-Bis(4-hydroxyphenyl)-4-methyl-5-[4-(2-piperidylethoxy)phenol]-1H-pyrazole dihydrochloride (MPP), in their studies, as compared to the use of the specific agonist G1 and antagonist G15 of GPER in our study. Interestingly, a recent study reported that G1 treatment suppressed proliferation and induced apoptosis of KGN cells (a human ovarian granulosa cell tumor cell line) in a GPER-independent manner [16]. This surprised observation was probably explained that tremendous heterogeneity was exhibited among different ovarian cancer cell lines [48,49]. Therefore, alteration of GPER expression was detected after G1 and G15 treatment for 24 h in our study. As Figure S2 shown, the level of GPER was increased by G1 treatment, and G15 treatment decreased GPER expression in Caov3 and Caov4 cells.

GPER (G-protein-coupled estrogen receptor) was discovered as a member of the G-protein-coupled receptor (GPCR) family [50]. The activation of GPER could regulate the activities of multiple downstream signals, such as PI3K/Akt and EGFR/ERK signaling [10]. A previous study suggested that ERK1/2 was a reliable marker of agonist-mediated GPCR and used to measure the functional outcome of receptor stimulation [51]. Additionally, regardless of the signaling pathway, phosphorylated ERK1/2 was typically regarded as a common endpoint of activation for GPER [41]. Our data revealed that G1 treatment rapidly increased p-ERK1/2 and could sustain the p-ERK1/2 level for 24 h. Similar results were also observed in breast [52], prostate [14] and adrenocortical cancer cells [53]. Furthermore, the level of H3K4me3 was promoted by G1 treatment in a time-dependent manner. All the results suggest that, in our study, GPER and its downstream targets were indeed activated by G1 treatment for 24 h.

A previous study by others suggested that a functional interaction between GPER and ER α might occur when the tumor cells expressed both of the receptors [12]. As Caov4 expressed ER α as well as GPER (Figure 3), it was difficult to pinpoint which of both receptors was responsible for regulating the signaling pathway and growth-inhibitory action. To investigate the specific effect of GPER in ovarian cancer cells. We used G1 (a selective ligand for GPER) in our study. Although G36 was seen a more selective GPER antagonist than G15 [54], our data showed only suppression of cell proliferation was found for a very high concentration of G36-treated Caov3 cells (Figure S1). G15 has a similar structure to G1 [20], and is effective in inhibiting all G1-mediated effects [20,55,56]. Therefore, G15 was used to block GPER and the actions of the G1 treatment in our experiments. G1 and G15 both have no affinity for ER α [20,57]. According to the estimated IC₅₀ of G1 for the Caov3 and Caov4 cell lines, we used 1 μ M G1, 1 μ M G15 and 1 μ M G1 + 1 μ M G15 to treat cells. Our results suggested that inhibition of the proliferation and migration of Caov3 and Caov4 cells was attributable primarily to activation of GPER by G1 treatment. This hypothesis was confirmed by siRNA knockdown of GPER, which blocked the G1 inhibitory

effect on cell growth of Caov3 and Caov4 cells. Several recent investigations suggested that activation of GPER by high concentration (1 μ M) G1 treatment played an inhibitory role in various cancer cells [15,19,53], which are in agreement with our findings. Furthermore, 24 h treatment with G15 reversed the inhibitory effect of G1 and blocked the actions of G1 in our extended experiments. Our study provided evidence that G1 treatment suppressed proliferation and migration of Caov3 and Caov4 cells via activation of GPER.

The mode of action of G1 and its interaction with GPER in Caov3 and Caov4 cells have not been studied previously. In the ER α -negative breast cancer cells (MDA-MB-468 and MDA-MB-436 cells), rapid activation of ERK1/2 (<30min) was induced by G1 treatment via GPER/EGFR/ERK signaling, leading to cell proliferation and cell migration [58]. On the contrary, G1 treatment was shown to induce sustained ERK1/2 in Caov3 and Caov4 cells, but the biological consequence was a profound inhibition of cell proliferation and migration in our study. Our results are supported by previous findings, which showed that p-ERK1/2 was maintained for 24 h and cell growth was suppressed under the treatment of G1 in breast [52], prostate [14] and adrenocortical cancer cells [53]. Both ERK1/2 activation and cell growth suppression were dependent on GPER, as siRNA knockdown and the antagonist of GPER effectively blocked the actions of G1.

It has been demonstrated that ERK1/2 is part of the GPER-mediated pathway [7]. The activation of ERK1/2 plays a central role in cell proliferation control [59]. Activation of ERK1/2 (p-ERK1/2) is able to translocate from the cytoplasm to the nucleus to phosphorylate their nuclear targets for transcriptional regulation [60]. A previous study has suggested cytosolic ERK1/2 activation inhibits survival and proliferation signals in the nucleus [60]. Moreover, the duration of ERK1/2 phosphorylation can determine a cell's fate, with transient p-ERK1/2 resulting in cell survival and proliferation and prolonged p-ERK1/2 with nuclear accumulation of activated ERK1/2 transmitting anti-proliferation signals [61–63]. In our study, we demonstrated that activation of GPER by G1 induced phosphorylated ERK1/2 in Caov3 and Caov4 cells, rapidly, and ERK1/2 activation was maintained for 24 h. Compared with another study of MCF-7 cells, the peak of the p-ERK1/2 level appeared at 1 h and disappeared after 24 h during G1 treatment [14]. Whether sustained p-ERK1/2 is a bridge to the H3K4me3 accumulation and inhibition of cell growth response to activation of GPER by G1 requires further study in the future.

As we know, H3K4me3 has been generally recognized as an active promoter mark while broad H3K4me3 at the tumor suppressor genes leads to tumor suppression [25]. A previous study suggested that KDM5B, a histone demethylase, demethylated H3K4me3 to an inactive transcription state and reduced the transcription of tumor suppressor genes, then promoted gastric cancer cell proliferation and migration [28]. In addition, $1\alpha,25(\text{OH})_2\text{D}_3$ exerted anti-tumoral effects on breast cancer epithelial cells by increasing the level of H3K4me3 at the target gene promoters [64]. In accordance with previous studies, our study first released that GPER activation by G1 treatment had an inhibitory effect on cell growth, accompanied by elevating the level of H3K4me3 in ovarian cancer cells.

So far three main human estrogen receptors (ER α , ER β and GPER) have been identified as potential targets for tailored endocrine therapies to treat ovarian cancer, although these approaches have not been implemented into clinical routine so far. Regarding histone modifications, previous analyses have shown that an activated endogenous estrogen-responsive TFF1 gene results in promoter recruitment of menin (MLL1/MLL2 histone methyltransferase complexes), and in the elevated trimethylation of H3K4 [65]. Moreover, the accumulation of H3K4me3 was induced on ER α -suppressed genes in the presence of ER β , followed by epigenetic activation of transcription of tumor suppressor p53 [33]. The G1 treatment induced p53 via transcriptional and post-transcriptional pathways to suppress breast cancer cells [66]. Whether p53-dependent transcription can be activated by G1 recruitment to H3K4me3 in ovarian cancer needs further research. The relation of the GPER activation-induced p-ERK1/2 pathway with H3K4me3 in ovarian cancer need to be investigated for further therapeutic interventions or combination therapies in the future. Many substrates of ERK1/2 were found in the nucleus: they were nuclear transcriptional

factors and took part in gene transcription, cell proliferation and differentiation. This is promising, because ovarian cancer cells facilitates migration and proliferation by activating the MAPK/ERK1/2 pathway [67]. On the other hand, the PI3K/AKT and ERK cascade activation induces chemotherapy resistance in endothelial ovarian cancer cells [68]. Therefore, this axis seems to be involved in the two processes that determine ovarian cancer survival most and merits further consideration.

Indirect confirmation of these results could be provided with the observation that suppression of GPER via G15 conversely promotes cell migration and proliferation of ovarian cancer cells with attenuation of p-ERK1/2 and H3K4me3 expression. The consistent results were obtained in Caov4 cells. Additionally, G15 blocked the actions of G1 partly in Caov3 cell line, in that G15 could not decrease the levels of p-ERK1/2 and H3K4me3 with promoting cell growth of Caov3 cells. The significant differences in GPER levels in Caov3 and Caov4 cells probably caused the various impacts of G15 treatment. Interestingly, in KGN cells (a human ovarian granulosa cell tumor cell line), G15 did not have an effect on cell proliferation [14]. These results might reflect the differentiation grade of granulosa tumors versus ovarian cancer subtypes at a cellular level [3]. A previous study reported that the GPER-specific antagonist G15 was able to impair GPER function and inhibit the proliferation of endometriotic cells [69]. All the observations could be explained by heterogeneity of different ovarian cell lines and different types of cancers. Our study has some limitations. One limitation is that the downstream regulators of the GPER pathway maintain phosphorylated ERK1/2 and increasing H3K4me3 levels; the localization of sustained p-ERK1/2 also was not investigated. Another limitation is that the functional cross-talk between GPER and ER α was not further studied in the present study. However, the effects of G1-induced activation of GPER on Caov3 and Caov4 cell lines are virtually identical.

5. Conclusions

In conclusion, our data suggests that GPER is involved in mediating the epigenetic regulation of H3K4me3 expression in ovarian cancer. Apart from the prognostic impact of the correlation of GPER and H3K4me3, we present, for the first time, that levels of phosphorylated ERK1/2 and H3K4me3 are elevated via activation of GPER by G1 treatment. Moreover, activation of GPER has an inhibitory effect on the proliferation and migration of ovarian cancer cells. Although further studies are needed, our findings are important. According to these results, the interplay of GPER and H3K4me3 could represent a biological rationale for therapeutic approaches addressing GPER as a potential target in future investigation.

Supplementary Materials: The following are available online at <https://www.mdpi.com/2073-4409/10/3/619/s1>, Figure S1: The effect of G36 on Caov3 and Caov4 cells; Figure S2: GPER expression after G1 or G15 treatment for 24 h in Caov3 and Caov4 cell lines; Figure S3: M30 cyto-death assay; Figure S4: H3K4me3 immunocytochemistry staining of Caov3 and Caov4 cells after G1 or G15 treatment for 24 h; Figure S5: Positive and negative controls for GPER and H3K4me3 in placental tissue.

Author Contributions: Conceptualization, F.T., U.J. and E.S.; formal analysis, U.J., S.H., M.R. and E.S.; funding acquisition, F.T. and U.J.; investigation, N.H., C.K., B.C., A.H., D.M., U.J. and E.S.; methodology, F.T., D.M., U.J. and E.S.; project administration, F.T. and U.J.; supervision, S.M., D.M. and U.J.; validation, F.T., S.M., D.M. and U.J.; visualization, N.H.; writing—original draft, N.H. and F.T.; writing—review and editing, B.C., A.H., S.M., D.M., U.J. and E.S. All authors have read and agreed to the published version of the manuscript.

Funding: This research was funded by the LMU Munich Medical Faculty. We further acknowledge financial support by China Scholarship Council (CSC) for Han Nan.

Institutional Review Board Statement: The study was conducted according to the guidelines of the Declaration of Helsinki, and approved by the Ethics Committee of the Ludwig-Maximilians-University (Date: 30 September 2009; approval number: 227-09; Munich, Germany).

Informed Consent Statement: Informed consent was obtained from all subjects involved in the study.

Data Availability Statement: The data presented in this study are available on request from the corresponding author. The data are not publicly available due to ethical issues.

Acknowledgments: The authors would like to thank Simone Hofmann for excellent technical support. We further thank Sabina K. Page for proofreading the manuscript as a native speaker of the English language.

Conflicts of Interest: S.M. reports grants and personal fees from AstraZeneca, Clovis, Medac, MSD, PharmaMar, Roche, Sensor Kinesis, Tesaro, and Teva outside the submitted work. F.T. has received grants and personal fees from AstraZeneca, Clovis, Medac, PharmaMar, Roche, and Tesaro outside the submitted work. The other authors declare no conflict of interest.

References

1. Siegel, R.L.; Miller, K.D.; Jemal, A. Cancer statistics, 2020. *CA Cancer J. Clin.* **2020**, *70*, 7–30. [[CrossRef](#)]
2. Jayson, G.C.; Kohn, E.C.; Kitchener, H.C.; Ledermann, J.A. Ovarian cancer. *Lancet* **2014**, *384*, 1376–1388. [[CrossRef](#)]
3. Bast, R.C.; Hennessy, B.; Mills, G.B. The biology of ovarian cancer: New opportunities for translation. *Nat. Rev. Cancer* **2009**, *9*, 415–428. [[CrossRef](#)]
4. Hunn, J.; Rodriguez, G.C. Ovarian Cancer. *Clin. Obstet. Gynecol.* **2012**, *55*, 3–23. [[CrossRef](#)] [[PubMed](#)]
5. Persson, I. Estrogens in the causation of breast, endometrial and ovarian cancers—evidence and hypotheses from epidemiological findings. *J. Steroid Biochem. Mol. Biol.* **2000**, *74*, 357–364. [[CrossRef](#)]
6. Prossnitz, E.R.; Barton, M. The G-protein-coupled estrogen receptor GPER in health and disease. *Nat. Rev. Endocrinol.* **2011**, *7*, 715–726. [[CrossRef](#)]
7. Filardo, E.J.; Quinn, J.A.; Bland, K.I.; Frackelton, A.R. Estrogen-Induced Activation of Erk-1 and Erk-2 Requires the G Protein-Coupled Receptor Homolog, GPR30, and Occurs via Trans-Activation of the Epidermal Growth Factor Receptor through Release of HB-EGF. *Mol. Endocrinol.* **2000**, *14*, 1649–1660. [[CrossRef](#)] [[PubMed](#)]
8. Revankar, C.M.; Cimino, D.F.; Sklar, L.A.; Arterburn, J.B.; Prossnitz, E.R. A Transmembrane Intracellular Estrogen Receptor Mediates Rapid Cell Signaling. *Science* **2005**, *307*, 1625–1630. [[CrossRef](#)]
9. Prossnitz, E.R.; Barton, M. Signaling, physiological functions and clinical relevance of the G protein-coupled estrogen receptor GPER. *Prostaglandins Other Lipid Mediat.* **2009**, *89*, 89–97. [[CrossRef](#)]
10. Prossnitz, E.R.; Barton, M. Estrogen biology: New insights into GPER function and clinical opportunities. *Mol. Cell. Endocrinol.* **2014**, *389*, 71–83. [[CrossRef](#)]
11. Albanito, L.; Madeo, A.; Lappano, R.; Vivacqua, A.; Rago, V.; Carpino, A.; Oprea, T.I.; Prossnitz, E.R.; Musti, A.M.; Andò, S.; et al. G Protein-Coupled Receptor 30 (GPR30) Mediates Gene Expression Changes and Growth Response to 17 β -Estradiol and Selective GPR30 Ligand G-1 in Ovarian Cancer Cells. *Cancer Res.* **2007**, *67*, 1859–1866. [[CrossRef](#)]
12. Barton, M.; Filardo, E.J.; Lolait, S.J.; Thomas, P.; Maggiolini, M.; Prossnitz, E.R. Twenty years of the G protein-coupled estrogen receptor GPER: Historical and personal perspectives. *J. Steroid Biochem. Mol. Biol.* **2018**, *176*, 4–15. [[CrossRef](#)] [[PubMed](#)]
13. Ariazi, E.A.; Brailoiu, E.; Yerrum, S.; Shupp, H.A.; Slifker, M.J.; Cunliffe, H.E.; Black, M.A.; Donato, A.L.; Arterburn, J.B.; Oprea, T.I.; et al. The G Protein-Coupled Receptor GPR30 Inhibits Proliferation of Estrogen Receptor-Positive Breast Cancer Cells. *Cancer Res.* **2010**, *70*, 1184–1194. [[CrossRef](#)]
14. Chan, Q.K.; Lam, H.-M.; Ng, C.-F.; Lee, A.Y.Y.; Chan, E.S.; Ng, H.-K.; Ho, S.-M.; Lau, K.-M. Activation of GPR30 inhibits the growth of prostate cancer cells through sustained activation of Erk1/2, c-jun/c-fos-dependent upregulation of p21, and induction of G2 cell-cycle arrest. *Cell Death Differ.* **2010**, *17*, 1511–1523. [[CrossRef](#)]
15. Liu, Q.; Chen, Z.; Jiang, G.; Zhou, Y.; Yang, X.; Huang, H.; Liu, H.; Du, J.; Wang, H. Epigenetic down regulation of G protein-coupled estrogen receptor (GPER) functions as a tumor suppressor in colorectal cancer. *Mol. Cancer* **2017**, *16*, 1–14. [[CrossRef](#)]
16. Wang, C.; Lv, X.; Jiang, C.; Davis, J.S. The putative G-protein coupled estrogen receptor agonist G-1 suppresses proliferation of ovarian and breast cancer cells in a GPER-independent manner. *Am. J. Transl. Res.* **2012**, *4*, 390–402.
17. Yan, Y.; Jiang, X.; Zhao, Y.; Wen, H.; Liu, G. Role of GPER on proliferation, migration and invasion in ligand-independent manner in human ovarian cancer cell line SKOV3. *Cell Biochem. Funct.* **2015**, *33*, 552–559. [[CrossRef](#)]
18. Yan, Y.; Liu, H.; Wen, H.; Jiang, X.; Cao, X.; Zhang, G.; Liu, G. The novel estrogen receptor GPER regulates the migration and invasion of ovarian cancer cells. *Mol. Cell. Biochem.* **2013**, *378*, 1–7. [[CrossRef](#)] [[PubMed](#)]
19. Ignatov, T.; Modl, S.; Thulig, M.; Weissenborn, C.; Treeck, O.; Ortman, O.; Zenclussen, A.; Costa, S.D.; Kalinski, T.; Ignatov, A. GPER-1 acts as a tumor suppressor in ovarian cancer. *J. Ovarian Res.* **2013**, *6*, 51. [[CrossRef](#)] [[PubMed](#)]
20. Dennis, M.K.; Burai, R.; Ramesh, C.; Petrie, W.K.; Alcon, S.N.; Nayak, T.K.; Bologna, C.G.; Leitao, A.; Brailoiu, E.; Deliu, E.; et al. In vivo effects of a GPR30 antagonist. *Nat. Chem. Biol.* **2009**, *5*, 421–427. [[CrossRef](#)]
21. Dawson, M.A.; Kouzarides, T. Cancer Epigenetics: From Mechanism to Therapy. *Cell* **2012**, *150*, 12–27. [[CrossRef](#)] [[PubMed](#)]
22. Park, S.; Kim, G.W.; Kwon, S.H.; Lee, J. Broad domains of histone H3 lysine 4 trimethylation in transcriptional regulation and disease. *FEBS J.* **2020**, *287*, 2891–2902. [[CrossRef](#)] [[PubMed](#)]

23. Koch, C.M.; Andrews, R.M.; Flicek, P.; Dillon, S.C.; Karaöz, U.; Clelland, G.K.; Wilcox, S.; Beare, D.M.; Fowler, J.C.; Couttet, P.; et al. The landscape of histone modifications across 1% of the human genome in five human cell lines. *Genome Res.* **2007**, *17*, 691–707. [[CrossRef](#)] [[PubMed](#)]
24. Barski, A.; Cuddapah, S.; Cui, K.; Roh, T.-Y.; Schones, D.E.; Wang, Z.; Wei, G.; Chepelev, I.; Zhao, K. High-Resolution Profiling of Histone Methylations in the Human Genome. *Cell* **2007**, *129*, 823–837. [[CrossRef](#)]
25. Chen, K.; Chen, Z.; Wu, D.; Zhang, L.; Lin, X.; Su, J.; Rodriguez, B.; Xi, Y.; Xia, Z.; Chen, X.; et al. Broad H3K4me3 is associated with increased transcription elongation and enhancer activity at tumor-suppressor genes. *Nat. Genet.* **2015**, *47*, 1149–1157. [[CrossRef](#)] [[PubMed](#)]
26. Chapman-Rothe, N.; Curry, E.; Zeller, C.; Liber, D.; Stronach, E.; Gabra, H.; Ghaem-Maghami, S.; Brown, R. Chromatin H3K27me3/H3K4me3 histone marks define gene sets in high-grade serous ovarian cancer that distinguish malignant, tumour-sustaining and chemo-resistant ovarian tumour cells. *Oncogene* **2012**, *32*, 4586–4592. [[CrossRef](#)]
27. Lu, C.; Yang, D.; Sabbatini, M.E.; Colby, A.H.; Grinstaff, M.W.; Oberlies, N.H.; Pearce, C.; Liu, K. Contrasting roles of H3K4me3 and H3K9me3 in regulation of apoptosis and gemcitabine resistance in human pancreatic cancer cells. *BMC Cancer* **2018**, *18*, 149. [[CrossRef](#)] [[PubMed](#)]
28. Li, Y.; Chen, L.; Feng, L.; Zhu, M.; Shen, Q.; Fang, Y.; Liu, X.; Zhang, X. NEK2 promotes proliferation, migration and tumor growth of gastric cancer cells via regulating KDM5B/H3K4me3. *Am. J. Cancer Res.* **2019**, *9*, 2364–2378. [[PubMed](#)]
29. Dhar, S.S.; Zhao, D.; Lin, T.; Gu, B.; Pal, K.; Wu, S.J.; Alam, H.; Lv, J.; Yun, K.; Gopalakrishnan, V.; et al. MLL4 Is Required to Maintain Broad H3K4me3 Peaks and Super-Enhancers at Tumor Suppressor Genes. *Mol. Cell* **2018**, *70*, 825–841.e6. [[CrossRef](#)] [[PubMed](#)]
30. Han, N.; Jeschke, U.; Kuhn, C.; Hester, A.; Czogalla, B.; Mahner, S.; Rottmann, M.; Mayr, D.; Schmoeckel, E.; Trillsch, F. H3K4me3 Is a Potential Mediator for Antiproliferative Effects of Calcitriol (1 α ,25(OH) $_2$ D $_3$) in Ovarian Cancer Biology. *Int. J. Mol. Sci.* **2020**, *21*, 2151. [[CrossRef](#)] [[PubMed](#)]
31. Mann, M.; Cortez, V.; Vadlamudi, R.K. Epigenetics of Estrogen Receptor Signaling: Role in Hormonal Cancer Progression and Therapy. *Cancers* **2011**, *3*, 1691–1707. [[CrossRef](#)]
32. Li, Y.; Sun, L.; Zhang, Y.; Wang, D.; Wang, F.; Liang, J.; Gui, B.; Shang, Y. The Histone Modifications Governing TFF1 Transcription Mediated by Estrogen Receptor. *J. Biol. Chem.* **2011**, *286*, 13925–13936. [[CrossRef](#)] [[PubMed](#)]
33. Lu, W.; Katzenellenbogen, B.S. Estrogen Receptor- β Modulation of the ER α -p53 Loop Regulating Gene Expression, Proliferation, and Apoptosis in Breast Cancer. *Horm. Cancer* **2017**, *8*, 230–242. [[CrossRef](#)] [[PubMed](#)]
34. Templin, M.F.; Stoll, D.; Schrenk, M.; Traub, P.C.; Vöhlinger, C.F.; Joos, T.O. Protein microarray technology. *Drug Discov. Today* **2002**, *7*, 815–822. [[CrossRef](#)]
35. Heublein, S.; Mayr, D.; Vrekoussis, T.; Friese, K.; Hofmann, S.S.; Jeschke, U.; Lenhard, M. The G-Protein Coupled Estrogen Receptor (GPER/GPR30) is a Gonadotropin Receptor Dependent Positive Prognosticator in Ovarian Carcinoma Patients. *PLoS ONE* **2013**, *8*, e71791. [[CrossRef](#)]
36. Friese, K.; Kost, B.; Vattai, A.; Marmé, F.; Kuhn, C.; Mahner, S.; Dannecker, C.; Jeschke, U.; Heublein, S. The G protein-coupled estrogen receptor (GPER/GPR30) may serve as a prognostic marker in early-stage cervical cancer. *J. Cancer Res. Clin. Oncol.* **2017**, *144*, 13–19. [[CrossRef](#)] [[PubMed](#)]
37. Heublein, S.; Mayr, D.; Friese, K.; Jarrin-Franco, M.C.; Lenhard, M.; Mayerhofer, A.; Jeschke, U. The G-Protein-Coupled Estrogen Receptor (GPER/GPR30) in Ovarian Granulosa Cell Tumors. *Int. J. Mol. Sci.* **2014**, *15*, 15161–15172. [[CrossRef](#)]
38. Heublein, S.; Vrekoussis, T.; Kühn, C.; Friese, K.; Makrigiannakis, A.; Mayr, D.; Lenhard, M.; Jeschke, U. Inducers of G-protein coupled estrogen receptor (GPER) in endometriosis: Potential implications for macrophages and follicle maturation. *J. Reprod. Immunol.* **2013**, *97*, 95–103. [[CrossRef](#)] [[PubMed](#)]
39. Fluss, R.; Faraggi, D.; Reiser, B. Estimation of the Youden Index and its Associated Cutoff Point. *Biom. J.* **2005**, *47*, 458–472. [[CrossRef](#)]
40. Perkins, N.J.; Schisterman, E.F. The Inconsistency of “Optimal” Cutpoints Obtained using Two Criteria based on the Receiver Operating Characteristic Curve. *Am. J. Epidemiol.* **2006**, *163*, 670–675. [[CrossRef](#)] [[PubMed](#)]
41. Eishingdrelo, H.; Kongsamut, S. Minireview: Targeting GPCR Activated ERK Pathways for Drug Discovery. *Curr. Chem. Genomics Transl. Med.* **2013**, *7*, 9–15. [[CrossRef](#)]
42. Smith, H.O.; Arias-Pulido, H.; Kuo, D.Y.; Howard, T.; Qualls, C.R.; Lee, S.-J.; Verschraegen, C.F.; Hathaway, H.J.; Joste, N.E.; Prossnitz, E.R. GPR30 predicts poor survival for ovarian cancer. *Gynecol. Oncol.* **2009**, *114*, 465–471. [[CrossRef](#)] [[PubMed](#)]
43. Schneider, A.-C.; Heukamp, L.C.; Rogenhofer, S.; Fechner, G.; Bastian, P.J.; Von Ruecker, A.; Müller, S.C.; Ellinger, J. Global histone H4K20 trimethylation predicts cancer-specific survival in patients with muscle-invasive bladder cancer. *BJU Int.* **2011**, *108*, E290–E296. [[CrossRef](#)]
44. Ellinger, J.; Kahl, P.; Mertens, C.; Rogenhofer, S.; Hauser, S.; Hartmann, W.; Bastian, P.J.; Büttner, R.; Müller, S.C.; von Ruecker, A. Prognostic relevance of global histone H3 lysine 4 (H3K4) methylation in renal cell carcinoma. *Int. J. Cancer* **2010**, *127*, 2360–2366. [[CrossRef](#)] [[PubMed](#)]
45. He, C.; Xu, J.; Zhang, J.; Xie, D.; Ye, H.; Xiao, Z.; Cai, M.; Xu, K.; Zeng, Y.; Li, H.; et al. High expression of trimethylated histone H3 lysine 4 is associated with poor prognosis in hepatocellular carcinoma. *Hum. Pathol.* **2012**, *43*, 1425–1435. [[CrossRef](#)] [[PubMed](#)]

46. Messier, T.L.; Gordon, J.A.R.; Boyd, J.R.; Tye, C.E.; Browne, G.; Stein, J.L.; Lian, J.B.; Stein, G.S. Histone H3 lysine 4 acetylation and methylation dynamics define breast cancer subtypes. *Oncotarget* **2016**, *7*, 5094–5109. [[CrossRef](#)] [[PubMed](#)]
47. Liu, H.; Li, Y.; Li, J.; Liu, Y.; Cui, B. H3K4me3 and Wdr82 are associated with tumor progression and a favorable prognosis in human colorectal cancer. *Oncol. Lett.* **2018**, *16*, 2125–2134. [[CrossRef](#)]
48. Boesch, M.; Zeimet, A.G.; Reimer, D.; Schmidt, S.; Gastl, G.; Parson, W.; Spoeck, F.; Hatina, J.; Wolf, D.; Sopper, S. The side population of ovarian cancer cells defines a heterogeneous compartment exhibiting stem cell characteristics. *Oncotarget* **2014**, *5*, 7027–7039. [[CrossRef](#)] [[PubMed](#)]
49. Testa, U.; Petrucci, E.; Pasquini, L.; Castelli, G.; Pelosi, E. Ovarian Cancers: Genetic Abnormalities, Tumor Heterogeneity and Progression, Clonal Evolution and Cancer Stem Cells. *Medicines* **2018**, *5*, 16. [[CrossRef](#)]
50. Gaudet, H.; Cheng, S.; Christensen, E.; Filardo, E. The G-protein coupled estrogen receptor, GPER: The inside and inside-out story. *Mol. Cell. Endocrinol.* **2015**, *418*, 207–219. [[CrossRef](#)] [[PubMed](#)]
51. Osmond, R.I.W.; Sheehan, A.; Borowicz, R.; Barnett, E.; Harvey, G.; Turner, C.; Brown, A.; Crouch, M.F.; Dyer, A.R. GPCR Screening via ERK 1/2: A Novel Platform for Screening G Protein–Coupled Receptors. *J. Biomol. Screen.* **2005**, *10*, 730–737. [[CrossRef](#)] [[PubMed](#)]
52. Chen, Z.-J.; Wei, W.-D.; Jiang, G.-M.; Liu, H.; Yang, X.; Wu, Y.-M.; Liu, H.; Wong, C.K.; Du, J.; Wang, H.-S. Activation of GPER suppresses epithelial mesenchymal transition of triple negative breast cancer cells via NF- κ B signals. *Mol. Oncol.* **2016**, *10*, 775–788. [[CrossRef](#)]
53. Chimento, A.; Sirianni, R.; Casaburi, I.; Zolea, F.; Rizza, P.; Avena, P.; Malivindi, R.; De Luca, A.; Campana, C.; Martire, E.; et al. GPER agonist G-1 decreases adrenocortical carcinoma (ACC) cell growth in vitro and in vivo. *Oncotarget* **2015**, *6*, 19190–19203. [[CrossRef](#)] [[PubMed](#)]
54. Dennis, M.K.; Field, A.S.; Burai, R.; Ramesh, C.; Petrie, W.K.; Bologna, C.G.; Oprea, T.I.; Yamaguchi, Y.; Hayashi, S.-I.; Sklar, S.L.A.; et al. Identification of a GPER/GPR30 antagonist with improved estrogen receptor counterselectivity. *J. Steroid Biochem. Mol. Biol.* **2011**, *127*, 358–366. [[CrossRef](#)]
55. Jenei-Lanzl, Z.; Straub, R.H.; Dienstknecht, T.; Huber, M.; Hager, M.; Grässel, S.; Kujat, R.; Angele, M.K.; Nerlich, M.; Angele, P. Estradiol inhibits chondrogenic differentiation of mesenchymal stem cells via nonclassic signaling. *Arthritis Rheum.* **2010**, *62*, 1088–1096. [[CrossRef](#)]
56. Lindsey, S.H.; Carver, K.A.; Prossnitz, E.R.; Chappell, M.C. Vasodilation in Response to the GPR30 Agonist G-1 is Not Different from Estradiol in the mRen2.Lewis Female Rat. *J. Cardiovasc. Pharmacol.* **2011**, *57*, 598–603. [[CrossRef](#)]
57. Bologna, C.G.; Revankar, C.M.; Young, S.M.; Edwards, B.S.; Arterburn, J.B.; Kiselyov, A.S.; Parker, M.A.; Tkachenko, S.E.; Savchuck, N.P.; Sklar, L.A.; et al. Virtual and biomolecular screening converge on a selective agonist for GPR30. *Nat. Chem. Biol.* **2006**, *2*, 207–212. [[CrossRef](#)] [[PubMed](#)]
58. Yu, T.; Liu, M.; Luo, H.; Wu, C.; Tang, X.; Tang, S.; Hu, P.; Yan, Y.; Wang, Z.; Tu, G. GPER mediates enhanced cell viability and motility via non-genomic signaling induced by 17 β -estradiol in triple-negative breast cancer cells. *J. Steroid Biochem. Mol. Biol.* **2014**, *143*, 392–403. [[CrossRef](#)]
59. Meloche, S.; Pouyssegur, J. The ERK1/2 mitogen-activated protein kinase pathway as a master regulator of the G1- to S-phase transition. *Oncogene* **2007**, *26*, 3227–3239. [[CrossRef](#)] [[PubMed](#)]
60. Mebratu, Y.; Tesfaygi, Y. How ERK1/2 activation controls cell proliferation and cell death: Is subcellular localization the answer? *Cell Cycle* **2009**, *8*, 1168–1175. [[CrossRef](#)] [[PubMed](#)]
61. Chen, J.-R.; Plotkin, L.L.; Aguirre, J.I.; Han, L.; Jilka, R.L.; Kousteni, S.; Bellido, T.; Manolagas, S.C. Transient Versus Sustained Phosphorylation and Nuclear Accumulation of ERKs Underlie Anti-Versus Pro-apoptotic Effects of Estrogens. *J. Biol. Chem.* **2005**, *280*, 4632–4638. [[CrossRef](#)]
62. Marshall, C. Specificity of receptor tyrosine kinase signaling: Transient versus sustained extracellular signal-regulated kinase activation. *Cell* **1995**, *80*, 179–185. [[CrossRef](#)]
63. Adachi, T.; Kar, S.; Wang, M.; Carr, B.I. Transient and sustained ERK phosphorylation and nuclear translocation in growth control. *J. Cell. Physiol.* **2002**, *192*, 151–159. [[CrossRef](#)] [[PubMed](#)]
64. Goeman, F.; De Nicola, F.; De Meo, P.D.; Pallocca, M.; Elmi, B.; Castrignanò, T.; Pesole, G.; Strano, S.; Blandino, G.; Fanciulli, M.; et al. VDR primary targets by genome-wide transcriptional profiling. *J. Steroid Biochem. Mol. Biol.* **2014**, *143*, 348–356. [[CrossRef](#)] [[PubMed](#)]
65. Dreijerink, K.M.; Mulder, K.W.; Winkler, G.S.; Höppener, J.W.; Lips, C.J.; Timmers, H.M. Menin Links Estrogen Receptor Activation to Histone H3K4 Trimethylation. *Cancer Res.* **2006**, *66*, 4929–4935. [[CrossRef](#)] [[PubMed](#)]
66. Wei, W.; Chen, Z.-J.; Zhang, K.-S.; Yang, X.-L.; Wu, Y.-M.; Chen, X.-H.; Huang, H.-B.; Liu, H.-L.; Cai, S.-H.; Du, J.; et al. The activation of G protein-coupled receptor 30 (GPR30) inhibits proliferation of estrogen receptor-negative breast cancer cells in vitro and in vivo. *Cell Death Dis.* **2014**, *5*, e1428. [[CrossRef](#)] [[PubMed](#)]
67. Mertens-Walker, I.; Bolitho, C.; Baxter, R.C.; Marsh, D.J. Gonadotropin-induced ovarian cancer cell migration and proliferation require extracellular signal-regulated kinase 1/2 activation regulated by calcium and protein kinase C δ . *Endocr. Relat. Cancer* **2010**, *17*, 335–349. [[CrossRef](#)]

68. Zhang, P.-F.; Wu, J.; Luo, J.-H.; Li, K.-S.; Wang, F.; Huang, W.; Wu, Y.; Gao, S.-P.; Zhang, X.-M. SNHG22 overexpression indicates poor prognosis and induces chemotherapy resistance via the miR-2467/Gal-1 signaling pathway in epithelial ovarian carcinoma. *Aging* **2019**, *11*, 8204–8216. [[CrossRef](#)]
69. Imesch, P.; Samartzis, E.P.; Dedes, K.J.; Fink, D.; Fedier, A. Histone deacetylase inhibitors down-regulate G-protein-coupled estrogen receptor and the GPER-antagonist G-15 inhibits proliferation in endometriotic cells. *Fertil. Steril.* **2013**, *100*, 770–776. [[CrossRef](#)]

Supplementary Materials:

1. The Effect of G36 on Caov3 and Caov4 Cells

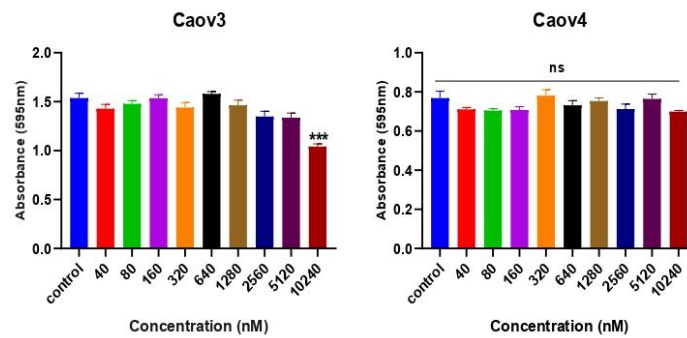


Figure S1. G36 had no effect on Caov3 and Caov4 cells. Both ovarian cancer cell lines were incubated with an increasing concentration of G36 for 24 h and the cell growth was evaluated by MTT assay. The result was presented as effective absorbance at 595 nm. Each experiment was repeated six times ($n = 6$) and the results expressed as the means \pm SEM. Statistical analysis were performed by one-way ANOVA test ($ns > 0.05$, $*** p < 0.001$ vs. control group).

2. GPER Expression after G1 or G15 Treatment for 24 h in Caov3 and Caov4 Cell Lines

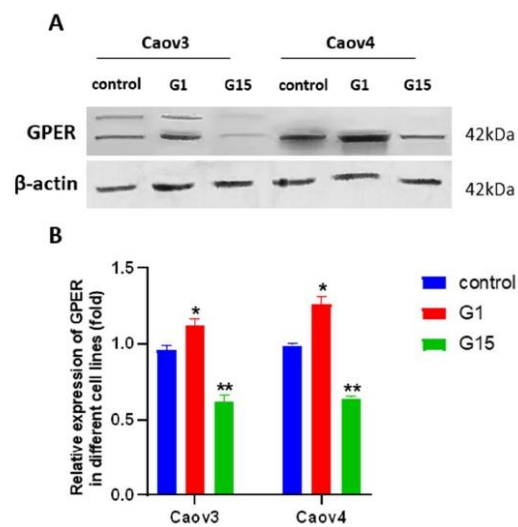


Figure S2. Caov3 and Caov4 cells were treated with $1 \mu\text{M}$ G1 or $1 \mu\text{M}$ G15 for 24 h. The levels of GPER protein were detected by western blot analysis. (A) Representative example of GPER protein expression in Caov3 and Caov4 cells after G1 or G15 treatment. (B) Histogram illustrates the ratio of GPER in Caov3

and Caov4 cell lines. * $p < 0.05$, ** $p < 0.01$ compared with control. β -actin was used as a loading control. Each experiment was repeated at least three times. The results are shown as the means \pm SEM.

3. M30 Cyto-Death Assay

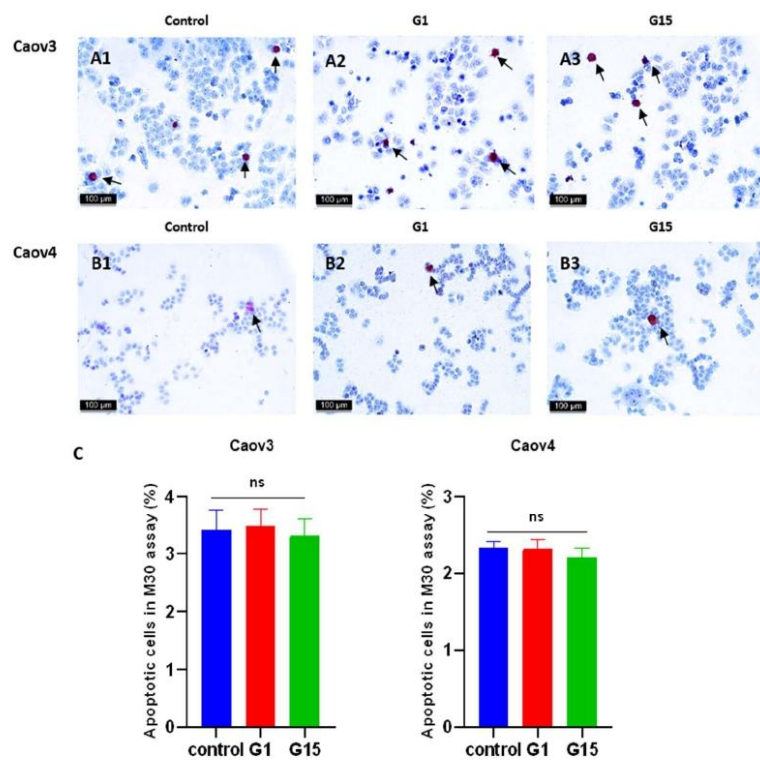
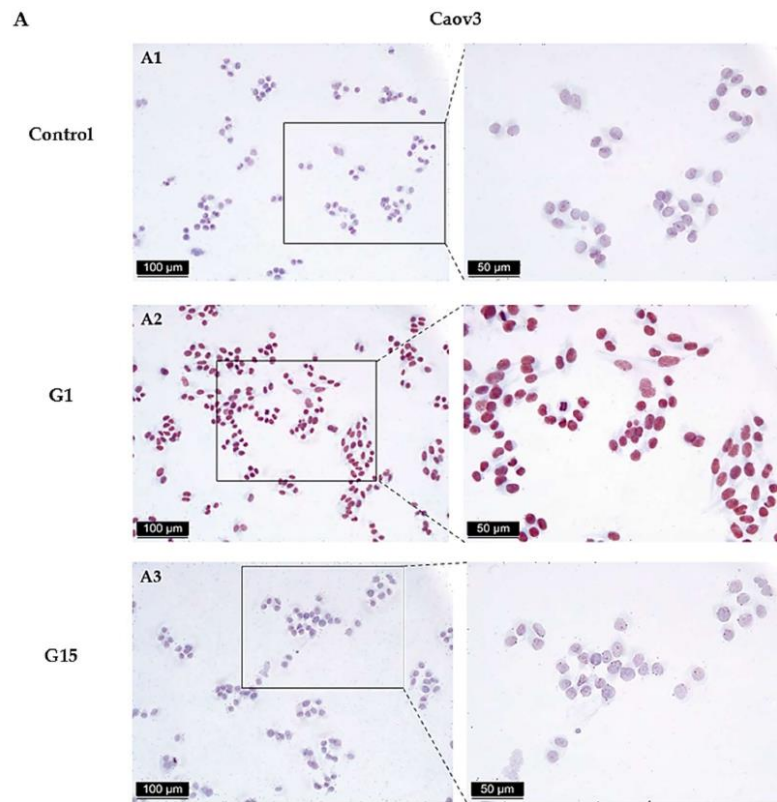


Figure S3. The detection of apoptotic cells using the M30 antibody after treatment with G1 or G15 for 24 h. The upper panel shows Caov3 cells treated with G1 and G15, respectively: (A1) control; (A2) G1; (A3) G15. The middle panel shows Caov4 cells treated with G1 and G15 respectively: (B1) control; (B2) G1; (B3) G15. The apoptotic cells stand out due to red staining (arrows) and negative cells show blue. (C) Results of M30 assay are summarized ($n = 10$). M30-positive cells are expressed as the number of positive cells $\times 100\%$ /total number of cells analyzed. Values are expressed as the mean \pm SEM. Scale bar = 100 μ m.

4. H3K4me3 Immunocytochemistry Staining of Caov3 and Caov4 Cells after G1 or G15 Treatment for 24 h



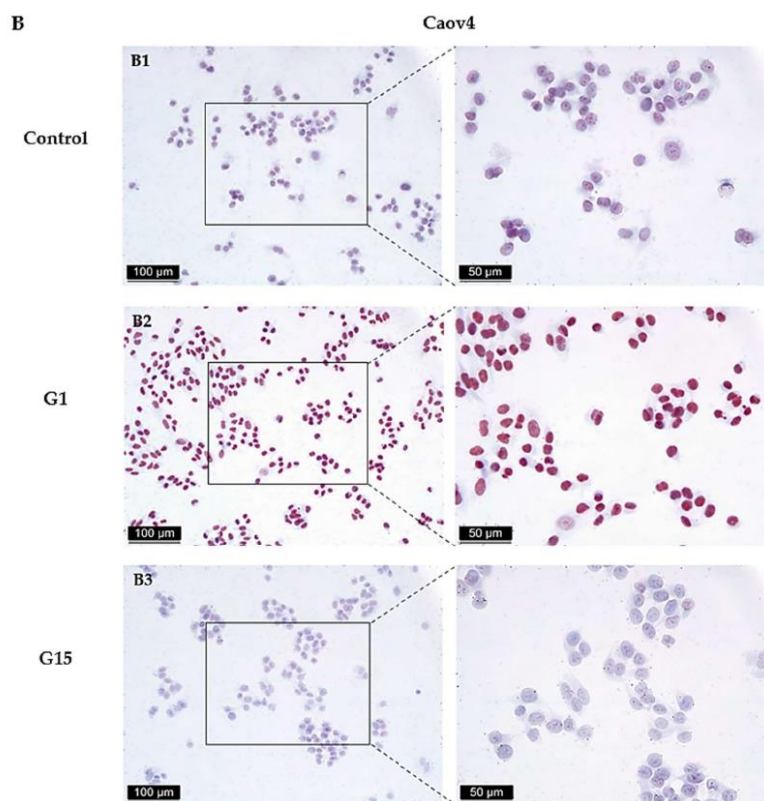


Figure 54. Representative pictures of H3K4me3 immunocytochemistry staining of Caov3 (A) and Caov4 (B) cells compared to the control (A1, B1), 1 μ M G1 (A2, B2) and 1 μ M G15 (A3, B3) for 24 h. Red staining is positive and blue staining is negative. Left panel: scale bar = 100 μ m; right panel: scale bar = 50 μ m.

5. Positive and Negative Controls for GPER and H3K4me3 in Placental Tissue

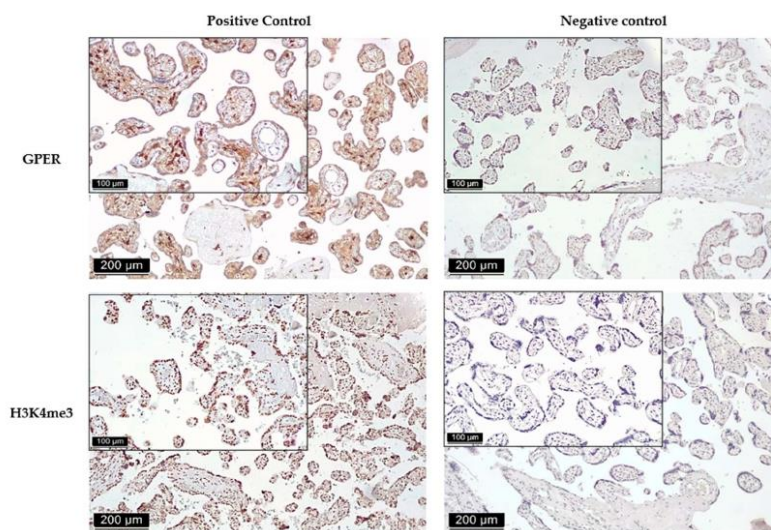


Figure S5. Positive and negative controls of the GPER and H3K4me3 stainings, respectively. We used the term placental villous tissue for positive and negative controls (scale bar = 200 µm, small pictures 100 µm).

5.Summary

Histone modification is closely related to the development of cancer. H3K4me3 has been identified as a possible tumour prognosis marker that mediates the level of tumour-associated gene expression. In my dissertation, the role and clinical significance of H3K4me3 were assessed in ovarian cancer patients. In addition, the activation of VDR or GPER through the stimulation of $1\alpha,25(\text{OH})_2\text{D}_3$ or selective agonist G1 was able to elevate the level of H3K4me3 in ovarian cancer cells with an obvious inhibition of cell growth. Therefore, my results suggest a potential effect of H3K4me3 level on prognosis of ovarian cancer patients as well as its associations to $1\alpha,25(\text{OH})_2\text{D}_3$ or G1 treatment in vitro model of ovarian cancer cells.

5.1 H3K4me3 expression in EOC patients and relation to treatment of $1\alpha,25(\text{OH})_2\text{D}_3$ Ovarian Cancer cells

In first study, we have discovered that high level of H3K4me3 expression was associated with a better outcome in EOC patients and co-expressions of H3K4me3 and VDR are observed in EOC patient tissue. Our findings have indicated that the utilization of $1\alpha,25(\text{OH})_2\text{D}_3$ is able to induce H3K4me3 levels and suppress cell proliferation in ovarian cancer cells. As a result, our findings may provide new insight into how calcitriol exerts its tumour-suppressive effects and highlight the potential advantage of calcitriol supplementation in the treatment of ovarian cancer.

5.2 The level of H3K4me3 and cell growth are mediated by GPER in ovarian cancer cells

In the second study, we have elucidated that high levels of GPER and H3K4me3 are related to more favourable outcomes in EOC patients. We have first suggested that G1-induced activation of GPER could inhibit cell proliferation and migration of ovarian cancer while elevating the levels of phosphorylated ERK1/2 and H3K4me3 through *in vitro* experimental models. The GPER antagonist G15, on the other hand, could neutralize the inhibitory actions of G1 on cell growth and induced decreased levels of H3K4me3 in ovarian cancer cells. As a result, we hypothesized that activation of GPER caused an increasing level of H3K4me3 and that treatment strategies addressing these interactions might have the potential to suppress cell proliferation and migration of ovarian cancer cells, thereby affecting the clinical conduction of disease. Although further research is required, our present discoveries can be considered as important insights in the biology of the disease. Interactions of GPER and VDR with H3K4me3 may provide a biological basis for therapeutic strategies targeting H3K4me3 as a promising marker in future research.

As a conclusion, H3K4 trimethylation as an important type of histone modifications seems to have a significant role in the development ovarian cancer. Because H3K4me3 makes a crucial contribution to transcriptional cycle in human cells, alterations of H3K4me3 level have an additional effect on various types of human cancers including ovarian cancer. My studies suggest that high levels of H3K4me3 are able to predict a favourable outcome in EOC patients. The results imply that H3K4me3 likely engages with the antiproliferative action of calcitriol in ovarian cancer cells.

Additionally, it has also been reported that the levels of phosphorylated ERK1/2 and H3K4me3 could be increased via activation of GPER implying that H3K4me3 has an additional function in inhibition of ovarian cancer cells of GPER signalling pathway. While the findings need further investigations, the current studies at least provide a novel strategy of EOC treatment.

6. Zusammenfassung

Histonmodifikationen stehen in engem Zusammenhang mit der Entstehung von Krebs. H3K4me3 wurde als ein möglicher Tumorprognosemarker identifiziert, der das Niveau der tumorassoziierten Genexpression vermittelt. In meiner Dissertation wurde die Rolle und die klinische Bedeutung von H3K4me3 bei Eierstockkrebs-Patientinnen untersucht. Darüber hinaus konnte durch die Aktivierung von VDR oder GPER, mittels Stimulation von $1\alpha,25(\text{OH})_2\text{D}_3$ oder dem selektiven Agonisten G1, das Niveau von H3K4me3 in Ovarialkarzinomzellen erhöht werden, was zu einer deutlichen Hemmung des Zellwachstums geführt hat. Daher deuten meine Ergebnisse darauf hin, dass ein potenzieller Effekt des H3K4me3-Niveaus auf die Prognose von Eierstockkrebs-Patientinnen sowie seine Assoziationen zu $1\alpha,25(\text{OH})_2\text{D}_3$ oder G1-Behandlung im In-vitro-Modell von Eierstockkrebszellen besteht.

6.1 H3K4me3-Expression bei EOC-Patientinnen und Beziehung zur Behandlung von $1\alpha,25(\text{OH})_2\text{D}_3$ -Eierstockkrebszellen

In einer ersten Studie haben wir herausgefunden, dass eine hohe H3K4me3-Expression mit einem besseren Outcome bei EOC-Patientinnen verbunden ist und eine Co-Expressionen von H3K4me3 und VDR im Gewebe von EOC-Patientinnen beobachtet werden kann. Unsere Ergebnisse deuten darauf hin, dass die Verwendung von $1\alpha,25(\text{OH})_2\text{D}_3$ in der Lage ist, den H3K4me3-Spiegel zu induzieren und die Zellproliferation in Eierstockkrebszellen zu unterdrücken. Daher können unsere Ergebnisse neue Erkenntnisse darüber liefern, wie Calcitriol seine tumorsuppressiven Effekte ausübt und den potenziellen Vorteil einer Calcitriol-Supplementierung bei der Behandlung von Ovarialkarzinom-Patientinnen verdeutlichen.

6.2 Das Niveau von H3K4me3 und das Zellwachstum werden durch GPER in Eierstockkrebszellen vermittelt

In der zweiten Studie haben wir aufgeklärt, dass hohe Spiegel von GPER und H3K4me3 mit einer günstigen Prognose verbunden sind. Wir haben zunächst gezeigt, dass die G1-induzierte Aktivierung von GPER die Zellproliferation und Migration von Ovarialkarzinomen hemmen könnte, während die Spiegel von phosphoryliertem ERK1/2 und H3K4me durch die experimentellen vitro-Modelle erhöht werden. Der GPER-Antagonist G15 konnte hingegen die hemmenden Wirkungen von G1 auf das Zellwachstum neutralisieren, sowie verminderte Spiegel von H3K4me3 in Ovarialkarzinomzellen in vitro induzieren. Infolgedessen stellten wir die Hypothese auf, dass die Aktivierung von GPER ein erhöhtes Niveau von H3K4me3 verursachte und dass Behandlungsstrategien, die auf diese Wechselwirkungen abzielen, wahrscheinlich vielversprechend sind, um die Zellproliferation und Migration von Ovarialkarzinomzellen zu unterdrücken und dadurch den klinischen Verlauf der Krankheit zu beeinflussen. Obwohl weitere Forschung erforderlich ist, liefern die derzeitigen Entdeckungen einen wichtigen Beitrag zum Verständnis der Biologie des Ovarialkarzinoms. Interaktionen von GPER oder VDR mit H3K4me3 könnten eine biologische Grundlage für therapeutische Strategien bilden, die auf H3K4me3 als vielversprechenden Marker in der zukünftigen Forschung abzielen.

Zusammenfassend kann gesagt werden: Die Veränderung der H3K4-Trimethylierung als ein wichtiger Typ von Histon-Modifikationen spielt eine bedeutende Rolle bei der Entwicklung von Eierstockkrebs. Da H3K4me3 einen entscheidenden Beitrag zum Transkriptionszyklus in menschlichen Zellen leistet, spielt die Veränderung des H3K4me3-Niveaus auch eine wichtige Rolle bei verschiedenen Arten von menschlichen Krebserkrankungen, einschließlich Eierstockkrebs. Meine Studien haben gezeigt, dass ein

hohes Niveau von H3K4me3 in der Lage ist, einen günstigen Ausgang bei EOC-Patientinnen vorherzusagen. Die weiteren Ergebnisse deuteten darauf hin, dass H3K4me3 wahrscheinlich an der antiproliferativen Wirkung von Calcitriol in Eierstockkrebszellen beteiligt ist. Darüber hinaus wurde berichtet, dass die Spiegel von phosphoryliertem ERK1/2 und H3K4me3 durch die Aktivierung von GPER erhöht werden könnten, was darauf hindeutet, dass H3K4me3 eine Rolle bei der Hemmung des GPER-Signalweges in Eierstockkrebszellen spielt. Obwohl die Ergebnisse weitere Untersuchungen erfordern, deuten die aktuellen Studien auf vielversprechende, neue Strategien für die Behandlung des EOC hin.

7. References

1. Jayson, G.C.; Kohn, E.C.; Kitchener, H.C.; Ledermann, J.A. Ovarian cancer. *The Lancet* **2014**, *384*, 1376-1388, doi:10.1016/s0140-6736(13)62146-7.
2. Quirk, J.T.; Natarajan, N. Ovarian cancer incidence in the United States, 1992–1999. *Gynecologic Oncology* **2005**, *97*, 519-523, doi:10.1016/j.ygyno.2005.02.007.
3. Siegel, R.L.; Miller, K.D.; Jemal, A. Cancer statistics, 2019. *CA: A Cancer Journal for Clinicians* **2019**, *69*, 7-34, doi:10.3322/caac.21551.
4. Bhoola, S.; Hoskins, W.J. Diagnosis and Management of Epithelial Ovarian Cancer. *Obstetrics & Gynecology* **2006**, *107*, 1399-1410, doi:10.1097/01.Aog.0000220516.34053.48.
5. Burger, R.A.; Brady, M.F.; Bookman, M.A.; Fleming, G.F.; Monk, B.J.; Huang, H.; Mannel, R.S.; Homesley, H.D.; Fowler, J.; Greer, B.E., et al. Incorporation of Bevacizumab in the Primary Treatment of Ovarian Cancer. *New England Journal of Medicine* **2011**, *365*, 2473-2483, doi:10.1056/NEJMoa1104390.
6. Moore, K.N.; DiSilvestro, P.; Lowe, E.S.; Garnett, S.; Pujade-Lauraine, E. SOLO1 and SOLO2: Randomized phase III trials of olaparib in patients (pts) with ovarian cancer and a BRCA1/2 mutation (BRCAm). *Journal of Clinical Oncology* **2014**, *32*, TPS5616-TPS5616, doi:10.1200/jco.2014.32.15_suppl.tps5616.
7. Ray-Coquard, I.L.; Harter, P.; Gonzalez Martin, A.; Cropet, C.; Pignata, S.; Fujiwara, K.; Marth, C.; Vergote, I.; Mirza, M.R.; Colombo, N., et al. PAOLA-1: An ENGOT/GCIG phase III trial of olaparib versus placebo combined with bevacizumab as maintenance treatment in patients with advanced ovarian cancer following first-line platinum-based chemotherapy plus bevacizumab. *Journal of Clinical Oncology* **2017**, *35*, TPS5605-TPS5605, doi:10.1200/JCO.2017.35.15_suppl.TPS5605.
8. Vaughan, S.; Coward, J.I.; Bast, R.C.; Berchuck, A.; Berek, J.S.; Brenton, J.D.; Coukos, G.; Crum, C.C.; Drapkin, R.; Etemadmoghadam, D., et al. Rethinking ovarian cancer: recommendations for improving outcomes. *Nature Reviews Cancer* **2011**, *11*, 719-725, doi:10.1038/nrc3144.
9. Meacham, C.E.; Morrison, S.J. Tumour heterogeneity and cancer cell plasticity. *Nature* **2013**, *501*, 328-337, doi:10.1038/nature12624.
10. Kossai, M.; Leary, A.; Scoazec, J.-Y.; Genestie, C. Ovarian Cancer: A Heterogeneous Disease. *Pathobiology* **2018**, *85*, 41-49, doi:10.1159/000479006.
11. Kaku, T.; Ogawa, S.; Kawano, Y.; Ohishi, Y.; Kobayashi, H.; Hirakawa, T.; Nakano, H. Histological classification of ovarian cancer. *Medical Electron Microscopy* **2003**, *36*, 9-17, doi:10.1007/s007950300002.
12. Kurman, R.J.; Shih, I.-M. Molecular pathogenesis and extraovarian origin of epithelial ovarian cancer—Shifting the paradigm. *Human Pathology* **2011**, *42*, 918-931, doi:10.1016/j.humpath.2011.03.003.
13. Shih, I.-M.; Kurman, R.J. Ovarian Tumorigenesis. *The American Journal of Pathology* **2004**, *164*, 1511-1518, doi:10.1016/s0002-9440(10)63708-x.
14. Jones, S.; Wang, T.-L.; Shih, I.-M.; Mao, T.-L.; Nakayama, K.; Roden, R.; Glas, R.; Slamon, D.; Diaz, L.A.; Vogelstein, B., et al. Frequent Mutations of Chromatin Remodeling Gene ARID1A in Ovarian Clear Cell Carcinoma. *Science* **2010**, *330*, 228-231, doi:10.1126/science.1196333.
15. Wiegand, K.C.; Shah, S.P.; Al-Agha, O.M.; Zhao, Y.; Tse, K.; Zeng, T.; Senz, J.; McConechy, M.K.; Anglesio, M.S.; Kalloger, S.E., et al. ARID1A mutations in endometriosis-associated ovarian carcinomas. *N Engl J Med* **2010**, *363*, 1532-1543, doi:10.1056/NEJMoa1008433.
16. Ahmed, A.A.; Etemadmoghadam, D.; Temple, J.; Lynch, A.G.; Riad, M.; Sharma, R.; Stewart, C.; Fereday, S.; Caldas, C.; deFazio, A., et al. Driver mutations in TP53 are ubiquitous in high grade serous carcinoma of the ovary. *The Journal of Pathology* **2010**, *221*, 49-56, doi:10.1002/path.2696.
17. Köbel, M.; Reuss, A.; Bois, A.d.; Kommoss, S.; Kommoss, F.; Gao, D.; Kalloger, S.E.; Huntsman, D.G.; Gilks, C.B. The biological and clinical value of p53 expression in pelvic high-grade serous carcinomas. *The Journal of Pathology* **2010**, *222*, 191-198, doi:10.1002/path.2744.
18. Asadollahi, R.; Hyde, C.A.C.; Zhong, X.Y. Epigenetics of ovarian cancer: From the lab

- to the clinic. *Gynecologic Oncology* **2010**, *118*, 81-87, doi:10.1016/j.ygyno.2010.03.015.
19. Esteller, M. Epigenetics in Cancer. *New England Journal of Medicine* **2008**, *358*, 1148-1159, doi:10.1056/NEJMra072067.
 20. Jones, P.A.; Baylin, S.B. The fundamental role of epigenetic events in cancer. *Nature Reviews Genetics* **2002**, *3*, 415-428, doi:10.1038/nrg816.
 21. Jones, P.A.; Baylin, S.B. The Epigenomics of Cancer. *Cell* **2007**, *128*, 683-692, doi:10.1016/j.cell.2007.01.029.
 22. Goldberg, A.D.; Allis, C.D.; Bernstein, E. Epigenetics: A Landscape Takes Shape. *Cell* **2007**, *128*, 635-638, doi:10.1016/j.cell.2007.02.006.
 23. Kwon, M.J.; Shin, Y.K. Epigenetic Regulation of Cancer-Associated Genes in Ovarian Cancer. *International Journal of Molecular Sciences* **2011**, *12*, 983-1008, doi:10.3390/ijms12020983.
 24. Marsh, D.J.; Shah, J.S.; Cole, A.J. Histones and Their Modifications in Ovarian Cancer—Drivers of Disease and Therapeutic Targets. *Frontiers in Oncology* **2014**, *4*, doi:10.3389/fonc.2014.00144.
 25. Luger, K.; Mäder, A.W.; Richmond, R.K.; Sargent, D.F.; Richmond, T.J. Crystal structure of the nucleosome core particle at 2.8 Å resolution. *Nature* **1997**, *389*, 251-260, doi:10.1038/38444.
 26. Kornberg, R.D. Chromatin Structure: A Repeating Unit of Histones and DNA. *Science* **1974**, *184*, 868-871, doi:10.1126/science.184.4139.868.
 27. Hergeth, S.P.; Schneider, R. The H1 linker histones: multifunctional proteins beyond the nucleosomal core particle. *EMBO reports* **2015**, *16*, 1439-1453, doi:10.15252/embr.201540749.
 28. Kouzarides, T. Chromatin Modifications and Their Function. *Cell* **2007**, *128*, 693-705, doi:10.1016/j.cell.2007.02.005.
 29. Strahl, B.D.; Allis, C.D. The language of covalent histone modifications. *Nature* **2000**, *403*, 41-45, doi:10.1038/47412.
 30. Chi, P.; Allis, C.D.; Wang, G.G. Covalent histone modifications — miswritten, misinterpreted and mis-erased in human cancers. *Nature Reviews Cancer* **2010**, *10*, 457-469, doi:10.1038/nrc2876.
 31. Bhaumik, S.R.; Smith, E.; Shilatifard, A. Covalent modifications of histones during development and disease pathogenesis. *Nature Structural & Molecular Biology* **2007**, *14*, 1008-1016, doi:10.1038/nsmb1337.
 32. Greer, E.L.; Shi, Y. Histone methylation: a dynamic mark in health, disease and inheritance. *Nature Reviews Genetics* **2012**, *13*, 343-357, doi:10.1038/nrg3173.
 33. Byvoet, P.; Shepherd, G.R.; Hardin, J.M.; Noland, B.J. The distribution and turnover of labeled methyl groups in histone fractions of cultured mammalian cells. *Archives of Biochemistry and Biophysics* **1972**, *148*, 558-567, doi:10.1016/0003-9861(72)90174-9.
 34. Shi, Y.; Lan, F.; Matson, C.; Mulligan, P.; Whetstine, J.R.; Cole, P.A.; Casero, R.A.; Shi, Y. Histone Demethylation Mediated by the Nuclear Amine Oxidase Homolog LSD1. *Cell* **2004**, *119*, 941-953, doi:10.1016/j.cell.2004.12.012.
 35. Hyun, K.; Jeon, J.; Park, K.; Kim, J. Writing, erasing and reading histone lysine methylations. *Experimental & Molecular Medicine* **2017**, *49*, e324-e324, doi:10.1038/emm.2017.11.
 36. Ruthenburg, A.J.; Allis, C.D.; Wysocka, J. Methylation of Lysine 4 on Histone H3: Intricacy of Writing and Reading a Single Epigenetic Mark. *Molecular Cell* **2007**, *25*, 15-30, doi:10.1016/j.molcel.2006.12.014.
 37. Kusch, T. Histone H3 lysine 4 methylation revisited. *Transcription* **2014**, *3*, 310-314, doi:10.4161/trns.21911.
 38. Pinskaya, M.; Morillon, A. Histone H3 Lysine 4 di-methylation: A novel mark for transcriptional fidelity? *Epigenetics* **2009**, *4*, 302-306, doi:10.4161/epi.4.5.9369.
 39. Heintzman, N.D.; Stuart, R.K.; Hon, G.; Fu, Y.; Ching, C.W.; Hawkins, R.D.; Barrera, L.O.; Van Calcar, S.; Qu, C.; Ching, K.A., et al. Distinct and predictive chromatin signatures of transcriptional promoters and enhancers in the human genome. *Nature Genetics* **2007**, *39*, 311-318, doi:10.1038/ng1966.
 40. Rada-Iglesias, A. Is H3K4me1 at enhancers correlative or causative? *Nature Genetics* **2017**, *50*, 4-5, doi:10.1038/s41588-017-0018-3.
 41. Pekowska, A.; Benoukraf, T.; Ferrier, P.; Spicuglia, S. A unique H3K4me2 profile marks tissue-specific gene regulation. *Genome Research* **2010**, *20*, 1493-1502, doi:10.1101/gr.109389.110.
 42. Okitsu, C.Y.; Hsieh, J.C.F.; Hsieh, C.-L. Transcriptional Activity Affects the H3K4me3 Level and Distribution in the Coding Region. *Molecular and Cellular Biology* **2010**, *30*,

- 2933-2946, doi:10.1128/mcb.01478-09.
43. Dong, X.; Greven, M.C.; Kundaje, A.; Djebali, S.; Brown, J.B.; Cheng, C.; Gingeras, T.R.; Gerstein, M.; Guigó, R.; Birney, E., et al. Modeling gene expression using chromatin features in various cellular contexts. *Genome Biology* **2012**, *13*, doi:10.1186/gb-2012-13-9-r53.
 44. Howe, F.S.; Fischl, H.; Murray, S.C.; Mellor, J. Is H3K4me3 instructive for transcription activation? *BioEssays* **2017**, *39*, doi:10.1002/bies.201600095.
 45. Bernstein, B.E.; Kamal, M.; Lindblad-Toh, K.; Bekiranov, S.; Bailey, D.K.; Huebert, D.J.; McMahon, S.; Karlsson, E.K.; Kulbokas, E.J., 3rd; Gingeras, T.R., et al. Genomic maps and comparative analysis of histone modifications in human and mouse. *Cell* **2005**, *120*, 169-181, doi:10.1016/j.cell.2005.01.001.
 46. Barski, A.; Cuddapah, S.; Cui, K.; Roh, T.-Y.; Schones, D.E.; Wang, Z.; Wei, G.; Chepelev, I.; Zhao, K. High-Resolution Profiling of Histone Methylations in the Human Genome. *Cell* **2007**, *129*, 823-837, doi:10.1016/j.cell.2007.05.009.
 47. Pokholok, D.K.; Harbison, C.T.; Levine, S.; Cole, M.; Hannett, N.M.; Lee, T.I.; Bell, G.W.; Walker, K.; Rolfe, P.A.; Herbolsheimer, E., et al. Genome-wide Map of Nucleosome Acetylation and Methylation in Yeast. *Cell* **2005**, *122*, 517-527, doi:10.1016/j.cell.2005.06.026.
 48. Park, S.; Kim, G.W.; Kwon, S.H.; Lee, J.S. Broad domains of histone H3 lysine 4 trimethylation in transcriptional regulation and disease. *The FEBS Journal* **2020**, 10.1111/febs.15219, doi:10.1111/febs.15219.
 49. Adli, M.; Zhu, J.; Bernstein, B.E. Genome-wide chromatin maps derived from limited numbers of hematopoietic progenitors. *Nature Methods* **2010**, *7*, 615-618, doi:10.1038/nmeth.1478.
 50. Lien, W.-H.; Guo, X.; Polak, L.; Lawton, Lee N.; Young, Richard A.; Zheng, D.; Fuchs, E. Genome-wide Maps of Histone Modifications Unwind In Vivo Chromatin States of the Hair Follicle Lineage. *Cell Stem Cell* **2011**, *9*, 219-232, doi:10.1016/j.stem.2011.07.015.
 51. Aiden, A.P.; Rivera, M.N.; Rheinbay, E.; Ku, M.; Coffman, E.J.; Truong, T.T.; Vargas, S.O.; Lander, E.S.; Haber, D.A.; Bernstein, B.E. Wilms Tumor Chromatin Profiles Highlight Stem Cell Properties and a Renal Developmental Network. *Cell Stem Cell* **2010**, *6*, 591-602, doi:10.1016/j.stem.2010.03.016.
 52. Benayoun, Bérénice A.; Pollina, Elizabeth A.; Ucar, D.; Mahmoudi, S.; Karra, K.; Wong, Edith D.; Devarajan, K.; Daugherty, Aaron C.; Kundaje, Anshul B.; Mancini, E., et al. H3K4me3 Breadth Is Linked to Cell Identity and Transcriptional Consistency. *Cell* **2014**, *158*, 673-688, doi:10.1016/j.cell.2014.06.027.
 53. Chen, K.; Chen, Z.; Wu, D.; Zhang, L.; Lin, X.; Su, J.; Rodriguez, B.; Xi, Y.; Xia, Z.; Chen, X., et al. Broad H3K4me3 is associated with increased transcription elongation and enhancer activity at tumor-suppressor genes. *Nature Genetics* **2015**, *47*, 1149-1157, doi:10.1038/ng.3385.
 54. Shilatifard, A. The COMPASS Family of Histone H3K4 Methylases: Mechanisms of Regulation in Development and Disease Pathogenesis. *Annual Review of Biochemistry* **2012**, *81*, 65-95, doi:10.1146/annurev-biochem-051710-134100.
 55. Miller, T.; Krogan, N.J.; Dover, J.; Erdjument-Bromage, H.; Tempst, P.; Johnston, M.; Greenblatt, J.F.; Shilatifard, A. COMPASS: A complex of proteins associated with a trithorax-related SET domain protein. *Proceedings of the National Academy of Sciences* **2001**, *98*, 12902-12907, doi:10.1073/pnas.231473398.
 56. Roguev, A. The *Saccharomyces cerevisiae* Set1 complex includes an Ash2 homologue and methylates histone 3 lysine 4. *The EMBO Journal* **2001**, *20*, 7137-7148, doi:10.1093/emboj/20.24.7137.
 57. Santos-Rosa, H.; Schneider, R.; Bannister, A.J.; Sherriff, J.; Bernstein, B.E.; Emre, N.C.T.; Schreiber, S.L.; Mellor, J.; Kouzarides, T. Active genes are tri-methylated at K4 of histone H3. *Nature* **2002**, *419*, 407-411, doi:10.1038/nature01080.
 58. Milne, T.A.; Briggs, S.D.; Brock, H.W.; Martin, M.E.; Gibbs, D.; Allis, C.D.; Hess, J.L. MLL Targets SET Domain Methyltransferase Activity to Hox Gene Promoters. *Molecular Cell* **2002**, *10*, 1107-1117, doi:10.1016/s1097-2765(02)00741-4.
 59. Zhao, X.D.; Han, X.; Chew, J.L.; Liu, J.; Chiu, K.P.; Choo, A.; Orlov, Y.L.; Sung, W.-K.; Shahab, A.; Kuznetsov, V.A., et al. Whole-Genome Mapping of Histone H3 Lys4 and 27 Trimethylations Reveals Distinct Genomic Compartments in Human Embryonic Stem Cells. *Cell Stem Cell* **2007**, *1*, 286-298, doi:10.1016/j.stem.2007.08.004.
 60. Lee, J.-H.; Skalnik, D.G. Wdr82 Is a C-Terminal Domain-Binding Protein That Recruits the Setd1A Histone H3-Lys4 Methyltransferase Complex to Transcription Start Sites of Transcribed Human Genes. *Molecular and Cellular Biology* **2008**, *28*, 609-618,

- doi:10.1128/mcb.01356-07.
61. Louder, R.K.; He, Y.; López-Blanco, J.R.; Fang, J.; Chacón, P.; Nogales, E. Structure of promoter-bound TFIID and model of human pre-initiation complex assembly. *Nature* **2016**, *531*, 604-609, doi:10.1038/nature17394.
 62. Burley, S.K.; Roeder, R.G. Biochemistry and Structural Biology of Transcription Factor IID (TFIID). *Annual Review of Biochemistry* **1996**, *65*, 769-799, doi:10.1146/annurev.bi.65.070196.004005.
 63. Albright, S.R.; Tjian, R. TAFs revisited: more data reveal new twists and confirm old ideas. *Gene* **2000**, *242*, 1-13, doi:10.1016/s0378-1119(99)00495-3.
 64. Vermeulen, M.; Mulder, K.W.; Denissov, S.; Pijnappel, W.W.M.P.; van Schaik, F.M.A.; Varier, R.A.; Baltissen, M.P.A.; Stunnenberg, H.G.; Mann, M.; Timmers, H.T.M. Selective Anchoring of TFIID to Nucleosomes by Trimethylation of Histone H3 Lysine 4. *Cell* **2007**, *131*, 58-69, doi:10.1016/j.cell.2007.08.016.
 65. Lauberth, Shannon M.; Nakayama, T.; Wu, X.; Ferris, Andrea L.; Tang, Z.; Hughes, Stephen H.; Roeder, Robert G. H3K4me3 Interactions with TAF3 Regulate Preinitiation Complex Assembly and Selective Gene Activation. *Cell* **2013**, *152*, 1021-1036, doi:10.1016/j.cell.2013.01.052.
 66. Sims, R.J. Elongation by RNA polymerase II: the short and long of it. *Genes & Development* **2004**, *18*, 2437-2468, doi:10.1101/gad.1235904.
 67. Hirose, Y.; Manley, J.L. RNA polymerase II and the integration of nuclear events. *Genes Dev* **2000**, *14*, 1415-1429.
 68. Fasken, M.B.; Corbett, A.H. Process or perish: quality control in mRNA biogenesis. *Nature Structural & Molecular Biology* **2005**, *12*, 482-488, doi:10.1038/nsmb945.
 69. Simic, R. Chromatin remodeling protein Chd1 interacts with transcription elongation factors and localizes to transcribed genes. *The EMBO Journal* **2003**, *22*, 1846-1856, doi:10.1093/emboj/cdg179.
 70. Sims, R.J.; Chen, C.-F.; Santos-Rosa, H.; Kouzarides, T.; Patel, S.S.; Reinberg, D. Human but Not Yeast CHD1 Binds Directly and Selectively to Histone H3 Methylated at Lysine 4 via Its Tandem Chromodomains. *Journal of Biological Chemistry* **2005**, *280*, 41789-41792, doi:10.1074/jbc.C500395200.
 71. Sims, R.J.; Millhouse, S.; Chen, C.-F.; Lewis, B.A.; Erdjument-Bromage, H.; Tempst, P.; Manley, J.L.; Reinberg, D. Recognition of Trimethylated Histone H3 Lysine 4 Facilitates the Recruitment of Transcription Postinitiation Factors and Pre-mRNA Splicing. *Molecular Cell* **2007**, *28*, 665-676, doi:10.1016/j.molcel.2007.11.010.
 72. Tanackovic, G.; Krämer, A. Human Splicing Factor SF3a, but Not SF1, Is Essential for Pre-mRNA Splicing In Vivo. *Molecular Biology of the Cell* **2005**, *16*, 1366-1377, doi:10.1091/mbc.e04-11-1034.
 73. Rahl, P.B.; Lin, C.Y.; Seila, A.C.; Flynn, R.A.; McCuine, S.; Burge, C.B.; Sharp, P.A.; Young, R.A. c-Myc Regulates Transcriptional Pause Release. *Cell* **2010**, *141*, 432-445, doi:10.1016/j.cell.2010.03.030.
 74. Ng, H.H.; Robert, F.; Young, R.A.; Struhl, K. Targeted Recruitment of Set1 Histone Methylase by Elongating Pol II Provides a Localized Mark and Memory of Recent Transcriptional Activity. *Molecular Cell* **2003**, *11*, 709-719, doi:10.1016/s1097-2765(03)00092-3.
 75. Hödl, M.; Basler, K. Transcription in the Absence of Histone H3.2 and H3K4 Methylation. *Current Biology* **2012**, *22*, 2253-2257, doi:10.1016/j.cub.2012.10.008.
 76. Peña, P.V.; Hom, R.A.; Hung, T.; Lin, H.; Kuo, A.J.; Wong, R.P.C.; Subach, O.M.; Champagne, K.S.; Zhao, R.; Verkhusha, V.V., et al. Histone H3K4me3 Binding Is Required for the DNA Repair and Apoptotic Activities of ING1 Tumor Suppressor. *Journal of Molecular Biology* **2008**, *380*, 303-312, doi:10.1016/j.jmb.2008.04.061.
 77. Dou, Y.; Milne, T.A.; Ruthenburg, A.J.; Lee, S.; Lee, J.W.; Verdine, G.L.; Allis, C.D.; Roeder, R.G. Regulation of MLL1 H3K4 methyltransferase activity by its core components. *Nature Structural & Molecular Biology* **2006**, *13*, 713-719, doi:10.1038/nsmb1128.
 78. Wang, Y.; Shi, J.; Chai, K.; Ying, X.; Zhou, B.P. The Role of Snail in EMT and Tumorigenesis. *Curr Cancer Drug Targets* **2013**, *13*, 963-972, doi:10.2174/15680096113136660102.
 79. Li, D.; Sun, H.; Sun, W.-j.; Bao, H.-b.; Si, S.-h.; Fan, J.-l.; Lin, P.; Cui, R.-j.; Pan, Y.-j.; Wen, S.-m., et al. Role of RbBP5 and H3K4me3 in the vicinity of Snail transcription start site during epithelial-mesenchymal transition in prostate cancer cell. *Oncotarget* **2016**, *7*, 65553-65567, doi:10.18632/oncotarget.11549.
 80. Ballabio, E.; Milne, T.A. Molecular and Epigenetic Mechanisms of MLL in Human

- Leukemogenesis. *Cancers* **2012**, *4*, 904-944, doi:10.3390/cancers4030904.
81. Fang, Y.; Zhang, D.; Hu, T.; Zhao, H.; Zhao, X.; Lou, Z.; He, Y.; Qin, W.; Xia, J.; Zhang, X., et al. KMT2A histone methyltransferase contributes to colorectal cancer development by promoting cathepsin Z transcriptional activation. *Cancer Medicine* **2019**, *8*, 3544-3552, doi:10.1002/cam4.2226.
82. Klose, R.J.; Zhang, Y. Regulation of histone methylation by demethylation and demethylation. *Nature Reviews Molecular Cell Biology* **2007**, *8*, 307-318, doi:10.1038/nrm2143.
83. Xiang, Y.; Zhu, Z.; Han, G.; Ye, X.; Xu, B.; Peng, Z.; Ma, Y.; Yu, Y.; Lin, H.; Chen, A.P., et al. JARID1B is a histone H3 lysine 4 demethylase up-regulated in prostate cancer. *Proceedings of the National Academy of Sciences* **2007**, *104*, 19226-19231, doi:10.1073/pnas.0700735104.
84. Yamane, K.; Tateishi, K.; Klose, R.J.; Fang, J.; Fabrizio, L.A.; Erdjument-Bromage, H.; Taylor-Papadimitriou, J.; Tempst, P.; Zhang, Y. PLU-1 Is an H3K4 Demethylase Involved in Transcriptional Repression and Breast Cancer Cell Proliferation. *Molecular Cell* **2007**, *25*, 801-812, doi:10.1016/j.molcel.2007.03.001.
85. Tan, K.; Shaw, A.L.; Madsen, B.; Jensen, K.; Taylor-Papadimitriou, J.; Freemont, P.S. Human PLU-1 Has Transcriptional Repression Properties and Interacts with the Developmental Transcription Factors BF-1 and PAX9. *Journal of Biological Chemistry* **2003**, *278*, 20507-20513, doi:10.1074/jbc.M301994200.
86. Weinberg, R. Tumor suppressor genes. *Science* **1991**, *254*, 1138-1146, doi:10.1126/science.1659741.
87. Dhar, S.S.; Zhao, D.; Lin, T.; Gu, B.; Pal, K.; Wu, S.J.; Alam, H.; Lv, J.; Yun, K.; Gopalakrishnan, V., et al. MLL4 Is Required to Maintain Broad H3K4me3 Peaks and Super-Enhancers at Tumor Suppressor Genes. *Molecular Cell* **2018**, *70*, 825-841.e826, doi:10.1016/j.molcel.2018.04.028.
88. Dagogo-Jack, I.; Shaw, A.T. Tumour heterogeneity and resistance to cancer therapies. *Nature Reviews Clinical Oncology* **2017**, *15*, 81-94, doi:10.1038/nrclinonc.2017.166.
89. Kurdistani, S.K. Histone Modifications in Cancer Biology and Prognosis. In *Epigenetics and Disease*, 2011; 10.1007/978-3-7643-8989-5_5pp. 91-106.
90. Ludwig, J.A.; Weinstein, J.N. Biomarkers in Cancer Staging, Prognosis and Treatment Selection. *Nature Reviews Cancer* **2005**, *5*, 845-856, doi:10.1038/nrc1739.
91. Sharma, S.; Kelly, T.K.; Jones, P.A. Epigenetics in cancer. *Carcinogenesis* **2009**, *31*, 27-36, doi:10.1093/carcin/bgp220.
92. Li, S.; Shen, L.; Chen, K.-N. Association between H3K4 methylation and cancer prognosis: A meta-analysis. *Thoracic Cancer* **2018**, *9*, 794-799, doi:10.1111/1759-7714.12647.
93. He, C.; Xu, J.; Zhang, J.; Xie, D.; Ye, H.; Xiao, Z.; Cai, M.; Xu, K.; Zeng, Y.; Li, H., et al. High expression of trimethylated histone H3 lysine 4 is associated with poor prognosis in hepatocellular carcinoma. *Human Pathology* **2012**, *43*, 1425-1435, doi:10.1016/j.humpath.2011.11.003.
94. Beyer, S.; Zhu, J.; Mayr, D.; Kuhn, C.; Schulze, S.; Hofmann, S.; Dannecker, C.; Jeschke, U.; Kost, B. Histone H3 Acetyl K9 and Histone H3 Tri Methyl K4 as Prognostic Markers for Patients with Cervical Cancer. *International Journal of Molecular Sciences* **2017**, *18*, doi:10.3390/ijms18030477.
95. Berger, L.; Kolben, T.; Meister, S.; Kolben, T.M.; Schmoeckel, E.; Mayr, D.; Mahner, S.; Jeschke, U.; Ditsch, N.; Beyer, S. Expression of H3K4me3 and H3K9ac in breast cancer. *Journal of Cancer Research and Clinical Oncology* **2020**, *146*, 2017-2027, doi:10.1007/s00432-020-03265-z.
96. Ye, X.-D.; Qiu, B.-Q.; Xiong, D.; Pei, X.; Jie, N.; Xu, H.; Zhu, S.-Q.; Long, X.; Xu, Z.; Wu, H.-B., et al. High level of H3K4 tri-methylation modification predicts poor prognosis in esophageal cancer. *Journal of Cancer* **2020**, *11*, 3256-3263, doi:10.7150/jca.36801.
97. Liu, H.; Li, Y.; Li, J.; Liu, Y.; Cui, B. H3K4me3 and Wdr82 are associated with tumor progression and a favorable prognosis in human colorectal cancer. *Oncology Letters* **2018**, *10*, 3892/ol.2018.8902, doi:10.3892/ol.2018.8902.
98. Dubuc, A.M.; Remke, M.; Korshunov, A.; Northcott, P.A.; Zhan, S.H.; Mendez-Lago, M.; Kool, M.; Jones, D.T.W.; Unterberger, A.; Morrissy, A.S., et al. Aberrant patterns of H3K4 and H3K27 histone lysine methylation occur across subgroups in medulloblastoma. *Acta Neuropathologica* **2012**, *125*, 373-384, doi:10.1007/s00401-012-1070-9.
99. Ellinger, J.; Kahl, P.; Mertens, C.; Rogenhofer, S.; Hauser, S.; Hartmann, W.; Bastian, P.J.; Büttner, R.; Müller, S.C.; von Ruecker, A. Prognostic relevance of global histone H3 lysine 4 (H3K4) methylation in renal cell carcinoma. *International Journal of Cancer*

- 2010**, 127, 2360-2366, doi:10.1002/ijc.25250.
100. Schneider, A.-C.; Heukamp, L.C.; Rogenhofer, S.; Fechner, G.; Bastian, P.J.; von Ruecker, A.; Müller, S.C.; Ellinger, J. Global histone H4K20 trimethylation predicts cancer-specific survival in patients with muscle-invasive bladder cancer. *BJU International* **2011**, 108, E290-E296, doi:10.1111/j.1464-410X.2011.10203.x.
 101. Ellinger, J.; Kahl, P.; von der Gathen, J.; Rogenhofer, S.; Heukamp, L.C.; Gütgemann, I.; Walter, B.; Hofstädter, F.; Büttner, R.; Müller, S.C., et al. Global levels of histone modifications predict prostate cancer recurrence. *The Prostate* **2010**, 70, 61-69, doi:10.1002/pros.21038.
 102. Zhou, M.; Li, Y.; Lin, S.; Chen, Y.; Qian, Y.; Zhao, Z.; Fan, H. H3K9me3, H3K36me3, and H4K20me3 Expression Correlates with Patient Outcome in Esophageal Squamous Cell Carcinoma as Epigenetic Markers. *Digestive Diseases and Sciences* **2019**, 64, 2147-2157, doi:10.1007/s10620-019-05529-2.
 103. Chen, Y.-W.; Kao, S.-Y.; Wang, H.-J.; Yang, M.-H. Histone modification patterns correlate with patient outcome in oral squamous cell carcinoma. *Cancer* **2013**, 119, 4259-4267, doi:10.1002/cncr.28356.
 104. Moore, D.D.; Kato, S.; Xie, W.; Mangelsdorf, D.J.; Schmidt, D.R.; Xiao, R.; Kliewer, S.A. International Union of Pharmacology. LXII. The NR1H and NR1I Receptors: Constitutive Androstane Receptor, Pregnane X Receptor, Farnesoid X Receptor α , Farnesoid X Receptor β , Liver X Receptor α , Liver X Receptor β , and Vitamin D Receptor. *Pharmacological Reviews* **2006**, 58, 742-759, doi:10.1124/pr.58.4.6.
 105. Fetahu, I.S.; Höbaus, J.; Kállay, E. Vitamin D and the epigenome. *Frontiers in Physiology* **2014**, 5, doi:10.3389/fphys.2014.00164.
 106. Nurminen, V.; Neme, A.; Seuter, S.; Carlberg, C. The impact of the vitamin D-modulated epigenome on VDR target gene regulation. *Biochimica et Biophysica Acta (BBA) - Gene Regulatory Mechanisms* **2018**, 1861, 697-705, doi:10.1016/j.bbagr.2018.05.006.
 107. Thorne, J.L.; Maguire, O.; Doig, C.L.; Battaglia, S.; Fehr, L.; Sucheston, L.E.; Heinaniemi, M.; O'Neill, L.P.; McCabe, C.J.; Turner, B.M., et al. Epigenetic control of a VDR-governed feed-forward loop that regulates p21 (waf1/cip1) expression and function in non-malignant prostate cells. *Nucleic Acids Research* **2011**, 39, 2045-2056, doi:10.1093/nar/gkq875.
 108. LaPorta, E.; Welsh, J. Modeling vitamin D actions in triple negative/basal-like breast cancer. *The Journal of Steroid Biochemistry and Molecular Biology* **2014**, 144, 65-73, doi:10.1016/j.jsbmb.2013.10.022.
 109. Goeman, F.; De Nicola, F.; D'Onorio De Meo, P.; Pallocca, M.; Elmi, B.; Castrignanò, T.; Pesole, G.; Strano, S.; Blandino, G.; Fanciulli, M., et al. VDR primary targets by genome-wide transcriptional profiling. *The Journal of Steroid Biochemistry and Molecular Biology* **2014**, 143, 348-356, doi:10.1016/j.jsbmb.2014.03.007.
 110. Langdon, S.P.; Herrington, C.S.; Hollis, R.L.; Gourley, C. Estrogen Signaling and Its Potential as a Target for Therapy in Ovarian Cancer. *Cancers* **2020**, 12, doi:10.3390/cancers12061647.
 111. Jensen, E.V. On the Mechanism of Estrogen Action. *Perspectives in Biology and Medicine* **1962**, 6, 47-60, doi:10.1353/pbm.1963.0005.
 112. Kuiper, G.G.; Enmark, E.; Peltö-Huikko, M.; Nilsson, S.; Gustafsson, J.A. Cloning of a novel receptor expressed in rat prostate and ovary. *Proceedings of the National Academy of Sciences* **1996**, 93, 5925-5930, doi:10.1073/pnas.93.12.5925.
 113. Lee, H.-R.; Kim, T.-H.; Choi, K.-C. Functions and physiological roles of two types of estrogen receptors, ER α and ER β , identified by estrogen receptor knockout mouse. *Laboratory Animal Research* **2012**, 28, doi:10.5625/lar.2012.28.2.71.
 114. Björnström, L.; Sjöberg, M. Mechanisms of Estrogen Receptor Signaling: Convergence of Genomic and Nongenomic Actions on Target Genes. *Molecular Endocrinology* **2005**, 19, 833-842, doi:10.1210/me.2004-0486.
 115. Hurtado, A.; Holmes, K.A.; Ross-Innes, C.S.; Schmidt, D.; Carroll, J.S. FOXA1 is a key determinant of estrogen receptor function and endocrine response. *Nature Genetics* **2010**, 43, 27-33, doi:10.1038/ng.730.
 116. Ernst, J.; Kheradpour, P.; Mikkelsen, T.S.; Shores, N.; Ward, L.D.; Epstein, C.B.; Zhang, X.; Wang, L.; Issner, R.; Coyne, M., et al. Mapping and analysis of chromatin state dynamics in nine human cell types. *Nature* **2011**, 473, 43-49, doi:10.1038/nature09906.
 117. Li, Y.; Sun, L.; Zhang, Y.; Wang, D.; Wang, F.; Liang, J.; Gui, B.; Shang, Y. The Histone Modifications Governing TFF1 Transcription Mediated by Estrogen Receptor. *Journal of Biological Chemistry* **2011**, 286, 13925-13936, doi:10.1074/jbc.M111.223198.

118. Bernstein, B.E.; Humphrey, E.L.; Erlich, R.L.; Schneider, R.; Bouman, P.; Liu, J.S.; Kouzarides, T.; Schreiber, S.L. Methylation of histone H3 Lys 4 in coding regions of active genes. *Proceedings of the National Academy of Sciences* **2002**, *99*, 8695-8700, doi:10.1073/pnas.082249499.
119. Dreijerink, K.M.A.; Mulder, K.W.; Winkler, G.S.; Höppener, J.W.M.; Lips, C.J.M.; Timmers, H.T.M. Menin Links Estrogen Receptor Activation to Histone H3K4 Trimethylation. *Cancer Research* **2006**, *66*, 4929-4935, doi:10.1158/0008-5472.Can-05-4461.
120. Sun, G.; Wang, C.; Wang, S.; Sun, H.; Zeng, K.; Zou, R.; Lin, L.; Liu, W.; Sun, N.; Song, H., et al. An H3K4me3 reader, BAP18 as an adaptor of COMPASS-like core subunits co-activates ER α action and associates with the sensitivity of antiestrogen in breast cancer. *Nucleic Acids Research* **2020**, *48*, 10768-10784, doi:10.1093/nar/gkaa787.
121. Drummond, A.E.; Fuller, P.J. The importance of ER β signalling in the ovary. *Journal of Endocrinology* **2010**, *205*, 15-23, doi:10.1677/joe-09-0379.
122. Dago, D.N.; Scafoglio, C.; Rinaldi, A.; Memoli, D.; Giurato, G.; Nassa, G.; Ravo, M.; Rizzo, F.; Tarallo, R.; Weisz, A. Estrogen receptor beta impacts hormone-induced alternative mRNA splicing in breast cancer cells. *BMC Genomics* **2015**, *16*, doi:10.1186/s12864-015-1541-1.
123. Lu, W.; Katzenellenbogen, B.S. Estrogen Receptor- β Modulation of the ER α -p53 Loop Regulating Gene Expression, Proliferation, and Apoptosis in Breast Cancer. *Hormones and Cancer* **2017**, *8*, 230-242, doi:10.1007/s12672-017-0298-1.
124. Prossnitz, E.R.; Barton, M. The G-protein-coupled estrogen receptor GPER in health and disease. *Nature Reviews Endocrinology* **2011**, *7*, 715-726, doi:10.1038/nrendo.2011.122.
125. O'Dowd, B.F.; Nguyen, T.; Marchese, A.; Cheng, R.; Lynch, K.R.; Heng, H.H.Q.; Kolakowski, L.F.; George, S.R. Discovery of Three Novel G-Protein-Coupled Receptor Genes. *Genomics* **1998**, *47*, 310-313, doi:10.1006/geno.1998.5095.
126. Carmeci, C.; Thompson, D.A.; Ring, H.Z.; Francke, U.; Weigel, R.J. Identification of a Gene (GPR30) with Homology to the G-Protein-Coupled Receptor Superfamily Associated with Estrogen Receptor Expression in Breast Cancer. *Genomics* **1997**, *45*, 607-617, doi:10.1006/geno.1997.4972.
127. Kvingedal, A.M.; Smeland, E.B. A novel putative G-protein-coupled receptor expressed in lung, heart and lymphoid tissue. *FEBS Letters* **1997**, *407*, 59-62, doi:10.1016/s0014-5793(97)00278-0.
128. Revankar, C.M. A Transmembrane Intracellular Estrogen Receptor Mediates Rapid Cell Signaling. *Science* **2005**, *307*, 1625-1630, doi:10.1126/science.1106943.
129. Prossnitz, E.R.; Barton, M. Signaling, physiological functions and clinical relevance of the G protein-coupled estrogen receptor GPER. *Prostaglandins & Other Lipid Mediators* **2009**, *89*, 89-97, doi:10.1016/j.prostaglandins.2009.05.001.
130. Prossnitz, E.R.; Barton, M. Estrogen biology: New insights into GPER function and clinical opportunities. *Molecular and Cellular Endocrinology* **2014**, *389*, 71-83, doi:10.1016/j.mce.2014.02.002.
131. Anbalagan, M.; Huderson, B.; Murphy, L.; Rowan, B.G. Post-Translational Modifications of Nuclear Receptors and Human Disease. *Nuclear Receptor Signaling* **2012**, *10*, doi:10.1621/nrs.10001.
132. Weißborn, C.; Ignatov, T.; Ochel, H.-J.; Costa, S.D.; Zenclussen, A.C.; Ignatova, Z.; Ignatov, A. GPER functions as a tumor suppressor in triple-negative breast cancer cells. *Journal of Cancer Research and Clinical Oncology* **2014**, *140*, 713-723, doi:10.1007/s00432-014-1620-8.
133. Li, Y.; Birnbaumer, L.; Teng, C.T. Regulation of ER α Gene Expression by Estrogen Receptor Agonists and Antagonists in SKBR3 Breast Cancer Cells: Differential Molecular Mechanisms Mediated by G Protein-Coupled Receptor GPR30/GPER-1. *Molecular Endocrinology* **2010**, *24*, 969-980, doi:10.1210/me.2009-0148.

Acknowledgements

Foremost, I would like to give my special thanks of gratitude to Prof.Dr. Udo Jeschke who gave me the golden opportunity to do this research in the Department of Obstetrics and Gynecology, Ludwig-Maximilians-Universität for my doctoral degree.

I would like to express my sincere gratitude to my primary supervisor, Prof.Dr. Udo Jeschke, who provided the continuous guidance and feedback throughout this research project. His patience, motivation and immense knowledge helped me complete the research successfully. His dynamism, vision and sincerity have deeply inspired me. He has taught me the methodology to perform the research and to present my research works as clearly as possible. His words 'Science is to find the reason' have always inspired me to be a good scientific worker. It was a great privilege and honour to work and study under his guidance.

Secondly, I would like to thank my secondary supervisor, Dr. Fabian Trillsch, for his revisions and suggestions of my publications. I would also like to thank him for his friendship, enthusiasm and great sense of humour. In addition, I'd like to show my deep appreciation to my supervisors who helped me finalize my project.

Besides my supervisors, I wish to acknowledge the help provided by the technical and support staff in our work group. They taught me a lot of technique of molecular biology experiments with their great patience. They also offered a tremendous support during the entire experimental period. For example, they helped me order all kinds of antibodies and reagents what were used in the research as well as solve various experimental troubles.

I am extremely grateful to my parents for their love, prayers, caring and sacrifices for my future. Additionally, I would like to thank my friends who supported me and offered deep insight into the study.

Finally, many thanks to all participants that took part in the study and enable this research to be possible.